Univerzita Karlova
Přírodovědecká fakulta

Studijní program: Biologie
Studijní program: Buněčná a vývojová biologie - fyziologie buňky

Bc. Erna Šljivnjak

Stimulace osteogenní differenciace mesenchymálních kmenových buněk pomocí perfúzního bioreaktoru

Stimulation of mesenchymal stem cell osteogenic differentiation using perfusion bioreactor

Diplomová práce

Vedoucí diplomové práce: Mgr. Michala Rampichová, Ph.D.

Praha 2022

Prohlašuji, že jsem závěrečnou práci zpracovala samostatně a že jsem uvedla všechny použité informační zdroje a literaturu. Tato práce ani její podstatná část nebyla předložena k získání jiného nebo stejného akademického titulu.

V Praze, 26.04.2022

_____

Bc. Erna Šljivnjak

Poděkování

Ráda bych touto cestou poděkovala své školitelce Mgr. Michale Rampichové, Ph.D. za vedení práce, její čas a oporu, Mgr. Věře Hedvičákové, Ph.D. za její pomoc při práci v laboratoři. Také jsem vděčná za technickou asistenci Mgr. Veroniky Hefka Blahnové, a rovněž bych chtěla poděkovat celé laboratoři Tkáňového inženýrství. Obzvlášt bych chtěla poděkovat Mgr. Matěji Buzgovi za stereologickou analýzu a doc. Ing. Jiřímu Chvojkovi, Ph.D. a Ing. Jakubu Erbenovi z TUL za poskytnutí nosičů použitých v experimentech. A v neposlední řadě i mé sestře a přítelovi, kteří mi byli rovněž oporou.

Abstract

Bone cells *in vivo* reside in a dynamic environment exposed to constant chemical and mechanical stimuli caused by the interstitial fluid flow. It is hypothesized that perfusion of the medium through the scaffold increases the mass transport and creates at the same time shear stress, thereby *in vitro* simulating the interstitial fluid effects and bone tissue formation conditions. This work examined the effects of perfusion flow rates on cell viability, proliferation, migration and osteogenic differentiation of human mesenchymal stem cells within cell-seeded 3D poly-ε-caprolactone scaffolds. Scaffolds were perfused for 21 days at flow rates 1, 3 and 5 mL/min and were compared to the scaffolds from static culture. Cells were most viable, had upregulated expression of osteogenic markers collagen type I and highest alkaline phosphatase activity under flow rate 1 mL/min when compared to their static counterparts. Cells proliferated the most under flow rate 3 mL/min when compared to their static counterparts. Flow rate 5 mL/min did not significantly differ from the static culture in any of the examined parameters. Cell migration into the scaffold was not improved upon exposure to perfusion. This data confirms that medium perfusion may benefit cell proliferation and osteogenic differentiation by enhancing the mass transport in the scaffolds, as well as mechanical stimulation. Dynamic culturing is a valuable tool in tissue engineering and the flow rate and shear stress are important coupled parameters.

Key words: stem cells, perfusion flow, tissue engineering, osteogenic differentiation, dynamic culture

Abstrakt

Kostní buňky jsou *in vivo* vystaveny neustálým chemickým a mechanickým podnětům, způsobených prouděním intersticiální tekutiny. V *in vitro* prostředí je možné napodobit účinky intersticiální tekutiny a podmínky tvorby kostní tkáně pomocí perfúzního bioreaktoru. Perfuze média přes tkáňový nosič zlepšuje transport živin a současně vytváří smykové tření, napodobující *in vivo* podmínky. Tato práce zkoumala účinky rychlostí perfuzního toku na buněčnou životaschopnost, proliferaci, migraci a osteogenní diferenciaci lidských mezenchymálních kmenových buněk kultivovaných v 3D vlákenných nosičích připravených z poly-ε-kaprolaktonu. Nosiče byly vystaveny perfuzi po dobu 21 dnů při průtokových rychlostech 1, 3 a 5 ml/min a byly porovnány s nosiči kultivovanými ve statických podmínkách. Buňky kultivované při průtoku 1 ml/min vykazovaly ve srovnání se statickou kulturou vyšší životaschopnost, měly zvýšenou expresi osteogenního markeru kolagenu typu I a nejvyšší aktivitu alkalické fosfatázy. Nejvyšší buněčná proliferace ve srovnání se statickou kulturou byla sledována při průtoku 3 ml/min. Buňky kultivované v bioreaktoru pod průtokem 5 ml/min se v žádném ze zkoumaných parametrů významně nelišily od statické kultury. Migrace buněk do nosičů po vystavení perfuznímu proudění nebyla sledována. Tato data potvrzují, že perfuze média může prospět buněčné proliferaci a osteogenní diferenciaci zvýšením transportu živin do nosičů a mechanickou stimulací. Dynamická kultivace je cenným nástrojem v tkáňovém inženýrství a rychlost průtoku a smykové tření jsou její důležité parametry.

Key words: kmenové buňky, perfuzní proudění, tkáňové inženýrství, osteogenní diferenciace, dynamická kultivace

Table of Contents

Abstract 1
Abstrakt 2
Table of Contents 3
Abbreviations 6
1 Introduction 8
2 Tissue engineering 9
2.1 Scaffold materials 11
2.1.1 Non-degradable scaffold materials 11
2.1.2 Degradable scaffold materials 11
2.1.2.1 Poly-ε-caprolactone 13
2.2 Scaffold categories 15
2.2.1 Electrospinning 17
2.2.2 Melt-blown 18
3 Bone development 20
3.1 Bone tissue characterization 20
3.2 Bone cells 22
3.2.1 Osteoblasts 22
3.2.1.1 Osteogenic transcription factors 22
3.2.1.1.1 RunX2 23
3.2.1.1.2 Osterix 24
3.2.1.1.3 Dlx5 and Msx2 25
3.2.1.1.4 Id-protein family 25
3.2.1.1.5 Other TFs 26
3.2.1.2 Growth factors in MSC osteogenesis 26
3.2.1.2.1 TGF-β superfamily 27
3.2.1.2.2 Other GFs 28
3.2.2 Human mesenchymal stem cells 29
3.2.2.1 Characteristics 30
3.2.2.2 Niche 31
3.2.2.3 Source tissues of MSCs 32
3.2.2.4 Immune system interaction 33
3.2.2.5 Osteogenic differentiation *in vivo* 35

3.2.2.6 Osteogenic differentiation *in vitro* 37
3.2.2.7 Alkaline phosphatase 38
3.3 Bone ECM 39
3.4 Bone homeostasis 40
3.5 Role of fluid shear stress in bone formation 42
4 Perfusion bioreactor 45
4.1 Overview of bioreactor types 45
4.2 Perfusion bioreactor properties 46
4.2.1 Flow rate selection 47
5 Aims of the thesis 49
6 Methods 50
6.1 Scaffold preparation 52
6.2 Scanning electron microscopy 52
6.3 Cell subculturing 52
6.4 Seeding of hMSCs 53
6.5 Perfusion bioreactor set up 53
6.6 Colorimetric assay for assessing cell metabolic activity 54
6.6.1 MTS assay protocol 55
6.7 Alkaline phosphatase assay 55
6.7.1 Alkaline phosphatase assay protocol 55
6.8 Quantification of DNA 56
6.8.1 PicoGreen assay protocol 56
6.9 RT-PCR analysis 57
6.9.1 qPCR protocol 57
6.10 Cell visualization 59
6.11 Statistical analysis 59
7 Results 60
7.1 Characterization of scaffolds 60
7.2 Cell metabolic activity 60
7.3 ALP activity 61
7.4 PicoGreen DNA quantitation 61
7.5 qPCR quantification of gene expression 62
7.5.1 RunX2 62
7.5.2 Type I collagen 62
7.5.3 OCN 63

7.5.4 IBSP 64
7.6 Cell visualization 65
7.6.1 Static sample vs dynamic sample 1 mL/min 65
7.6.2 Static sample vs dynamic sample 3 mL/min 66
7.6.3 Static sample vs dynamic sample 5 mL/min 68
8 Discussion 70
9 Conclusion 78
10 References 79

Abbreviations

3D Three-dimensional

ALP Alkaline phosphatase

AP1 Activator protein 1

Asc-2-P Ascorbic acid 2-phosphate

AT-MSC Adipose tissue originating MSCs

ATB Antibiotics

ATF4 Activating transcription factor 4

bFGF Basic FGF

BG Bioactive glasses

bHLH Alkaline helix-loop-helix

BM Bone marrow

BMP Bone morphogenetic protein

BSP Bone sialoprotein

C/EBP CCAAT Enhancer binding proteins co-activator core binding factor

CREB2 CAMP Response Element-Binding Protein

DBM Demineralized bone matrix

DiOC6(3) 3,3′-diethyloxacarbocyanine iodide

Dlx5 Distal-less homeobox 5

DNA Deoxyribonucleic acid

dsDNA Double-stranded deoxyribonucleic acid

ECM Extracellular matrix

EDTA Ethylenediaminetetraacetic acid

EEF1A1 Eukaryotic Translation Elongation Factor 1 Alpha 1

FBS Fetal bovine serum

FGF Fibroblast GF

GF Growth factor

GPI Glycosylphosphatidylinositol

HA Hydroxyapatite

HGF Hepatocyte growth factor

HIF-1 Hypoxia induces

Hoxa2 Homeobox protein

hMSC Human mesenchymal stem cells

HSCs Hematopoietic stem cells

IBSP Integrin-binding sialoprotein

IDO 3-dioxygenase

IGF Insulin-like Growth Factor

IFN-γ Interferon gamma

IL-β1 Interleukin

iPSCs Induced pluripotent stem cells

LCS Lacunocanalicular system

M-CSF Macrophage colony-stimulating factor

MAPK Mitogen -activated protein kinase

Mef2 Myocyte enhancer factor 2

MEM Minimum Essential Medium

MHC Major histocompatibility complex

MSC Mesenchymal stem cell

Msx 2 Msh homeobox 2

MTS 3-(4,5-dimethylthiazol-2-yl)-5-(3-carboxymethoxyphenyl)-2-(4-sulfophenyl)-2H-tetrazolium)

NF-κB Nuclear factor (NF)-kappa B

NFAT Nuclear factor of activated T cells

NK Natural killer

NPP1 Nucleotide pyrophosphatase/phosphodiesterase 1

NTP Nucleoside triphosphate

Oct4 Octamer-binding transcription factor 4

OSE2 Osteoblast specific cis-acting element

OCN Osteocalcin

Osx Osterix

PBS Phosphate buffered saline

PBT Poly (butylene terephthalate)

PCL Poly-ε-caprolactone

PDGF Platelet-derived growth factor

PEG Polyethylenglycol

PG PicoGreen

PGA Poly-glycolic acid

PGE2 Prostaglandin E2

PI Propidium iodide

PLA Poly-lactic acid

pNPP p-Nitrophenyl phosphate

PP Polypropylene

pRb Retinoblastoma protein

PS Polystyrene

RANKL Receptor Activator of Nuclear Factor Kappa B ligand

Rex1 Reduced expression transcription factor 1

RNA Ribonucleic acid

RunX2 Runt-related transcription factor 2

qPCR Quantitative polymerase chain reaction

SATB2 Special AT-rich sequence-binding protein 2

SD Standard deviation

STAT5 Signal transducer and activator of transcription 5

SVF Stromal vascular fraction

TCF/LEF1 T-cell factor/lymphoid enhancer factor

TGF-β Transforming growth factor β

TNAP Tissue-nonspecific alkaline phosphatase

TF Transcription factor

Tregs Regulatory T cells

VEGF Vascular endothelial growth factor

αSMA α-smooth muscle actin

***β*-TCP** β-tricalcium phosphate

1 Introduction

Mesenchymal stem cells (MSCs) are a multi-potent population of cells, which can be induced to differentiate into many cell types, first and foremost cells of connective tissue, by addition of appropriate signalling molecules. This property makes MSCs ideal candidates for usage in regenerative medicine and tissue engineering, where the main goal is to accelerate restoration of injured tissues and, alternatively, production of tissue replacements.

Developing homogeneous scaffolds in static culture conditions is a persisting issue in tissue engineering. Perfusion bioreactors are a tool that can be used to overcome limitations associated with oxygen and nutrient transport to cells in static cultures. They provide uniform continuous mixing and perfusion of the medium into the scaffold core, which are contained in chambers. This allows for better physical and chemical stimulation of the cells in scaffolds since the perfusion resembles the interstitial fluid flow of the bone. Mechanostimulation significantly maintains and induces the bone phenotype and should resemble *in vivo* conditions of bone growth.

The goal of my thesis is to examine three different perfusion flow rates in the bioreactor and to determine which are the ones stimulating MSCs the most to proliferate, migrate and to commit differentiation into osteoblasts on three-dimensional (3D) scaffolds for the application in bone tissue engineering. All scaffolds cultured under mechanical stimulation were compared to those that were cultured in static conditions.

This thesis consists of theoretical and experimental part. In the theoretical part I discuss first the tissue engineering principle, materials and methods. This is followed by description of bone tissue morphology and formation. MSCs, their characteristics, osteogenic differentiation and therapeutical potential, as well as their interaction with the immune system are then discussed within the framework of the bone tissue. Afterwards, properties of the perfusion bioreactors are discussed, as are the selected parameters for the perfusion. All materials used and methods performed in the experiments I described in the experimental part of the thesis. Chapter with the results of my experimental work contains numerical, graphical and photographical data. All of the results are discussed in a separate chapter.

2 Tissue engineering

The market for bone implants is growing at a rapid rate, with about 2.8 million bone repair procedures performed each year across the globe (Mailoo et al. 2019) and is expected to reach a size of $75 billion by 2023. More active population, democratization of high-risk sports, rising occurrence of bone diseases, obesity and increase in interest in owns' healthcare (Knowledge Enterprises 2006) are all factors contributing to this trend. Reparation of bones is a considerable aging-related socioeconomic burden (Clegg et al. 2013).

Bone grafts use mainly autogenous and allogenic bones. The challenge for the implant market lies, firstly, in the harvest of the graft, since harvesting autogenous bones injures the body, but also in the limitation of harvesting volume. Other possible complications of allogenic bone transplants are viral and bacterial infections, as well as immune reactions. An ideal bone substitute should not present a risk to the recipient with regards to the harvesting method, efficacy or supply limitations.

The field of tissue engineering is tremendously interdisciplinary and falls back on professionals from clinical medicine, mechanical engineering, genetics, materials science and other related sciences. It proposes the use of synthetic or naturally derived constructs enacting as templates for tissue formation, typically seeded with cells and at times stimulated by growth factors (GF) or bioreactors (Figure 1).

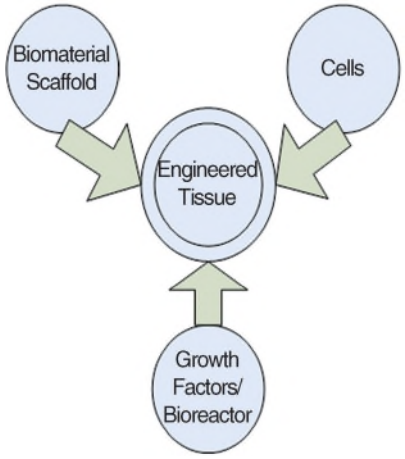

Figure 1 Cells, signals (chemical or physical) and the scaffold are the three pillars of tissue engineering. (Image from O'Brien, 2011)

Tissue engineering follows one of the two approaches, cell therapy or engineering of scaffolds, or combination of both (see Figure 2) (Kuo & Tuan 2003). Host's cells can be seeded

and cultured on the scaffold *in vitro* and subsequently implanted. Alternatively, the cells are stimulated *in vivo* to infiltrate the non-seeded implanted scaffold, differentiate and form new, fully functional tissue.

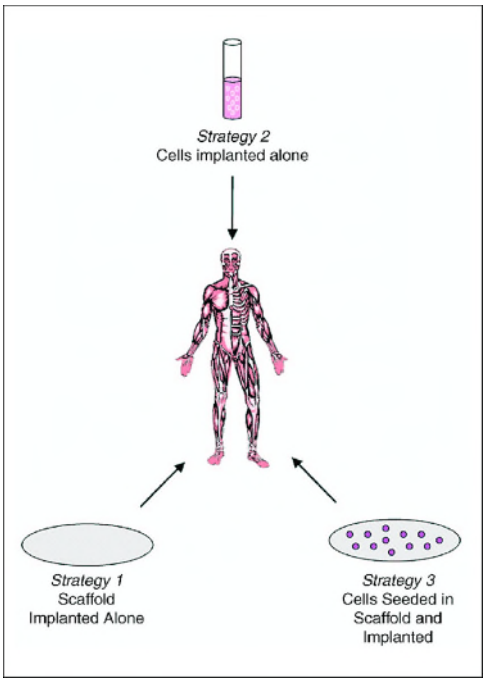

Figure 2 Three main strategies to tissue engineering. Strategy 1: To guide tissue regeneration using engineered matrices alone. Strategy 2: To inject autogenic, allogeneic, or xenogeneic cells alone. Strategy 3: To create constructs of cells placed on or within (Image from Kuo & Tuan, 2003*)*

Therefore, the concern of bone tissue engineering, regenerative medicine and cell therapy is mostly to develop an optimal artificial environment triggering a favourable response within the host tissue. This environment is accomplished by designing a scaffold that is well populated by host's cells or can be pre-colonized by adequate donor cells enhancing the process of tissue regeneration. Scaffolds are supposed to resemble not only the hierarchical structure of the extracellular matrix (ECM), but its native composition as well, which is unstable in artificial environments. Its 3D structure with an interconnected dense pore network facilitates cell and tissue growth and aids in diffusional transport of nutrients, oxygen and waste products (Kuo & Tuan 2003). The critical parameters of scaffold influencing cell behavior are its morphology, dimensionality and stability, which should respond to demands of target tissue (Li et al., 2005).

2.1 Scaffold materials

Scaffolds are distinguished by their mechanical properties which are deducted from difference in their chemical composition (Li et al., 2006) and methods of production. Materials used for tissue substitutes and scaffolds can be divided into *in vivo* stable materials and *in vivo* degrading materials, as well as naturally and synthetically derived materials. The stable materials are used in the cases, when mechanical stability is needed. On the other hand, in most of the cases of the tissue engineering applications it is advantageous to use biodegradable materials. The degradation of the scaffold should be in compliance with forming of new tissue by cells infiltrating the scaffold.

2.1.1 Non-degradable scaffold materials

One of the non-degradable stable synthetic materials is titanium. Titanium, tantalum and stainless-steel alloys are so far the most common choice for total bone replacement or implant fixations (Bose et al., 2012). Their main advantage is the inexpensive production process. They are biocompatible, corrosion resistant (Huang 2002), little immunogenic and meet the requirements for load-bearing bone utilization (Takemoto et al., 2005), even higher than in the native bone (Giannoudis et al., 2005). Due to high rigidity, metal implants cannot mechanically stimulate cells and induce their proliferation and differentiation. Even though a material containing magnesium ions was observed to degrade, a general disadvantage of metal implants is the non-degradability in the body (Bose et al., 2012).

2.1.2 Degradable scaffold materials

The following mentioned materials have shown the ability to degrade *in vivo*. First of them are ceramic materials composed of inorganic oxides and salts which exhibit a similarity with the mineral component of healthy bones, calcium phosphate. They are capable of strong bonding to osseous tissues (Stevens et al., 2008). Extensive research was mostly dedicated to calcium phosphates, hydroxyapatite (HA), β-tricalcium phosphate (β-TCP) and their composites, which are highly biocompatible (Bose et al., 2011). HA is not only similar to the bone in structure, but possesses osteoconductive properties (Kikuchi et al., 2001) improving the surrounding connective tissue, thus setting off regeneration and promoting osseointegration and osteoblast adhesion (Samavedi et al., 2013, Cunniffe et al., 2010). Ceramics on the other hand may exhibit low osteoinductivity and inappropriate resorption rates leading to a decline in mechanical

characteristics (Wang et al., 2018, Bohner, M., 2010). Natural and synthetic sources are used for commercial manufacturing of calcium phosphates, which are delivered in various physical configurations such as particles, blocks, cements, or applied as coatings to metallic implants or polymer composites. Some of the sources for production of calcium phosphates are cattle bones, corals (Guda et al., 2008), calcium carbonate and monoammonium phosphate (Verwilghen et al., 2009).

A subgroup of ceramic materials comprised of compounds with variable representation of SiO_2, Na_2O, CaO, and P_2O_5 is called bioactive glasses (BG) group. They help to dissolve a layer of HA on their own surface after implantation. HA then creates strong bonds with host's collagen fibers. Main characteristics of BGs are a high level of hardness, hence brittleness (Rahaman et al., 2011) and osteoconductivity (Wheeler et al., 1998). BGs added to poly-ε-caprolactone (PCL) and *β*-TCP were shown to be enhanced with regards to their disadvantages when alone and with regards to formation of new bone (Eqtesadi et al., 2016, Zhang et al., 2016).

One of the rare originally organic replacements, demineralized bone matrix (DBM), is made by decalcification of compact bone. The main component are collagen and non-collagenous proteins. The risk of infection and rejection by the recipient's immune system is minimized by radioactive and chemical treatment of the matrix. Growth factors of the bone are still present in the bone matrix, which take account for higher levels of osteoinduction than in regular allogenic implant (Flynn, 2011).

Material that can be divided into two groups based on the source of their origin, both displaying biocompatibility and degradability within the body (Liang et al., 2007) are polymers. Collagen, gelatin, hyaluronan, alginic acid and chitosan are found in polymers of natural origin. Commercially available synthetic polymers commonly used for biomedical applications are made of poly-α-hydroxy acids: poly-lactic acid (PLA) (Shastri et al., 2000; Zeng et al., 2003), poly-glycolic acid (PGA)(McKee et al., 2006), and their copolymers with 3-caprolactone, PCL (Ohkawa et al., 2004), and polyethylenglycol (PEG) (Shastri et al., 2000). It is important to mention that hydrolysis of certain synthetic compounds, such as PLA, may cause acidification of its' environment, which can have an impact on newly formed tissue (Athanasiou et al., 1998). Polymeric tissue-engineering scaffolds should support host-appropriate cell population and ECM component deposition precise to the tissue targeted for replacement. Bone tissue engineering uses scaffolds of both origins in abundance. Their surfaces can be chemically and physically modified

and bioactive molecules can be incorporated into scaffolds themselves in order to achieve high functionality and most suitable conditions for cells (Yoo et al., 2009).

Combining different characteristics of two or more polymers and ceramics, is a new group of materials called biocomposites. Commonly combined are HA or related calcium phosphate ceramics (biphasic calcium phosphate, β -TCP) with collagen, BGs or with PLA.

2.1.2.1 Poly-ε-caprolactone

Material used for scaffold production in this project is PCL. It was reported to be an excellent candidate for MSC transplantation and cell-based scaffold in tissue engineering (Li et al., 2005). It exhibited the most optimal structural integrity and desirable cellular response together in comparison to other four poly(α-hydroxy ester)-based fibrous scaffolds (Li et al., 2006).

Despite that non-enzymatic degradation of PCL is dominant *in vivo*, various enzymes can be a part of aliphatic polymer degradation through enzymatic hydrolysis particularly by esterases and lipases (Sivalingam et al. 2003). PCL degrades slowly by hydrolytic chain scission of the ester linkage (Kweon et al. 2003). Scaffolds based on PCL displayed ability to persist in a robust state in physiological buffer sufficiently long to allow new tissue to form and be replaced by it. They reduce physiological issues correlated to local pH changes due to acidic by-products of metabolism. All observable by-products are excreted by the completion of its degradation.

The scaffolds prepared from PCL demonstrated a considerable slow loss of its' molecular weight (up to 12 months, depending on the polymer composition) (Pitt et al., 1981) and preservation of ester and hydroxy end groups at room temperature (Ouhadi et al. 1976). This makes them favourable in mechanical support of cell proliferation and differentiation. These properties allow in turn for structurally stable connective tissue, such as bone, to be engineered (Li et al., 2005; Li et al., 2006). Thanks to its considerable degree of crystallinity and hydrophobicity, high molecular weight PCL exhibited *in vivo* a lengthy degradation time, up to 2 years (Sun et al. 2006). *In vitro* degradation rate of PCL is linear and *in vivo* this relationship seems to be exponential. It also seems to be quite independent of scaffold architecture and morphology (Bartnikowski et al. 2019).

In vivo initial reduction in molecular weight and subsequent breakdown on molecular level is followed by complete metabolization of tiny fragments (less than kDa) of polymer by cells or microorganisms (Rydz et al. 2014). Macrophages, cells from local tissue and other large cells

adhere to PCL and complete the fragmentation of structurally unstable material. The fragments are absorbed by cells (Pitt et al., 1981) and intracellular degradation occurs within 14 days (Woodward et al. 1985).

Degradation rate may be affected by local environment of the scaffolds, foreign body response, interactions with radical besides the hydrolysis type. Some studies have shown that porosity and size of fiber diameters may affect the rate of degradation of the scaffolds (Figure 3). The large surface of the scaffold resulting from high porosity could increase the hydrolysis rate. This leads to an increase in acidic by-products, however this finer porous network enhances fluid permeability diffusing them out and neutralizing the acidification (Zhang et al. 2013). In contrast, large diameter fibers have shown slower degradation rate *in vitro* (200 nm vs 700 nm), which supports degradation rate being impaired by bigger thickness of non-vowen scaffolds (Lee et al. 2014; Bölgen et al. 2012).

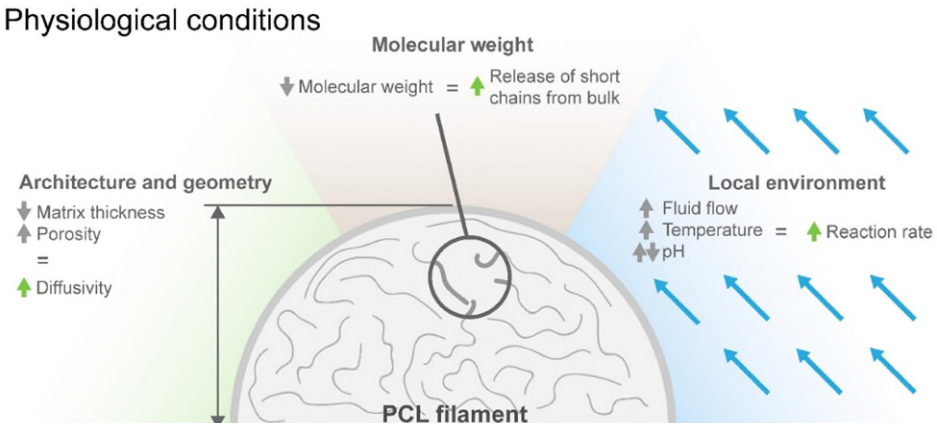

Figure 3 Graphical abstract of PCL degradation from material and environmental aspect. Physiological conditions that influence PCL degradation are the molecular weight and the architecture of the scaffold and the local environment. Image adapted from (Bartnikowski et al. 2019)

The ability of PCL constructs to upregulate gene expression and to stimulate cell proliferation was proved in a study by Li et al. (2003), which demonstrated that they are cytocompatible and can be used in maintenance of phenotypic nature. Human MSCs (hMSCs) derived from bone are able to differentiate into chondrogenic, adipogenic and lastly osteogenic lineages based on the selected culture media when seeded onto nanofibers of PCL scaffolds (Li et al. 2005). Neonatal rat MSCs were seeded on electrospun PCL scaffolds and cultured using a rotating bioreactor and after 4 weeks this lead to collagen type I deposition and matrix mineralization all through the scaffold (Shin et al. 2004). Park et al. used PCL scaffold in a 12-week study of regeneration of defects in rabbit tibia. Cells were not cultured on the scaffold prior

to insertion of PCL scaffolds into defects. New bone formation was observed at week 4. At week 12 the scaffold structure remained distinct and it appeared to guide bone tissue formation further (Park et al. 2012).

Thanks to superb properties of PCL, such as thermal stability, biocompatibility, slow rate of biodegradability by hydrolytic mechanisms, possibility of modifications, it can be employed not only in tissue engineering scaffolds, but it is used in wound dressing and targeted drug delivery systems in human medicine (J. J. Li et al. 2018; Hivechi et al., 2019; Houshyar et al. 2019). Its low melting temperature, fluctuating viscosity and versatility makes it highly appropriate to be processed via melting, for example 3D printing, electrospinning, melt-blown, and injection molding (Eshraghi & Das 2010; Correlo et al. 2005).

2.2 Scaffold categories

In order to choose the appropriate scaffold to engineer a tissue, it is important to take into consideration its final destination. The adequate scaffold needs to reflect structurally the environment in the organism where it is going to be implanted. Combinations of different materials and techniques try to accomplish this and give rise to forms such as gels, nanofibers, and porous foams.

Polymers can form networks by cross-linking hydrophilic chains to construct gels. Hydrophilicity enables extensive water absorption into the 3D network necessary for cell growth. Absorption fold can go up to 1000 times of their initial weight before dissolving (Ahmed, 2015; Chan et al. 2008) and that is why they are named hydrogels. High permeability to oxygen, nutrient and other water-soluble components (Wang et al., 2010) (Lai Y. and Baccei L. J., 1991) make them a desirable material for tissue engineering. Hydrogels promote osteoconductivity, angiogenesis, cell attachment and matrix integration and osseointegration (Li et al., 2016; Kim et al., 2007; Von See et al. 2010). ECM components, collagen and hyaluronan (Kim et al., 2007), are natural polymers behind hydrogels' low toxicity, high biocompatibility and cell adhesion. Other natural polymers that are used for hydrogel production are gelatin, agarose, chitosan and alginate (Tabriz et al., 2015). Thanks to the great elasticity of hydrogels, they are used in abundance in cartilage tissue engineering (Jin et al., 2009).

Different high-pressure gas foaming techniques aim to produce porous scaffolds that have large void spaces and surface for seeding and anchorage of cells. These techniques are dependent

on the specificity of clinical application of the scaffolds. They should remove use of organic solvent to avoid an inflammation after implantation (Thavornyutikarn et al. 2014). 45S5 Bioglass can be prepared by foaming to increase its porosity and thereby enhance its integration into the bone (Aguilar-Reyes et al. 2010). Particle leaching and textile techniques have foamed certain biodegradable polyurethane materials, which incorporate degradable aliphatic polyesters as soft segments (Q. Z. Chen 2011).

Nanofibers are another form of scaffolds that are considered to biomimic ECM filamentary architecture. Their production techniques can be split to physical synthetic routes (electrospinning, physical vapor deposition, etc.) and to chemical synthetic methods (e.g. sol-gel, electrochemical deposition, etc.). Nanofibers can be designed to have a high surface area-to-volume ratio, varying porosity and controlled degradability. It is possible to incorporate soluble chemicals or signalling molecules in fibers to enhance e.g. bone regeneration capacity (Andalib et al. 2016; Shin et al. 2004). Fibrous matrix of a PCL-based non-woven scaffold demonstrated remarkable penetration of neonatal rat mesenchymal stem cells (MSCs) implying PCL nanofiber scaffold application in bone tissue engineering (Yoshimoto et al. 2003). Nanofibrous morphology promotes mineralization process, thereby improves osteoconductivity of the scaffold (Yao et al. 2020). Furthermore, fibrous matrix system is sensitive to external and systemic cues. This sensitivity, which an organ such as the heart require, is supported by a structure based on fibrous (e. g. elastin and collagen) and adhesive proteins and proteoglycan (Parker & Ingber 2007). Moreover, such scaffolds produced by electrospinning proved to be a favourable substrate for differentiation of stem cells (Kazemnejad et al. 2009; Piryaei et al. 2010). The advantage of nanofiber scaffold lies in its nanometre range, as it is highly similar to the proportions of ECM components, which predisposes the cells to interact with it and to growth (W. J. Li et al. 2003; Dan Li and Xia 2004, Sur et al., 2015). Cells adhere and anchor onto the nanofibers and spread along the orientation of the fiber into the depth of scaffold (Mo et al. 2004), unlike in microfibers, where the cells would not proliferate and would round up (Geng, Kwon, and Jang 2005).

2.2.1 Electrospinning

Commonly used technique for polymer scaffold fabrication is electrospinning. It is considered to be economical, simple means of scaffold production from a range of polymers mimicking the structure and biological functions of the natural ECM (Huang et al. 2003). Electrospinning creates a non-vowen highly porous network of ultra-fine fibers (submicrometers or nanometers) by applying high-voltage and creating electrostatic field between two electrodes oriented against each other. Polymer solution gets then charged in the syringe needle. Thin threads of charged polymer solution from syringe needle are drawn by the force of strong electrostatic field of external source to an oppositely charged or grounded collector (Figure 4). The solution should have sufficient viscoelasticity and cohesiveness to endure threading process.

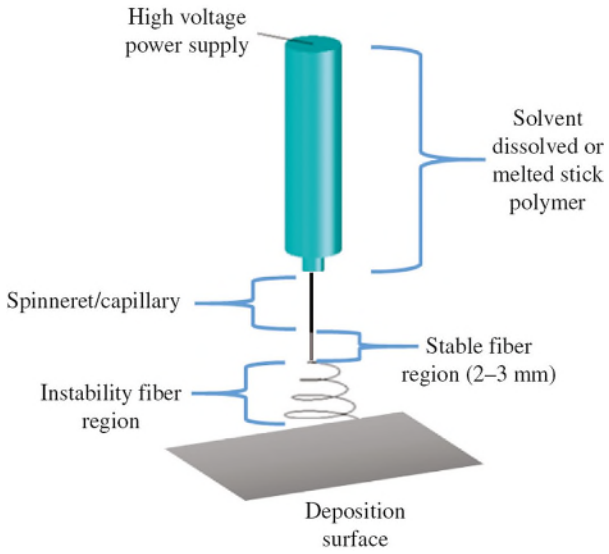

Figure 4 Illustration of electrospinning process for the preparation of nanofibers. Polymer is ejected via a syringe to the capillary. Electrostatic force created by the initiated voltage drags the polymer from the capillary tip to the deposition surface of the electrode. There are 2-3 mm of stable fiber path before the polymer jet turns into fiber and is deposited. (Image from Skinner et al., 2017)

Polymers can be dissolved in water or organic solutions. Solvent plays the biggest role in the morphology of the PCL fibers created by electrospinning. Solvent systems are various, and they include chloroform, acetic acid, formic acid, acetone and dichlormethane (Subbiah et al., 2005) or their combinations. Solvents evaporate over time. Their usage in different concentrations as well as addition of water influences the PCL to assume form of a droplet, bead, finer or larger fibers (Mochane et al. 2019).

Type and concentration of solvent selected is one of the parameters that can be adjusted to achieve variability in the morphology of the finished product of electrospinning. Other possible

adjustable parameters are electric field strength, polymer charge density, polymer molecular weight and the type of the collector.

The drawback of electrospinning is the use of organic solvents, which could be cytotoxic if not entirely cleared out (Mikos & Temenoff 2000), slow fiber production rates and high voltages required. Another limitation of this process is that is can work with conductive polymers only.

2.2.2 Melt-blown

Melt-blown is a technique used to produce the 3D fibrous scaffolds, which was used in this thesis. It is widely used in the textile industry and it was first developed in the 1950s to try trapping radioactive particles in the upper atmosphere with the submicron fibers. Not only is it a high-throughput option in comparison to electrospinning in terms of production capacity, but it also avoids high voltage usage (Ellison et al. 2007).

The process consists of polymer being melted and supplied through a die nosepiece (see Figure 5). Hot gas stream of high speed is directed onto the polymer being extruded to the blowing direction (Marla & Shambaugh 2003). The gas stream elongates the fibers onto a moving collector into particularly fine fibers of the diameter order 10^{-9} – 10^{-8} m, as the temperature of the gas is usually same as that of the molten polymer. Surrounding atmosphere at room temperature cools down the polymer jets at a distance from the nozzle exit. The resulting product is a solid non-woven which has randomly oriented fibers that is mechanically supportive and stable (Sinha-Ray et al. 2014).

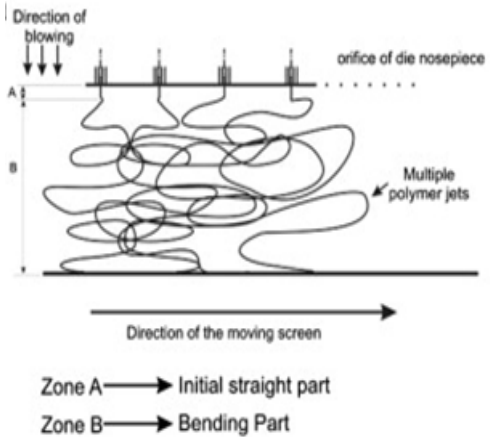

Figure 5 Schematic of the meltblowing process (Image adapted from (Sinha-Ray et al. 2013))

Factors such as speed of the collector, temperature of the hot gas, nozzles radius and polymer viscosity impact the size of the diameter of the fibers, the fiber looping on the collector, and mass distribution. It is possible to map and predict the melt-blowing process and the strength and homogeneity of the non-woven material by manipulating above-mentioned factors (Sinha-Ray et al. 2013).

A variety of polymers are used for melt-blown scaffold production and these include PCL, polypropylene (PP), polyethylene, poly(ethylene terephthalate), poly(methyl methacrylate), polyamides (e.g. nylon), poly(butylene terephthalate) (PBT), and polystyrene (PS). Even though the process seems to be independent on the polymer chemical structure, its final characteristics such as toughness, stiffness and solvent resistance are dependent on the polymer properties(Ellison et al. 2007).

Melt-blown is already utilized to produce oil sorbents (Zhao et al. 2013) and battery separators (Wang et al. 2016), filters (Deng et al. 2019). Relatively newly it is also used in bone tissue engineering for scaffolds fabrication. The melt-blown technology was also combined with electrospinning technique to achieve mechanical support of microfibers and pro-adhesive properties of nanofibers (Erben et al. 2015; Rampichová et al. 2018).

3 Bone development

The bone is the hardest among all connective tissues of the organism. After blood, it is the second most transplanted tissue in the human medicine practice. By weight, about 10-20 % of the bones is water, 60-70 % are inorganic components and the rest consists of organic components - approximately 8-10 % (Gong et al.1964). The bone is a dynamic, living tissue undergoing constant remodelling throughout life as a response to local and systemic factors (Robling et al. 2006). Its cells are productive, especially during growth. The process of growth requires cellular products, such as the growth factors, but also the blood supply and hormones, which are provided by vascular tissue. Bone growth is determined mainly by the bone-forming cells osteoblast and bone resorbing osteoclasts. Apart from the above-mentioned cells, osteoprogenitor cells and osteocytes are also found within bone tissue.

There are two processes that are responsible for bone development. The first is intramembranous ossification and it is responsible for formation of flat bones, such as bones of the skull. Here the MSC differentiate into osteoblasts directly to form the bone. The other process is endochondral ossification by which bones are regenerated and long bones, e.g. skull base, are formed. Here MSCs first form cartilage which is then replaced by bone. However, the final structural arrangement is not much different between the bone types and they share general chemical and structural features (Gamsjaeger et al. 2010). Apart from long and flat bones, there are short, sesamoid and irregular bones. Different parts of the bone grow at a different rate due to, diverse bone pressure direction, distribution and other factors. New bone is deposited under the periosteum in the form of circumferential lamellae.

Genetic and environmental factors, hormonal equilibrium, nutrition and mechanical factors influence bone growth (Aerssens et al. 1997; Fratzl et al. 2004). It stops in humans naturally around 18 years of age in females and 21 years in males. Nonetheless, bone remodelling continues throughout adulthood. It serves to repair damages from bone loading or to adapt to loading and metabolic changes. 2%-5% of cortical bone is being remodelled each year, whereas it is about 25% for trabecular bone due to much larger surface to volume ratio (Hadjidakis & Androulakis 2006a).

3.1 Bone tissue characterization

The organic component of a healthy bone consists of bone cells and ECM proteins, while the inorganic component consists of diverse minerals, mainly HA. HA provides structural rigidity

and compression strength, while ECM protein collagen gives bone flexibility and toughness, which prevent brittle cracking and improve tensile properties. In combination, they provide outstanding tensile strength and fracture resistance (Fratzl et al. 2004; Rho et al. 1998).

Hard outer shell that surrounds the bone marrow in long bones, is made of cortical bone. It mainly has as a mechanical function and is thick and dense. This is the area of the bone to which tendons and ligaments are attached. Sponge-resembling trabecular or cancellous bone fills cavities of epiphysis and other end bone regions. Trabecular bone is about 50-95 % more porous in comparison to cortical bone of 5-10 % (Cardoso et al. 2013; Doblaré et al.2004). It has mainly a metabolic function. It is found between layers of cortical bone and is exposed to the bone marrow and a higher turnover of blood flow than the cortical bone.

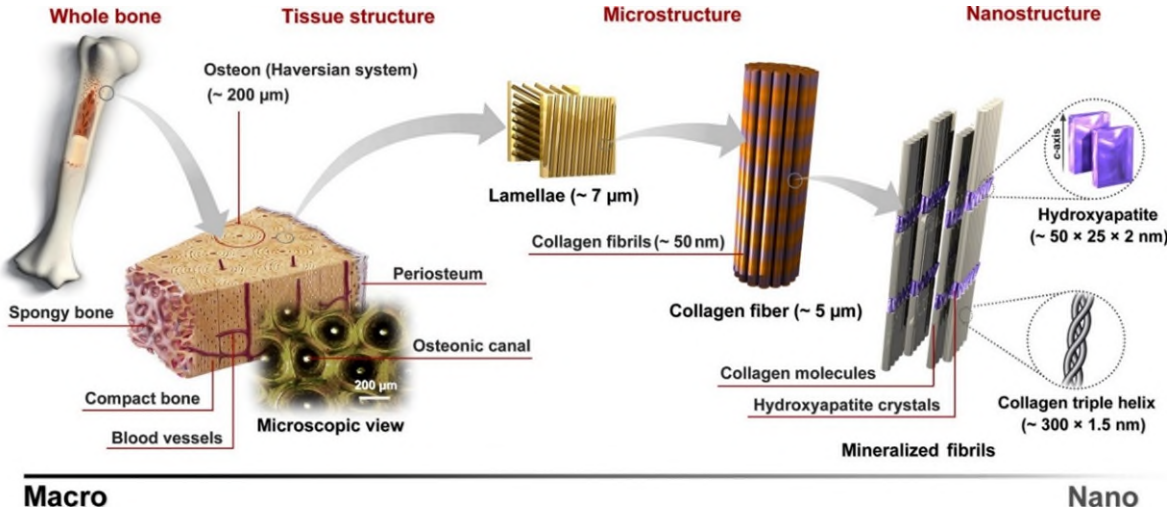

Figure 6 Hierarchical structure of a typical bone shown with size scale. Microstructures are Haversian canal, osteon, lamellae. Nanostructures are hydroxyapatite and collagen triple-helix fibrils. Image from (Sadat-Shojai et al. 2013)

The main compact bone structural unit in humans is the osteon. Its diameter ranges from 50-300 µm and it has a length of several millimetres. It runs lengthwise down the axis of long bones. The osteon is composed of central Haversian canal ringed by concentric lamellae, the mineralized matrix fibers. Neighbouring osteons are linked via perpendicular Volkmann's canals joined to capillaries and nerves of Haversian system (see Figure 6). Osteons that were once pushed out and replaced during remodelling are the interstitial lamellae. Individual protein fibers, lamellae, can be composed in a parallel manner, e.g. in trabecular bone and periosteum, or in a concentric manner, e.g. in cortical bones that have Haversian canal in the middle.

3.2 Bone cells

The internal structure of bones is continuously being changed by bone cells in order to maintain its functionality. Bone cells are osteoblasts, osteocytes, osteoclasts and bone lining cells.

3.2.1 Osteoblasts

Osteoblasts are a single-row of cuboidal-shaped cells predominantly found along the endosteum, which is generally a one-cell layer coating internal surfaces of the bones. This is where the bone formation is active. The intercellular contact and communication are done via adherence and gap junctions. Occasionally, they seem to have cytoplasmic processes towards the bone matrix, through which osteocyte processes are contacted (Capulli et al. 2014). Thanks to morphological characteristics of osteoblasts, including extensive rough endoplasmic reticulum, extrusive Golgi apparatus and plenty of secretory vesicles they can synthesize large amounts of ECM proteins (Capulli, Paone, and Rucci 2014). During ECM secretion osteoblasts can wrap themselves with ECM in empty spaces called lacunae and become osteocytes. These cells are linked to Haversian system via extensions of the cytoplasm that run through canaliculi, which are tiny interconnecting canals (Akter and Ibanez 2016).

Osteoblasts are derived from bone marrow MSCs committed towards osteoprogenitor lineage (Abdallah & Kassem 2007). They arise perinatally during foetal development and persist in the adult bone marrow making 4-6 % of the overall resident cells of the bone (Capulli et al. 2014). Osteogenic differentiation is described in the chapter 3.2.2.5 below.

3.2.1.1 Osteogenic transcription factors

Formation and regeneration of any tissue is coupled with relatively specific molecules that ensure precise course of all events. For this purpose, hormones and cytokines act as regulators together with growth and transcription factors (TFs). TFs are proteins that have a DNA-binding domain that ensures their targeted localization on a DNA sequence and, thus, regulation of transcription (Karin 1990). The activity of TFs is regulated in different ways. Some proteins can bind to their gene promotors, thereby, influencing their chromatin structure or they can get modified post-translationally.

Key master TFs which control proper maturation and osteoblast function are RunX2 and Osterix. Distal-less homeobox 5 (Dlx5), c-fos and Msh homeobox 2 (Msx2) are involved in

regulation of this process as well (Kirkham et al. 2012). All of these TFs lead to expression of bone tissue specific genes like collagen type I, osteopontine, osteocalcin, BSP and ALP, which are.

3.2.1.1.1 RunX2

RunX2 (also called Osf2) is a TF also known as core-binding factor alpha-1 (Cbfa-1). On a molecular level, RunX2 function is facilitated via its localization on the consensus sequence PuACCPuCA (e.g. or TGTGGT), also known as osteoblast specific *cis*-acting element (OSE2) (Marie 2008). OSE2 is present in promotors of all major genes leading to osteoblast phenotype manifestation. It belongs to runt family of TFs, which is characterized by being built of different α subunits and always same β subunit (Marie 2008; James 2013). In order for Runx2 to enhance DNA binding affinity it must create a heterodimer with transcription co-activator core binding factor (Cbfβ) (Nagata et al. 1999). The Runt family of proteins regulate diverse cell processes. Runt-related TF 2 (RunX2) can be activated by a plethora of signalling pathways, such as transforming growth factor β (TGF-β), BMP and Wingless (Wnt) (James 2013), as well as mitogen-activated protein kinase (MAPK) phosphorylation. MAPK kinase gets activated after collagen type I binds to α1β2 integrins on the osteoblast surface (Guozhi Xiao et al. 2000). Hormone regulation of RunX2 is executed via growth hormone, parathormone, vitamin D and oestrogens (Marie 2008).

RunX2 is crucial in the beginning of osteoblastogenesis of MSCs and it remains present during differentiation (Marie 2008). In later stages of osteoblast development, RunX2 dims down their proliferation and terminal differentiation. The level of ECM deposited by osteoblasts is regulated by RunX2 as well, as RunX2 has a role in maintenance in already differentiated osteoblasts.

Expression and activity of RunX2 is tightly regulated on several levels because it has an extremely important role in osteogenesis. DNA-protein and protein-protein interactions and other TFs are the tools used for this regulation. A prominent negative regulator of RunX2 expression is Hoxa2, a homeobox protein that belongs to Hox TF family (Dobreva et al. 2006). Hoxa2 expression is repressed by nuclear matrix protein Special AT-rich Binding 2 (SATB2) which also physically interacts with RunX2 and enhances its DNA binding. Both events lead to RunX2-dependent osteoblast differentiation (X. Huang et al. 2020). Other TFs that repress osteogenic

differentiation are Stat1, Sox8, Sox9 or p53 (Marie 2008). Stat1 binds the cytoplasmic RunX2, thereby lowering its nuclear concentration. On the other hand, there are proteins that enhance RunX2 expression. Some examples are retinoblastoma protein pRb, transacylase protein tafazzin and Hoxa10. Tafazzin also has a specific domain which directly interacts with RunX2 and acts as its co-activator. Another important regulator of RunX2 activity is the synergistic interaction with Smad proteins. These proteins are involved in signalling TGF-β pathway. RunX2 can also interact with factors such as p300/creb binding protein, that has a histone acetyl transferase activity (Westendorf 2006). This enables tight control of transcriptional activity through arrangement of acetylated and deacetylated chromatin. Moreover, proper function of Run X2 is controlled from stability point of view, through interaction of Smur1 ubiqutin ligase and C-terminus of Runx2 which leads to its degradation in proteasome (M. Zhao et al. 2004).

3.2.1.1.2 Osterix

Osterix (Osx or Sp7) is a zinc finger-containing osteoblast-specific nuclear TF. The zinc finger is located in its C-terminus. Osx function is to regulate expression of markers in late osteoblastogenesis and to direct pre-osteoblasts' maturation and bone mineralization (Nakashima et al. 2002) through induction of mature osteoblast genes such as collagen type I, osteonectin, osteocalcin, osteopontin and BSP (Figure 7). It is found, however, not only in osteoblast-lineage cells, but also in chondrocytes and is overexpressed in breast cancer and other cancer tissues (Qu et al. 2019). It has been recognized that RunX2 functions upstream of Osx. BMP-2 activates RunX2 via Smad signalling, and RunX2 binds to Osx promoter and upregulates it (Pérez-Campo et al. 2016). Ia positive loop Osx regulation RunX2 too indirectly, as it can form an enhanceosome with Dlx5 and myocyte enhancer factor 2 (Mef2) (Kawane et al. 2014). Osx transcription can be also regulated independently of RunX2, which was shown in RunX2 deficient MSCs. In this case, BMP-2 indirectly regulates Osx transcription, via other proteins such as Dlx, p38 or Msx2 (Liu et al. 2020).

It is not absolutely clear how Osx works. It interacts with nuclear factor of activated T cells (NFAT) and TF-IIB, which affects chromatin re-arrangement (Kirkham et al. 2012). It seems that RNA helicase A forms a complex with Osx, which could be a way to further regulate osteoblasts. Activity of Osx is most probably modulated also by post-translation modifications, such as glycosylation or phosphorylation (Chu & Ferro 2005).

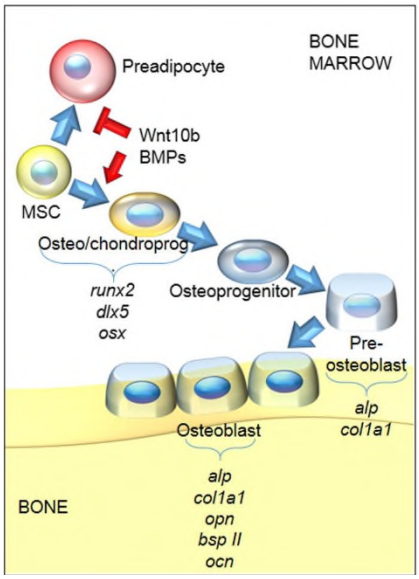

Figure 7 The basic criteria of the osteo/chondroprogenitor cells are defined when at least the following osteoblast-specific transcription factors are expressed: Runt-related transcription factor 2 (RunX2), Distal-less homeobox 5 (Dlx5) and Osterix (Osx)(Image adapted from Capulli et al. 2014)

3.2.1.1.3 Dlx5 and Msx2

Members of homeobox protein family, Dlx5 and Msx2, play a role in osteoblast differentiation (Marie 2008; H. Zhang et al. 1997). They are able to form heterodimers, cooperate and act as antagonists, activators or repressors. They are expressed at different stages of bone cell maturation. The presence of Dlx5 is constant in developing skeleton and its concentration rises in late stages of mature osteoblasts. It promotes osteogenesis under BMP control (Han et al. 2011). Its high concentration activates RunX2 and BSP transcription. It is unclear if osteocalcin (OCN) expression is positively or negatively influenced by Dlx5 or both; Msx2 may be associating with OCN promoter temporarily in osteoprogenitor cells repressing its activity. It represses collagen type I transcription too. On the other hand, when Dlx5 and RunX2 associate with OCN promoter in osteoblasts after the proliferation period they act as transcription enhancers (Hassan et al. 2004).

3.2.1.1.4 Id-protein family

Id-protein family is named after their function, to inhibit the DNA by binding to it. Id proteins impact BMP-induced osteoblast differentiation by dimerizing with bHLH – alkaline helix-loop-helix family of proteins (Williams et al. 2011). bHLH regulate cell development and differentiation by binding the so called E-box, which is a DNA-binding element (Lasorella et al. 2014). When Id proteins are absent, as during the terminal differentiation of committed osteoblasts,

the bHLH are bound to E-box and this induces expression of genes leading to cell cycle arrest and differentiation. If the Id proteins are present, in early osteoblast progenitor cells upon BMP9 stimulation, nuclear bHLH proteins are bound to them and the cell is free to proliferate (Peng et al. 2004). Tumours arise if this signalling is dysregulated. Id protein activity is regulated via ubiquitination.

3.2.1.1.5 Other TFs

Apart from the TFs mentioned above, following TFs are involved in osteogenesis regulation as well: AP1, ATF4, CCAAT/enhancer binding proteins (C/EBP) and peroxisome proliferator-activated receptor (PPARγ).

ATF4, known also as cAMP Response Element-Binding Protein (CREB2), interacts with RunX2 and thereby controls transcription activity of OCN. Posttranslational modifications regulate ATF4 by phosphorylation by Rsk2 kinase and this influences the ability of this TF to regulate transport amino acids into osteoblasts (Yang et al. 2004). CREB2 is also involved in regulation of Jun and Fos proteins by kinase A (Kirkham et al. 2012).

PPARγ steroid receptors are activated by non-saturated fatty acids (Ali et al. 2005). Their main role is to induce MSC adipogenesis, however they are involved in bone development as well. If a ligand binds to PPARγ, the expression of RunX2 and Osx is repressed. Nuclear membrane expression of PPARγ is reduced due to the activity of parathyroid hormone and vitamin D (Marie 2008). If adipogenetic signalisation prevails, bone mass may be reduced or lost.

Proteins Jun and Fos create a heterodimer which makes the TF AP1 (Marie 2008). It is involved in the fate of osteoblasts on many levels - commencing their differentiation, modulating them and thereby impacting proliferation and gene expression.

C/EBP control expression and activity of GFs specific for osteogenesis and GF receptors (Dhawan et al. 2005). The program of adipocyte differentiation is sequentially regulated by C/EBP as well. A synergistic relationship between Runx2 and C/EBP-β for osteoblastogenesis by binding to RunX2 promoter was observed (Henriquez et al. 2011). They induce OCN gene expression and ALP activity (Shirakawa et al. 2006).

3.2.1.2 Growth factors in MSC osteogenesis

Growth factors are polypeptide signal biomolecules, that bind to cell surface receptors to induce signalling, usually via signal cascades with purpose of expression of specific proteins and

formation of a specific tissue. That is how GFs have an impact on cell proliferation, differentiation, maturation, and also production of other GFs. Unlike hormones that act systemically, they only have a local effect and are secreted in low concentrations.

In induction of osteogenic differentiation widely used and investigated are GFs from TGF-β superfamily. Included in osteogenic differentiation are also Insulin-like Growth Factor (IGF), fibroblast GF (FGF), vascular endothelial GF (VEGF) and platelet-derived GF (PDGF) (Devescovi et al. 2008). They mutually influence each other and are produced in different cell cycle stages alone or together, in order to achieve the most precise effect in osteogenic induction. *In vitro* VEGF and IGF-1 were shown to be produced mainly during proliferation, and FGF-2 and BMP-2 were produced in cell differentiation and maturation (Dramowski et al. 2021).

3.2.1.2.1 TGF-β superfamily

GFs from the diverse TGF-beta superfamily are involved in bone healing and both types of ossification (Gerstenfeld et al. 2003). They ensure MSC proliferation, differentiation, and their chemotaxis. In mammals, this superfamily can be further divided to subfamilies TGF-β, activin/inhibin/nodal, and BMP, with similar but non-overlapping physiological functions (Chen et al. 2012; Shi & Massagué 2003).

TGF-β can be present in four isoforms, during bone healing and regeneration - TGF-β1, TGF-β2, TGF-β3 and TGF-β4(Rosier, O'Keefe, and Hicks 1998). Cells such as macrophages, MSCs, thrombocytes and some other types produce a pre-cursor of the GF, which then requires proteolytic cleavage (Yusuf et al. 2016; Massagué, Attisano, and Wrana 1994).In order to obtain the active form of the GF, they form dimers. TGF-β expression level is dependent on the amount of ECM protein collagen type I and II. Collagen type II decreases TGF-β1 expression, whereas collagen type I increases TGF-β1 expression (Bosnakovski et al. 2006). TGF-β restricts resorption of bone mass, by decreasing production of receptor activator of nuclear factor kappa-B ligand (RANKL), a differentiation factor of osteoclasts. This leads to bone formation to prevail (Vater et al. 2011). Another function of TGF-β1 is to activate osteoblast progenitors and stimulate it for early differentiation and ECM protein production. It increases RunX2 expression *in vivo* and decreases PPARγ expression (Cao and Chen 2005). In bone healing, it plays a role in supporting MSCs to migrate to the injured site so they can proliferate and differentiate (Jose A. Andrades 2013). BMP-2 effect is also potentiated by TGF-β1 (Chen et al. 2012).

Same as TGF-β, BMP, a diverse class of GFs, is also closely related to skeleton formation during organism development (Katz et al. 2009; Kim et al. 2013). Around 30 isoforms of BMPs are identified, but only a few of those are related to osteogenic differentiation. Those are BMP-4, -5, -6, -7 (Andrades 2013) and most importantly BMP-2. Production of osteoblast differentiation markers, e.g. OCN and increase in mineral deposition is dependent on BMP expression (Noël et al. 2004). BMP-2 induces irreversible osteogenic differentiation even after exposing cells to it for a short time. Together with BMP-4 they act as critical factors in proliferation and maturation of chondrocytes in process of endochondral ossification. BMP-2 is released by MSCs, osteoblasts and chondrocytes *in vivo* (Andrades 2013). In bone healing the concentration of BMP-2 peaks 24 hours after injury, which implies that it is involved in early phases of healing and probably controls the expression of other BMPs. Isoforms BMP-3 and BMP-4 appear during ECM mineralization, which is weeks after BMP-2 (Andrades et al. 2009).

Signalization via GFs from TGF-β superfamily operates via other biomolecules too, such as noggin, Smad proteins, etc., and they mutually influence each other in different signalling pathways.

3.2.1.2.2 Other GFs

Besides TGF-β there are other GFs that are involved in regulation of osteogenesis. One of them is hepatocyte growth factor (HGF), which regulates cell growth, movement and morphogenesis via activated tyrosine kinase. It is involved in angiogenesis, tumorigenesis and tissue regeneration (Jia et al. 2013). Aenlle et al. (2014) have shown in their study that HGF supports hMSC osteogenic differentiation by activating transcription of OCN, osteoprotegerin and Osx. Also, HGF is an indispensable molecule in ECM mineralization.

Since the bone is abundantly vascularized, in order to maintain proper process of MSC osteogenic differentiation, the presence of VEGF is absolutely essential. It regulates the formation of new blood vessels (Shibuya 2006). In osteogenesis, it has a supportive function in survival of osteoprogenitor cells and a chemotactic function in attracting main bone forming cells (Kempen et al. 2009).

Key regulator of osteoblast maturation is FGF (Jackson et al. 2006). Basic FGF (bFGF) or FGF-2 regulates proliferation, differentiation and the extent to which bone cells mineralize (Z. Huang et al. 2010). It protects osteoblasts against apoptosis. FGF-9 and -18 act at each stage of

osteoblast proliferation as well as the FGF-2 (Jackson et al. 2006). FGF-1 is involved in the process of endochondral ossification (Schindeler et al. 2008).

In high concentrations the PDGF is a potent osteoinductive factor (Davies et al. 2018) as it induces mineralization, proliferation and thereby differentiation of hMSCs (Pountos et al. 2010). It induces mitosis of cells of mesenchymal and neuro-ectodermal origin (Ross et al. 1990).

Experiments in IGF-deficient mice or sporadically present IGF in tissues showed delayed embryonal skeleton development, low bone mineralization levels and prolonged healing of bone fractures (Y. Wang et al. 2006). In humans, it was shown too that IGF concentration corelates positively with bone mineralization levels and negatively with the frequency of bone fractures (Langlois et al. 1998). Stem cells isolated from the tip of the tooth root showed increased proliferation, ALP activity and mineralization under IGF-1 influence (Wang et al. 2012).

3.2.2 Human mesenchymal stem cells

Individual types of stem cells are distinct in their differentiation potential. Totipotent cells have the highest differentiation potential, as they can create embryonic and extraembryonic tissues. These cells are zygotes. Lower level of pluripotency is the ability to differentiate into cells of the three germinal layers. Next are multipotent stem cells that differentiate only into the cell types of only one germinal layer from which the cells originate. Lastly, there are unipotent cells that are able to differentiate into only one cell type. It is worth mentioning induced pluripotent stem cells (iPSCs) that do not appear naturally in the organism. To obtain iPSCs it is necessary to artificially re-program non-stem somatic cell and force it to express genes and factors needed to temporarily have the characteristics of embryonic stem cells. iPSCs are used in *in vitro* experimental level.

MSCs belong to a group of multipotent cells and one of their main characteristics is the ability of self-renewal. They can also differentiate into various cell types (Dominici et al. 2006) and be responsible for regeneration of damaged tissues (Weissman 2000). MSCs are not specialized and can be inactive for long periods of time. If a need arises, they can start to proliferate and differentiate. If the tissue is damaged, it releases molecules that serve as MSCs activity stimulating factors. Thus, upon stem cell division they either self-renew and maintain multipotency or they become a pre-cursor for a specialized cell type. On top of these features, what makes these cells an excellent candidate to use in cell and gene therapy and in treatment of certain cancer types or autoimmune disorders is relatively simple harvest and isolation process.

Being multipotent, MSCs can give rise to whole series of mesoderm originating tissues and because of that they can be isolated from plethora of tissues (Prockop 1997; Pittenger et al. 1999; Kolf et al.2007)(Kolf, Cho, and Tuan 2007). MSCs can be isolated from various tissues such as the traditional bone marrow, then adipose tissue, dental and perinatal tissues, skin, foreskin, salivary gland, limb buds and menstrual blood. The most common method of isolation is based on the ability of the MSCs to selectively adhere to plastic surfaces and it involves using tissue mincing, optional enzymatic digestion and cell outgrowth on plastic (Mushahary et al. 2018).

3.2.2.1 Characteristics

MSCs are spindle-shaped fibroblast-like cells whose dimensions are in the order of micrometres depending on the cell cycle phase (Bruder et al. 1997). They are not much significantly different from other cell types in shape or size. Typical location in the organism for this population of stem cell is not yet clearly defined. In comparison to other cell types, there is no single surface antigen that would be explicitly expressed on MSC cell membrane. However, it is necessary, for therapeutic and experimental purposes, to define the properties based on which it will be determined whether the cells are MSCs. That is why The International Society for Cellular Therapy, established in 1992, formulated in 2006 the three criteria that cells must fulfil in order to be considered as 'mesenchymal stem cells'. The criteria consist of the cells being able to 1. adhere to plastic *in vitro*, 2. express surface antigens CD73, CD90 a CD105 while at the same time not expressing surface antigens CD45, CD14, CD34, CD11b, CD79αa or CD19 and 3. differentiate *in vitro* to adipogenic, osteogenic and chondrogenic lineages. Surface antigen of cells of immune system, hematopoietic cell line and cells of endothelium should not be present on the surface of MSCs (Dominici et al. 2006). Standard culturing conditions include minimal growth medium with 10% FBS.

Stro-1 is a marker that can be used to identify MSCs, however it is not present exclusively on their surface. Cells not expressing Stro-1 are unable to form colonies and cannot give rise to hematopoietic-supportive stromal cells (Simmons and Torok-Storb 1991), which is in fact one of the main functions of MSCs in the organism (Kolf, Cho, and Tuan 2007). Beside the above-mentioned surface antigens, the following markers are also expressed by MSCs: CD271/NGFR, CD90/Thy-1, CD106, CD44, CD13, Flk-1/CD309, CD29, Sca-1 a CD10 (Kolf, Cho, and Tuan

2007; Quirici et al. 2002). These markers nonetheless are not expressed consistently or are not specific and should be combined with other means of cell population characterization.

3.2.2.2 Niche

MSCs are found in a microenvironment, the so-called niche. The niche has all the factors immediately surrounding the MSCs. The function of the factors is to keep the cells in a state of naivety and in case of damage to stimulate them to migrate and differentiate (Kolf et al. 2007; Schofield 1978). This surrounding includes proteins of ECM, non-stem cells, that have specific surface antigens providing intercellular contact, and all dissolved substances and signal molecules, which warn stem cells where are they needed. Niche is also supposed to protect stem cells from accumulation of genetic mutations that could lead to tumour development. This is done, amongst other, by regulating the balance between symmetrical and asymmetric cell division which preserves optimal cell number necessary to repair surrounding damaged tissue. Deregulation in the niche environment has the main impact on the rise of pathological conditions as tumorigenesis and different degenerative diseases (Gattazzo et al. 2014).

Protein components of ECM create dynamically evolving 3D network and provide specific structural and biomechanical properties of the niche thanks to their diversity. Transmembrane proteins called integrins are for the most part responsible for the interaction between cells and ECM proteins (Legate et al. 2009). ECM proteins may be beneficial for lineage specification of certain sources of MSCs in terms of fabrication of scaffolds for therapeutic application of MSCs (Wang et al. 2013). However, no ECM component typical for MSC niche was yet discovered that would help to maintain the cells in their naïve state *ex vivo* (Kolf et al. 2007).

The last component of the niche are the cells themselves and the molecules expressed on their surfaces. Since α-smooth muscle actin (αSMA) was detected on hMSCs isolated from different tissues, perivascular localization of MSC niche was proposed (Kiel et al. 2005). Expression of Stro-1 and CD46 on MSCs, antigens associated with vascular tissue, was confirmed as well (Shi & Gronthos 2003). Perivascular niche localization would be convenient with regards to effective and fast transport of stem cells via blood vessels to any site where they are needed in the organism. However, majority of the researchers agree that the endosteum is a niche mostly for restricted hematopoietic progenitor lineage and that niches of hematopoietic stem cells (HSCs) are close to the sinusoids – perisinusoidal (Comazzetto et al. 2021).

3.2.2.3 Source tissues of MSCs

The origin of MSCs is substantial in research. They are commonly isolated from bone marrow of many mammalian model organisms (Otsuru et al. 2013) and other tissues of mesodermal origin, such as adipose tissue (Ghorbani et al. 2014). Different sources vary in difficulty of isolation and the quantity needed of the cells available for isolation, and they vary in cells' immunomodulatory or differentiation potential. Cells coming from different sources differ also genetically and production of different cytokines and chemokines (Wagner et al. 2005). The basic distinction is between foetal and adult source tissues. Ontogenetically most primitive populations of MSCs are isolated from tissues of organism that are in prenatal developmental phase and these cells have the most diverse therapeutical use (Wang et al. 2004). As a general rule, factors such as the age, sex, fitness, diet and, if applicable, the medication regime of the cell donor influences the capacity of the isolated MSCs to differentiate and proliferate.

Foetal tissue that contains MSCs is the so-called Wharton's jelly of the umbilical cord – jelly-like mass surrounding umbilical cord blood vessels, then umbilical cord blood, chorion, amnion and amniotic fluid (Kobolak et al. 2016). The main advantage of foetal tissues is that they are easily accessible, thus avoiding invasive isolation methods and ethical limitations. Umbilical cord is the most common MSC foetal source. It is removed after birth and frozen in order to be MSCs the HSCs, the colony-forming endothelial precursors. After extraction *ex vivo* expansion is needed to increase the cell number to achieve a dose needed for clinical indication (Hass et al. 2011; Otsuru et al. 2013).

MSCs derived from the bone marrow are a traditional source of MSCs for research and clinical applications. They are, however, low in abundance, and to obtain sufficient amounts of these cells it is necessary to culture them *in vitro* extensively and to expand them (Quirici et al. 2002). They are easy to isolate from the bone marrow, thus avoiding immunological issues. Their expansion in vitro can be done relatively quickly, and it is possible to preserve them not affecting greatly their potency. No serious side effects were reported during autologous or allogenic therapy (Bhat et al. 2021).

To the bone marrow, peripheral blood and adipose tissue are adult MSC-containing tissues conventionally used. In addition to these, isolation from cartilage, dental pulp, liver, kidneys, neural tissue, lungs, spleen, skeletal muscles, stroma of thymus and spleen, synovium and ligaments was described (Kobolak et al. 2016). A rich source of MSCs is adipose tissue. To

separate adipocytes from the adipose tissue-derived stromal vascular fraction (SVF) cell suspension is centrifuged after mechanical and enzymatic tissue breakdown. MSCs are obtained by washing away non-adherent cells after seeding of SVF on the dish. This is a quite simple isolation protocol, where from 1 gram of fatty tissue 5000 MSCs can be obtained, which is about 500× more than the isolation yield from the bone marrow (Pittenger et al. 1999). If isolation procedures from bone marrow and adipose tissue are compared, the extraction of fatty tissue is seen as less invasive, less painful and less risky while providing a reasonable amount of MSCs. However, these isolated cells from adipose tissue have shown a limited differential potential and from therapeutic standpoint their use is less advantageous (Kolf et al. 2007). A topic of discussion are also cells isolated from dental pulp. They may be highly proliferative and capable of pluripotent differentiation into many different tissue types, are less immunogenic and could substitute umbilical cord MSCs in stem cell banking. They reside within the perivascular niche of the dental pulp and are easily accessible especially during the replacement process of deciduous teeth with permanent ones. This process does not spike ethical controversy although much remains to be discovered (Hass et al. 2011, Miura et al. 2003).

3.2.2.4 Immune system interaction

One of the characteristics of MSCs is to interact with the immune system and modulate its response (Corcione et al. 2006). Thanks to this attribute, MSCs *in vivo* support their self-renewal, proliferation, differentiation. MSCs show low immunogenicity, because they lack expression of major histocompatibility complex (MHC) II glycoprotein family under normal circumstances and co-stimulatory molecules CD40, CD80 and CD86 and also because expression of MHC I is decreased. Not even differentiated MSCs express MHC II class nor do they induce lymphocyte alloreactivity (Fernández Vallone et al. 2013; Nauta & Fibbe 2007). This makes them a candidate for use in cell therapy of autoimmune diseases, graft-versus-host disease and to induce and maintain graft tolerance. *In vivo*, they are involved, for example, in the induction of peripheral tolerance or in pregnancy in tolerance mother-foetus (Nauta & Fibbe 2007). Microenvironment in the niche, local function of the cells or ontogenetic age could affect the differences in MSC immunological properties, however most of the data shows that MSCs differ only slightly. It is worth mentioning that originating MSCs have a slightly increased ability to supress immune reactions in comparison to bone marrow MSCs (Mattar & Bieback 2015) and that liver-derived

MSCs are superior in immunomodulation over adipose tissue MSCs and bone marrow MSCs (Taner et al. 2020, Yigitbilek et al. 2021).

MSCs can influence naïve, but also CD4+ and CD8+ cells independently on MHC glycoproteins. Influence is induced via allogeneic cells amongst other. Influenced cells have a lower expression of cycline D2 and higher expression of p27 protein. This arrests T lymphocytes in the cell cycle and prevents their accumulation in G0/G1 phase of the cell cycle (Shi et al. 2011). In foetal abortion models, MSCs have demonstrated to boost the suppressive regulation of T cells and macrophages (Li et al. 2019). Instead of influencing their maturation, cytokine production or cytolytic activity, MSCs suppress their proliferation. Process leading to suppression of T cell inflammatory response is triggered by direct intercellular contact and cell exposure to proinflammatory cytokines (e.g., interferon gamma (IFN-γ) and interleukin (IL)-β1) (Li et al. 2019; Nauta & Fibbe 2007). Molecules that are secreted by MSCs during immunosuppression and could be associated with modulation of the T cell response are TFG-β, HGF, indoleamine 2,3-dioxygenase (IDO) and prostaglandin E2, among many others (Li & Hua 2017). The mechanism of their action is not clear, however, their presence leads to inhibition of translocation of nuclear factor (NF)-kappa B complex to the nucleus and subsequently to suppression of T cell proliferation (Li & Ikehara 2013).

MSCs demonstrate the production of nitric oxide after migration to the site of injury, which inhibits the transcription factor signal transducer and activator of transcription 5 (STAT5) phosphorylation, STAT5 role is essential for T cell activation and proliferation. In addition to suppressing T cell proliferation, MSCs can also induce their apoptosis. A small amount of MSCs accumulates in secondary lymphatic organs, where it suppresses the delayed hypersensitivity response by inducing apoptosis of activated T cells (Mattar & Bieback 2015).

MSCs suppresses cell proliferation and secretion of IFN-γ by other components of cellular immunity as well, such as activated natural killer (NK) cells. Prostaglandin E2 (PGE2) (Dhingra et al. 2013) and to a lesser extent TGF-β1 and IDO (Meisel et al. 2004) are thought to play a role in this process. It has also been found that MSCs can suppress the cytotoxic action of NK cells against MHC I-expressing cells much more effectively than against MHC I-deficient cells. This is a phenomenon that, among other things, probably helps to protect the body's own tissues from the immune system (Fernández Vallone et al. 2013; M. Li & Ikehara 2013).

Dendritic cell are another component of immune systems and their function, e.g. their response to maturation signals, is disrupted by MSCs in several ways. Disruption of maturation leads to inhibition of their differentiation to cells that show an inhibitory or suppressing phenotype. Furthermore, the expression of co-stimulatory molecules is reduced and their ability to stimulate naïve T cells to proliferate and secrete proinflammatory IL-12 is negatively regulated. IL-6, macrophage colony-stimulating factor (M-CSF) and PGE2 produced by MSCs are involved in the above mentioned effects (Li & Ikehara 2013).

B cells are another component of humoral immunity, that can be affected by MSCs via physical contact and soluble molecules inducing the same effect as in T cells - cell division is arrested in the G0/G1 phase of the cell cycle. Proliferation is inhibited when cells are exposed to anti-CD40 ligand and IL-4 (Li & Ikehara 2013). MSCs produce IDO in the presence of IFN- γ, which leads to suppression of effector cell proliferation. Inhibition of immunoglobulin G activation and secretion has also been shown. Nonetheless, unlike for T cells, induction of apoptosis was not observed (Shi et al. 2011).

The immunomodulatory properties of MSCs also include the induction of regulatory T cells (Tregs). This is done via the atypical MHC class I glycoprotein HLA-G5 and via likely constitutively expressed TGF-β. Tregs can also be indirectly induced through Fas ligand/Fas-mediated death pathway through direct intercellular contact. Tregs, increased by MSCs, *in vivo* demonstrated amelioration of diseases and promoted experimental graft survival (Mattar & Bieback 2015).

In general, MSCs modulate the immune system by releasing three types of molecules: IL-1 receptor antagonists, PGE2 and multifunctional proteins, which translocate NF-kappa B to the nucleus in target cells (Prockop & Youn Oh 2012). All secreted molecules have a similar effect on the immune system and lead to the suppression of inflammatory responses. Under physiological conditions, MSCs also express proinflammatory cytokines (e.g., IL-1, IL-6, IL-8, and TNFα), however, only as a part of differentiation into certain cell types and not with the aim to stimulate an inflammatory response (Sumanasinghe et al. 2009).

3.2.2.5 Osteogenic differentiation *in vivo*

The journey of a mature bone cell starts with MSC. They have the ability to differentiate into several cell types, therefore they must commit to osteogenic differentiation to create a bone

cell (Vater et al.2011). Before the MSC fully matures into a bone cell there are several stages, in which different specific molecules are expressed.

Stages of osteoblast maturation are osteoprogenitors, preosteoblasts, mature osteoblasts and osteocytes or bone lining cells Observable changes during osteogenic differentiation are changes in morphology of MSCs. First osteoprogenitors have a spindle-like shape, which changes into polygonal shape of preosteoblasts. In the next stage the cells assume a cuboidal shape of an osteoblast. If the cells mature into osteocytes or bone lining cells then the shape further changes to, respectively, a spindle or they become flat (Malaval et al. 1999). Changes in cell shape may be transduced into a regulatory signal in MSC commitment by some structures in the cell, including the actomyosin cytoskeleton (McBeath et al. 2004).

MSC commitment and differentiation is regulated by RunX2 and Osx. These GFs were described above. It has several targets in this process, which are crucial proteins of bone tissue such as osteopontin, OCN, BSP-2 (known as integrin-binding sialoprotein (IBSP)) and ALP (Ducy et al. 1997). Differentiation factors, such as the TGF-β1 and FGF, and signalling pathways Wnt/β catenin and hedgehog activate RunX2 and osterix (Hayrapetyan et al.2014; Pérez-Campo et al. 2016). Relatively recently the level of reactive oxygen species was show to be a regulator of osteogenic differentiation (Atashi et al. 2015).

Typical molecules in osteogenic differentiation are collagen type I, OCN, osteopontin, osteonectin, IBSP and active ALP. Osteopontin, and sometimes a low level of IBSP which is usually found in mature osteoblasts, are synthesized in preosteoblast stage (Malaval et al. 1999; Bianco et al. 2017). Then, while the cells are still proliferating in the immature osteoblast stage, collagen type I and low levels of ALP are expressed. Collagen acts as a nucleation centre in mineralization of the ECM (Anderson 2003; Owen et al. 1990). Also, it interacts with preosteoblasts which promotes the maturation further by activating MAPK (G. Xiao et al. 2002). Late preosteoblast to mature stage is associated with high levels of ALP and its activity and a decrease in proliferation. This is when OCN expression appears, as it needs first the ECM mineralization to start and that is dependent on ALP activity (Owen et al. 1990). ECM maturation is associated also with increased levels of osteopontin and IBSP (Clarke 2008). Mineralization of the bone is preceded by decrease in ALP activity and is finalized by incorporation of HA into the new osteoid (Anderson 2003). The process of mineralization accommodates the supporting

function of bones. When the bone is formed, some osteoblast further differentiate into osteocytes, become bone-lining cells, or go through apoptosis (Bonewald 2011).

3.2.2.6 Osteogenic differentiation *in vitro*

In vitro osteogenic differentiation is similar to processes occurring in the bone *in vivo*. Differentiated osteoblasts express markers typical for the bone. Taken as positive markers of osteogenic differentiation are the increased expression of ALP, calcium deposition (Hadjidakis and Androulakis 2006b), expression of collagen type I, OCN, IBSP, osteopontin (Owen et al. 1990).

GFs are one of the basic tools in tissue engineering for *in vitro* differentiation. In order to achieve optimal results when differentiating MSCs, the most effective method is combining GFs and optimizing their ratios. The MSCs are stimulated to differentiate into osteoblasts by GFs from TGF- β family. Some GFs, such as BMP-2, FGF-2 and VEGF together support osteogenic differentiation of MSCs in rats in very low concentrations. If VEGF and FGF-2 are added in early proliferation phase, in the first 7 days, then the differentiation into osteoblasts is extremely enhanced, whereas BMP-2 has the same effect in the following 7 days showing that the timing and combination of GFs is important to obtain desired result (Bai et al. 2013). BMP-2 and BMP-7 are approved by Food and Drug Administration of the United States of America in spine injury therapy (Freire et al. 2011).

Besides the GFs, other compounds, referred to as supplements, have demonstrated to be valuable in tissue engineering. Typical protocol for *in vitro* osteogenic differentiation of MSCs includes culturing confluent cell layer for several weeks with addition of osteogenic supplements, which are dexamethasone, β-glycerol phosphate and ascorbate. The mentioned osteogenic supplements can be further combined with vitamin D3 and GFs from TGF-β and BMP family (Vater et al.2011). The supplements have an advantage over GFs thanks to their longer half-life *in vivo* (X. Shi et al. 2010).

Dexamethasone is a synthetic glucocorticoid which binds to glucocorticoid response element in promoter region of genes involved in osteogenesis. It stimulates integrin α5 and BSP transcription to a certain extent, and they take part in activation of RunX2-dependent gene transcription. It can inhibit functions of osteoblast in certain concentrations which can lead to osteoporosis. In general, glucocorticoids decrease collagen synthesis. In order to achieve total

stimulation of MSC osteogenic differentiation it is needed to culture the cells with dexamethasone at least for 3 weeks (Vater et al.2011).

The role of ascorbate is to act as a co-factor in hydroxylation of proline and lysine residues in collagen maturation. It is a strong mitogen for cells. The significant disadvantage of ascorbic acid is its instability in culture medium. That is why it is replaced by its more stable long-acting derivate vitamin C, the ascorbic acid 2-phosphate (Asc-2-P), concentrated 0.25 mM to 1 mM (Vater et al .2011). Asc-2-P showed stimulative effects in collagen synthesis and ALP activity. These effects depend on collagen synthesis and its inhibitors. Under Asc-2-P influence mature ECM and 3D shapes of collagen can be observed (Takamizawa et al. 2004).

Mineralization of ECM requires the presence of β-glycerophosphate which acts as a substrate for ALP because it has a -PO_4 group. ALP hydrolyses it and turns it into indispensable source of inorganic phosphates. When MSCs are cultured in medium with β-glycerophosphate the ALP activity, lactate, protein and phospholipid production is increased. As a consequence of ALP activity inorganic matter is deposited as initial mineralization sites are formed. Usual concentration in which β-glycerophosphate is added to the culture medium is 5-10 mM (Vater et al.2011).

It is possible to modify osteogenic medium with the addition of other supplements that have a positive impact on osteoblast generation. An example of such supplement is before-mentioned vitamin D3, which interacts with a nuclear receptor, This interaction leads to stimulation of osteogenic TFs RunX2 and Osx and expression osteoblast commitment markers ALP, collagen type I, OCN and osteopontin (Takamizawa et al. 2004).

3.2.2.7 Alkaline phosphatase

In alkaline environment (pH 9.5-10.5) monoesters of phosphate acids get hydrolysed to phosphate acid and alcohol by metalloproteinase ALP. The metabolism of macroergic phosphate bonds is influenced by ALP, which also helps to transport inorganic phosphates across cell membrane. ALP is located within cell membranes and matrix vesicles (Siller & Whyte 2018). The biggest proportion of ALP in the organism is produced by liver and bones (Štěpán, Volek, and Kolář 1976).

ALP was one of the first discovered bone markers (McComb et al. 1979). Increased ALP levels are observed in bone healing processes fracture repair and in bone growth in children, thanks to increased osteoblast activity. This is why it is called bone remodelling marker activity. It is

produced in osteoblast maturation phase and, amongst others, its function is cell proliferation regulation. Concentration of ALP in plasma is directly proportional to osteoblast activity, as the increase of ALP activity over 3 weeks points to osteogenic differentiation (Pittenger et al. 1999). Level of ALP is examined in blood analysis and increased ALP above 129 U/I can point to osteoporosis in men (Shetty et al. 2016; Pikner R et al. 2020; Fink et al. 2016).

Regulation of ALP expression is acomplex process that consists of multiple interlinked signalling pathways (Figure 8). During upregulation of certain genes such as OCN, reduction of ALP expression occurs, which clearly should not happen in early growth (Siller and Whyte 2018). Runx2 and/or TCF/LEF1 activate ALP expression, thereby promoting bone mineralization. This activation is induced via downstream signalling like Smad via BMP2 or MAPK/ERK/P13 K or through Wnt signalling via β-catenin (Ling et al. 2010).

There are 17 isoenzymes of this metalloenzyme. 1 of them is non-tissue specific, the TNAP, and 1 of its 3 isoforms appears in bones (T. R. Kuo and Chen 2017). TNAP can be found in membranes of osteoblasts concentrating specifically on the membranes of matrix vesicles. These 2 isoforms are difficult to distinguish due to their difference only in posttranslational glycosylation. Bone isoenzyme is thermolabile in comparison with the liver version (Shetty et al. 2016).

3.3 Bone ECM

ECM is a natural mechanical support for cells in all tissues. In the musculoskeletal system it highly mineralized and hard. Organic component of the bone is made 85 %-90 % out of collagen fibers, mainly type I. In some phases of bone development type III and V are present in trace amounts (Clarke 2008). Collagen protein structure ensures stability and organization of ECM. It is also crucial in the beginning phase of ECM mineralization. Osteonectin, OCN, osteopontin and BSP are the non-collagenous proteins that are present in the ECM (Fujisawa & Tamura 2012). The majority is synthesized by osteoblasts and approximately one fourth is obtained from blood serum. These proteins have the ability to bind HA [$3Ca_3(PO_4)_6(OH)_2$] and calcium ions (Clarke 2008). Nanocrystals of HA are stored in and around protein fiber network (Moreira et al. 2019).

Bone ECM maturation is associated with increased ALP activity and expression of OCN, osteonectin and BSP (Clarke 2008). It seems that these proteins aid in proper mineral compound deposition via regulating the amount and size of formed HA crystals. Mineralization is commenced

by vesicle secretion with high calcium and phosphate concentration (Anderson 2003). Phosphate is transported into the vesicles via type-III sodium-dependent phosphate transporters, whereas calcium is transported via annexin transmembrane channels (Golub 2009). Apart from inorganic component the vesicles contain nucleation centre where precipitation of HA crystals occurs (Anderson 2003). The mechanism by which the vesicles are directed to a specific site is not known. Nonetheless mineralization always begins at the ends of collagen fibers with which vesicle interact via e.g. annexins. Proteins that were identified to initiate crystal creation are BSP and dentin matrix acidic phosphoprotein 1. The vesicles contain ALP and nucleotide pyrophosphatase/phosphodiesterase 1 (NPP1) among other enzymes (Golub 2009). ALP is incorporated into the outer membrane of the vesicle undergone exocytosis via glycosylphosphatidylinositol (GPI) anchor. It supports the mineralization by decreasing extracellular level of pyrophosphate (PPi) and solubility of calcium and increasing level of inorganic phosphate. PPi, mainly produced from extracellular ATP, inhibits formation of HA, but in the presence of ALP it is hydrolysed to Pi. Subsequently inorganic phosphate is a substrate for HA production. Inorganic phosphate forms HA with calcium and magnesium (Pikner R et al. 2020). NPP1 works in the opposite way as it inhibits mineral deposition by increasing extracellular concentration of PPi which is synthesized from extracellular nucleoside triphosphate.

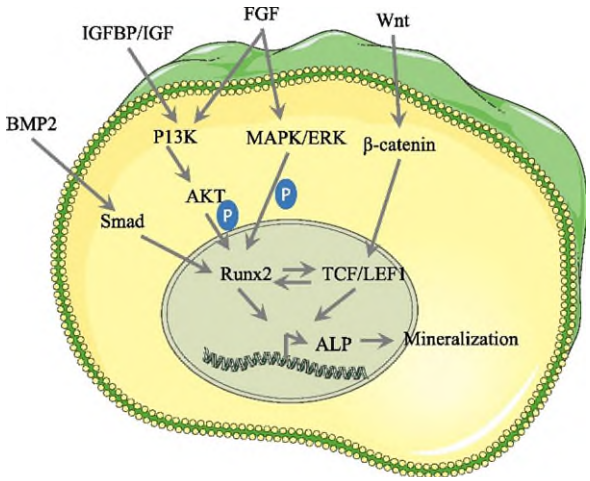

Figure 8 ALP expression induction. Runx2 expression is increased by BMP2 via downstream Smad signalling, or by IGFBP/IGF/FGF kinase downstream signalling. Runx2/TCF/LEF1 is increased via β-catenin and Wnt signalling. (Vimalraj 2020)

3.4 Bone homeostasis

It is known that bones have a structurally supportive function in the organism. They have other functions too and they involve protecting internal organs and central nervous system, as well as enabling movement. It was mentioned that a high amount of compounds with calcium and

phosphate is present in the bones. For this reason, the skeleton also plays an important role in maintaining the constant ionic environment in the body. The bone is a dynamic organ and its balance is kept by osteoblast and osteoclast activity. Optimal ratio of firmness of the bone and sufficient elasticity is ensured by the presence of specific proteins and ECM mineralization. This must be tightly regulated and harmonized in order to preserve skeletal health and integrity (Hadjidakis & Androulakis 2006a).

Human skeleton renews approximately once every ten years due to bone remodeling. This is determined by genetic blueprint and is regulated by local and systemic factors. Systemic factors are hormones such as androgen, estrogen, parathyroid hormone, and glucocorticoids, calcitriol, calcitonin, BMPs, and local regulators are cytokines, prostaglandins and GFs (Florencio-Silva et al. 2015). For example, the drop in estrogen level at menopause causes bone loss and osteoporosis therefore it has a key role in homeostasis of bone tissue. This process is not fully understood, but it seems that estrogen prevents immoderate bone resorption by inhibition of osteoblast and osteocyte apoptosis and osteoclast formation (Khosla et al. 2012).

The property of bone to change and adapt to external forces implies that these forces regulate bone remodelling. Increased mechanical load increases bone formation and decreases resorption. Unloading has the opposite effect and as a consequence the bone resorbs more (Hadjidakis & Androulakis 2006a). Bone remodelling guarantees tissue turnover whilst sustaining bone matter and ensuring adaptation to mechanical and calcium and phosphate metabolic requirements in grown skeleton. Destruction of bone carried out by osteoclasts is called resorption. This process is in balance and coupled with bone formation. It results in maintenance of constant amount of bone. The amount of formed bone is equal to the amount of resorbed bone, restoring the bone completely upon its removal. The imbalance between the processes results either in bone loss or excess of bone. In the absence of bone remodelling, if the bone turnover is turned off, the risk of fracture may increase (Rodan 1998).

Osteoblast, osteocytes and osteoclasts, are involved in the remodelling via regulation of signalling pathways, such as activation and impairment of WNT–β-catenin signaling which results in increase and decrease in bone mass (Baron & Kneissel 2013). Osteoclasts move on bone surfaces, pump hydrogen ions and by secretion of proteolytic enzymes they dissolve the ECM and resorb discrete zones of bones. This would not be possible without M-CSF and RANKL, because they are necessary for osteoclast differentiation (Vater et al.2011; Teitelbaum & Ross 2003).

RANK/RANKL signalling is regulated by osteoprotegerin, which prevents extensive osteoclast differentiation and by extension the bone resorption as well (Teitelbaum & Ross 2003). The resorbed bone is replaced by osteoblasts. First, the MSCs must migrate to the bone resorption cavity. This is facilitated by TGF-β1 PDGF, BMP-2 and BMP-4 regulation (Balogh et al.2018). In addition the activated osteoclast-derived chemokine sphingosine-1-phosphate is essential in recruiting the MSCs to the site of active resoprtion (Pederson et al. 2008). This process repairs micro-injuries of bones and adapt the bone niche for control of mechanical toughness. After ECM mineralization, osteocytes are differentiated from mature osteoblasts and are inserted in the matrix (Takayanagi 2007). During bone development, osteocytes fine tune the bone structure and during the remodelling they act as recyclers restoring and keeping skeletal health. After bone resorption, osteoblasts are activated to produce the ECM and to undertake mineralization (Al-Bari and Al Mamun 2020).

3.5 Role of fluid shear stress in bone formation

In the mineralized bone tissue, the cells are continuously washed by the interstitial fluid travelling over cell bodies and cytoplasmic processes. This creates shear stress along the pericellular space and tiny electrical potentials that are sensed by cell membranes. The created shear stress influences maintenance and healing of bone tissue. There is evidence that, amongst other, osteocytes are acting as mechanosensors of shear stress and as orchestrators of bone remodelling (Bonewald 2011; Robling & Bonewald 2020).

The body of an osteocyte is entrapped within the lacuna, but its cytoplasmic processes (up to 50 cytoplasmic processes per osteocyte) traverse little tunnels that stem from canaliculi, a lacuna space, reaching other osteocytes, osteoblasts and bone lining cells, thereby creating the lacunocanalicular system (Figure 9) (Manolagas 2006). This system allows for intercellular transport of small signalling molecules like nitric oxide and prostaglandins, and is located in vicinity of vascular supply, where oxygen and nutrients are available (Dallas et al. 2013; Civitelli et al. 2002). Besides the lacunocanalicular system, other porous spaces that are filled with interstitial fluid are Volkman and Haversian canals, and small spaces between crystallites of HA and collagen fibers; all in μm range (Cowin & Cardoso 2015).

Cell-cell communication is facilitated by interstitial fluid. It flows along cytoplasmic processes, canaliculi and lacunae (Mullender et al. 1996). The fluid flux movement is crucial for the two-way transport of solutes, influencing signaling and communication between bone cells. Osteocyte network can detect mechanical pressures and loads by the lacunocanalicular system. This helps the bone to adapt daily to mechanical strains and weight bearing loading forces (Rochefort et al. 2010). Mechanotransduction is the process by which external loads felt by the skeleton are transformed into biochemical signals that are used to direct cellular responses such as microdamage repair and bone remodeling (Huang et al. 2004). The mechanisms of conversion of mechanical stimuli to biochemical signals are not firmly established.

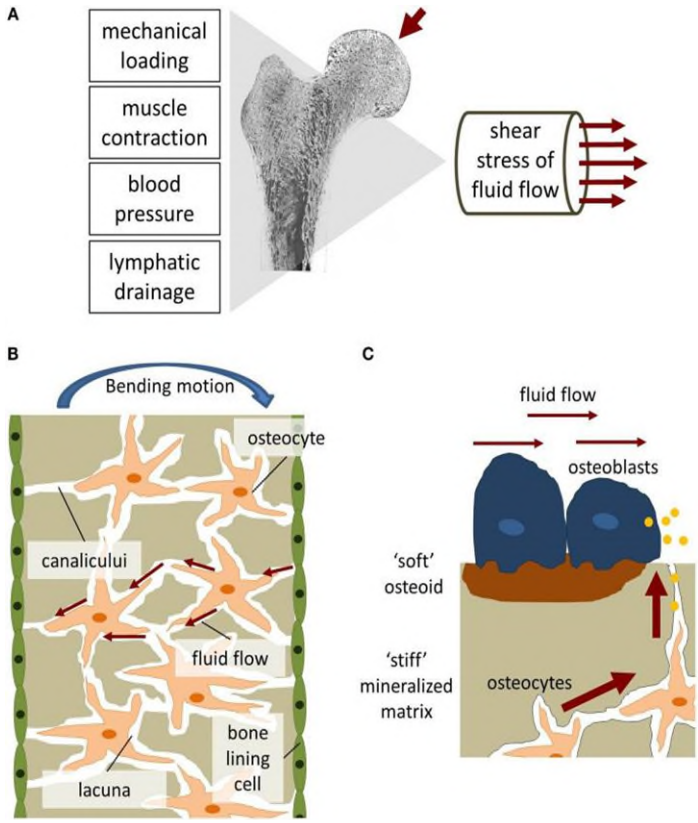

Figure 9 Fluid shear stress in bone. (A) Mechanical loading, muscle contraction, blood pressure, and lymphatic drainage generate the fluid flow. (B) Bone bending creates tension and compression forces which sets off interstitial fluid movement (Image adapted from Duncan and Turner 1995). (C) Flow velocities differ for osteocytes and osteoblast creating different biochemical environment. (Image adapted from Wittkowske et al. 2016)

Stress may be thought of as the internal force distribution felt throughout the bone as a consequence of an external force (Figure 9). External forces cause internal stress to which osteocytes are recognized to be sensitive to *in vitro*. Local cellular deformation occuring within the bone as a result of the local stress is strain (Smalt et al. 1997). Besides external forces, fluid

movement is subjected to strain amplification phenomenon. Most likely the osteocytes integrate stimuli coming from bone loading and strain amplification to appropriately signalize cues in bone adaptation maintenance (Robling & Bonewald 2020). Cells sensing shear stress respond to it by releasing osteogenic signalling factors such as nitric oxide, and prostaglandins (Figure 9C), and are thought to signalize osteoblasts and osteoclasts to start remodelling (Robling & Bonewald 2020). In resting periods without physical activity the driving forces for the slow constant flow of the interstitial fluid are the hydrostatic and osmotic pressure differences between the interstitium, blood and lymphatics (Xing et al. 2014).

4 Perfusion bioreactor

Systems that allow an *in vitro* recapitulation of relevant *in vivo* cell and tissue developmental and morphological events are continuously investigated. This *in vitro* approach is labeled as “biomimetic paradigm”. Myriad of aspects like different cell types, ECM, chemical and physical factors influence cell cultures in the dynamic course of tissue development.

Bioreactor technologies have been researched for tissue-engineering applications They follow the biomimetic paradigm. Every culturing method that concerns bioreactors begins with isolated cells that are seeded on 3D scaffolds. Appropriate stimuli are designed to be provided by the bioreactor. This reinforces new tissue development *in vitro*.

Most bioreactors are, however, restricted in regard to the size and number of scaffolds, automatization, control and supervision of the process. This makes the reproducibility and standardization of experiment with 3D cell cultures difficult.

4.1 Overview of bioreactor types

Simple bioreactor is the spinner flask (Sikavitsas et al. 2002). Here the scaffolds hang by needles from the flask lid. The medium in the flask reaches and covers the scaffolds. It is stirred by a magnetic stir bar which is on the bottom of the flask. This induces fluid movement and alleviates the concentration gradients of nutrients on the surface of the scaffolds.

Specialized cell culture vessel that allows growth of the cells under low physiological fluid shear circumstance is the rotating wall vessel. It was developed to simulate microgravity and to model its effects (Freed & Vunjak-Novakovic 1995). The motor drives a belt that rotates the cylindrical vessel with cell culture. The rotation is horizontal which creates a free fall environment of low-fluid shear. This enhances cell attachment and aggregation. The free fall is balanced by centrifugal forces due to rotation.

In cases when the mass transfer becomes a restrictive factor, that is when perfusion bioreactors are beneficial. In terms of the perfusion regime, there are intermittent, pulsatile and continuous perfusion bioreactor. The latter bioreactor type was used in this project and shall be described further below.

4.2 Perfusion bioreactor properties

Perfusion is a means to culture cells in a bioreactor in which medium is continuously flowing through the cell culture. Supply of oxygen and nutrient and waste elimination were shown to be enhanced in perfused environments (Volkmer et al. 2008). This removes the limitations of the mass transfer in culturing cells on scaffolds. Mass transfer proved to be dependent of the flow velocity and rate and resulted in better uniformity and density of the scaffolds (Grayson et al. 2011; Kleinhans et al. 2015). Moreover, in perfusion bioreactors there is a possibility to administer fluid shear stress. This is convenient in bone tissue engineering (Weinbaum et al. 1994) as it has mechanotransductive effect in osteogenic differentiation *in vivo* (Kleinhans et al. 2015; Goldstein et al. 2001). When the intrinsic properties of the scaffolds are established, the appropriate fluid shear stress can be determined and applied via varying flow rates (Guyot et al. 2015). Porosity of the scaffold plays a role in the local shear stress experience of each cell which varies. Another parameter that improves cellular viability and osteogenic differentiation is the hydrostatic pressure (Becquart et al. 2016). Research has shown that in order to achieve these benefits a higher pressure than the one naturally occurring *in vivo* is to be applied (Egger et al. 2017).

The concept of the fluid flow in the perfusion bioreactor I used is rather simple. Pump perfuses the medium in a continuous re-circulating manner through the porous scaffolds. The medium flows from top to bottom (Figure 10A). It is important to ensure that the medium passes through a confined space, a chamber, which is occupied by the scaffold in a manner that the medium does not flow around its edges (Figure 10B). This way the exchange of the medium within

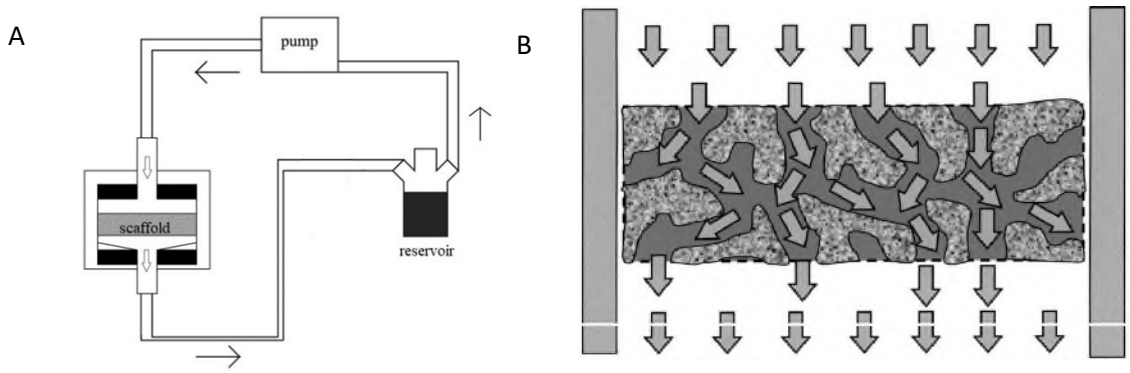

Figure 10 Perfusion system described by Bancroft et al. Figure 10A Scheme of the system with the scaffold, confined in the chamber. The medium reservoir provides the medium supply. Arrows represent medium flow. Image adapted from (Gaspar an 2012) Figure 10B Representation of interstitial flow through the scaffolds. The medium delivery is enhanced and mechanical force of the fluid shear stress increases differentiation of cells. Image taken from (Sikavitsas et al. 2002)

the interior of the porous network is guaranteed and cell viability, ALP activity and mineralization are enhanced (Mueller et al. 1999; Sikavitsas, et al. 2002).

Most of the perfusion bioreactor designs includes previously mentioned pump and a chamber, but also culture media reservoir (Figure 10A), cartridges, tubing circuit and stands for chambers and reservoirs (Gaspar et al. 2012).

4.2.1 Flow rate selection

In order to engineer thick bone constructs with the desired properties described above, there needs to be an understanding of the flow rate impact on cellular responses and morphology, osteogenic differentiation and ECM formation and organization. In a system with constant pore size, viscosity and porosity, the fluid shear stress will be conditioned by the flow rate of the medium applied (Hadida & Marchat 2020). The flow rate is determined by the cross-sectional area of the tube as the length of the column of fluid being pumped and the rate of pumping remains constant.

The same flow rate used in different types of perfusion bioreactor can give different results. The significant range, per the observations of Gaspar et al. (2012) are 0.2 to 1 mL/min, depending on the system used. These flow rates positively impact osteoblast differentiation, deposition and distribution of ECM. Higher values, e.g. 4 mL/min did not result in a significant difference in the bone formation when compared to static culture after 19 days (Janssen et al. 2006). Cell attachment may be disrupted by too high flow rate and the subsequent ECM formation and deposition are endangered. For Kleinhans et al. (2015) 0.8mL/min flow rate exhibited a sufficient suppy of nutrients and removal of the waste after 7 days of culturing hMSCs in the perfusion bioreactor. Higher values of the flow rate resulted in low cell density, which the authors presume is a due to cell death. Osteogenic differentiation may be decreased as a consequence of the loss of cell-scaffold and intracellular attachment. Guyot et al. (2015) used flow rate of 1mL/min to culture human periost-derived cells. These were able to infiltrate and fill up to 100% scaffold. In another study published in 2018, the computer models for bioreactor processes to design optimal conditions for culturing were investigated. Maximum neotissue filling was shown to be a result of 1.83 mL/min flow rate. All scaffolds that yielded high fillings were under flow rates between 1.5 – 2 mL/min (Mehrian et al. 2018). Egger et al. 2017 reports highest viability and ALP activity at a flow rate 1.5 mL/min, in addition to the dynamic cultures demonstrating significant higher ALP

activity in all dynamic conditions over the static ones. The samples were cultured for 6 days in dynamic conditions under three different hydrostatic pressures. In another study (Yaghoobi et al. 2019) with multilayered electrospun nanohydroxyapatite-PCL flow rates of 2 mL/min and 4.5 mL/min were applied in the bioreactor system and the cells were cultured for 14 days. It demonstrated that ALP activity, calcium content and RunX2 expression increased under both flow rates in comparison with static cultures. Higher cell differentiation was noticed in the group which was under mechanical pressure and the group that was subjected to parallel flow in particular. Overall there is almost no published literature on osteogenic differentiation of cells seeded on electrospun or melt-blown multilayered scaffolds.

5 Aims of the thesis

The aim of the work was to research the influence of mechanical stimulation on differentiation of hMSCs in 3D scaffolds. Combination of 3D environment of scaffold and mechanic stimulation using the bioreactor should imitate natural cell microenvironment and is theoretically more favourable to stimulate MSCs to proliferate and differentiate into osteoblasts than the conditions of the static culture.

The specific aims of the study were to:

- Learn hMSCs culture methods
- Finding optimal dynamic conditions needed for proliferation of hMSCs in terms of testing different medium flow rates
- Finding optimal dynamic conditions needed for stimulation of osteogenic differentiation of hMSCs in terms of testing different medium flow rates
- Finding optimal dynamic conditions needed for cell infiltration into the scaffolds in terms of testing different medium flow rates
- Characterization of hMSC osteogenic differentiation
- Comparison of static and dynamic culture conditions

6 Methods

Table 1 List of used chemicals, including the catalogue number, manufacturer, and country of origin

Chemical name		Catalogue number	Manufacturer	Country
Dexamethasone		-	Medochemie	Cyprus
DiOC6(3)		D2438	Sigma Aldrich	Germany
DMSO		D2438	Sigma Aldrich	Germany
EDTA		EDS	Sigma Aldrich	Germany
Ethanol 96%		70390	Penta	Czech Republic
FBS		10270106	Gibco®; Thermo Fisher Scientific	Brazil
		F7524	Sigma Aldrich	Germany
hMSCs		7500	ScienCell	USA
L-ascorbic acid 2-phosphate		A8960-5G	Sigma Aldrich	Germany
α-MEM		12571063	Gibco®; Thermo Fisher Scientific	USA
Methanol		21210	Penta	Czech Republic
MTS		G1111	Promega	USA
NaOH		15670	Penta	Czech Republic
PCR Grade Water		03315959001	Roche	
PCL		440752	Sigma Aldrich	Germany
Penicillin/Streptomycin		15140-122	Invitrogen	USA
		P4333-100ML	Sigma Aldrich	Germany
PicoGreen Quan-iT Assay kit		Q-33120	Invitrogen	USA
PNPP		37621	Thermo Fisher Scientific	USA
Propidium Iodide		P4864-10ML	Sigma Aldrich	Germany
RevertAid First Strand cDNA Synthesis Kit		K1622	ThermoFisher Scientific	USA
RNeasy Mini Kit		74104	Qiagen	USA
TaqMan® Gene Expression Assay	Hs00265885_g1	4331182	Thermo Fisher Scientific	USA
	Hs01047973_m1	4331182	Thermo Fisher Scientific	USA
	Hs00164004_m1	4331182	Thermo Fisher Scientific	USA

Chemical name		Catalogue number	Manufacturer	Country
	Hs01587814_g1	4331182	Thermo Fisher Scientific	USA
	Hs00173720_m1	4331182	Thermo Fisher Scientific	USA
TaqMan™ Gene Expression Master Mix		4369016	Life Technologies; Thermo Fisher Scientific	USA
Tris		T1503	Sigma Aldrich	Germany
TritonX-100		T8787	Sigma Aldrich	Germany
Trypsin-EDTA		59418C-100ML	Sigma Aldrich	Germany
β-glycerol phosphate		50020	Sigma Aldrich	Germany

Table 2 List of used appliances, including the manufacturer's model name, manufacturer and country of origin

Appliance model name	Manufacturer	Country of origin
Analytical scale T5939	Kern	Germany
Microcentrifuge Spectrafuge C2400 24D	Labnet Int	USA
Centrifuge NF800R	Nüve	Turkey
CO_2 incubator 2424-2	Shel Lab	USA
NB-203XL	N-Biotek	Korea
Confocal microscope LSM 5 DUO	Zeiss	Germany
Heating bath NB-301	BioTek	USA
Fume hood LK 1901	Komplet s.r.o.	Czech Republic
Laminar flow cabinet Safeflow 1.2	Bioair	Italy
Thermal cycler GenePro	Bioer Technology	China
qPCR thermal cycler LightCycler® 480	Roche	Switzerland
Light microscope TH4-200	Olympus	Japan
Ismatec Pump Tubing HV-06431-34	Ismatec; Masterflex® Bioprocessing	Germany
Microplate plate reader Infinite 200 PRO NanoQuant	Tecan	Switzerland
Perfusion bioreactor OsteoGen®	Bangalore Integrated System Solutions Pvt. Ltd	India
Quorum 150R S plus device	Quorum Technologies	United Kingdom
Tescan	Vega	Czech Republic
Vortex ZX Classic	VELP Scientifica	Italy

6.1 Scaffold preparation

Cell scaffolds made from PCL nano- and microfibers prepared by combining electrospinning and melt-technologies, as described in Rampichová et al. (2018), were kindly provided by Technical University in Liberec. For my experiments, 10 mm wide round-shaped scaffolds were prepared. They were firstly sterilized in 70% ethanol for 30 minutes and subsequently washed three times with sterile phosphate buffered saline (PBS). The second wash lasted 15 minutes. hMSCs were seeded on freshly sterilized scaffolds.

6.2 Scanning electron microscopy

Samples were cut and stuck onto the holders, then coated with a thin layer of gold in a Quorum 150R S plus device. Afterwards, the samples were visualized using scanning electron microscopy. The mean fiber size, pore size and porosity were calculated in ImageJ software.

In the course of this work I have benefited from the stereological analysis of the scaffold by Mgr. Matěj Buzgo.

6.3 Cell subculturing

Pre-isolated cells were used and passaging was performed when they were 80-90% confluent. This is done in order to keep their phenotype, viability and proliferation.

Growth medium and trypsin are warmed up in heating bath in 37ºC. The growth medium that used consisted of α-MEM, is supplemented with 10% fetal bovine serum (FBS) and antibiotics (ATB) (100 I.U./mL penicillin, 100 μg/mL streptomycin). The cells were checked under light microscope to confirm their confluence. After removing the medium from the flask, 5 mL of PBS with EDTA solution was added and the cells were washed. Subsequently, 2 mL of 1.5x concentrated trypsin-EDTA were added and the cells were incubated for 5 minutes in 0.5 mL 1.5x trypsin-EDTA in the incubator (5% CO_2, 37ºC). It was visually confirmed that cells are detached from the flask surface. Trypsin reaction was stopped by addition of 10 mL of medium containing 10% FBS and 1% ATB. The cell suspension was resuspended and split into new 150 mm^2 flasks in ration 1:2 or 1:3, depending on the original confluence and the medium was added to the total volume of 30 mL.

6.4 Seeding of hMSCs

The cells in Bürker chamber from passage 4 were counted and resuspended in growth medium in concentration 5×10^6 hMSCs/100 µL medium. Then 24 sterile scaffolds were placed on the bottom of 48-well plate and seed 100 µL of cell suspension on scaffolds and into 4 empty wells, which served as quality control of cells. 250 µL of growth medium was added into all 28 wells. Then, the plate was left for 2 hours in the incubator in order for the cells to adhere on the scaffolds before imposition of medium flow. After 2 hours, the growth medium was exchanged for 750 µL of differentiation medium to 12 wells with scaffolds, which serve as a static control, as well as to 4 wells without scaffolds. The remaining 12 scaffolds were used for culturing in dynamic conditions in differentiation medium in perfusion bioreactor. The differentiation medium consisted of α-MEM supplemented with 10% FBS, 1% ATB, 10 mM β-glycerol phosphate disodium salt hydrate, 100 nM dexamethasone and 40 µg/mL ascorbic acid-2-phosphate. The whole volume of the medium was changed every 2 days in static culture for the duration of the experiment which was 21 days.

6.5 Perfusion bioreactor set up

Assembly of the perfusion bioreactor was performed under sterile conditions. 12 available reservoirs were filled with 30 mL of differentiation medium and 12 scaffolds were prepared and implanted into chambers (Figure 11 A and B). The scaffold diameter was 10 mm, which is a bit over the diameter of the chamber (9.5 mm). This way flow of the medium through the scaffold was ensured. This was followed by connecting the reservoirs and the chambers by tubes that were also placed in the cartridges over the peristaltic pump (Figure 11C). Since the perfusion bioreactor is a closed system, sterile filters ensured gas exchange. The bioreactor is placed in an incubator, which provides adequate temperature of 37°C and level of CO_2, which was 5%. In this work 3 different flow rates were chosen based on preliminary studies (not presented here) to induce proliferation and osteogenic differentiation. Cells were cultured under three different flow rates of 1mL/min, 3 mL/min and 5 mL/min.

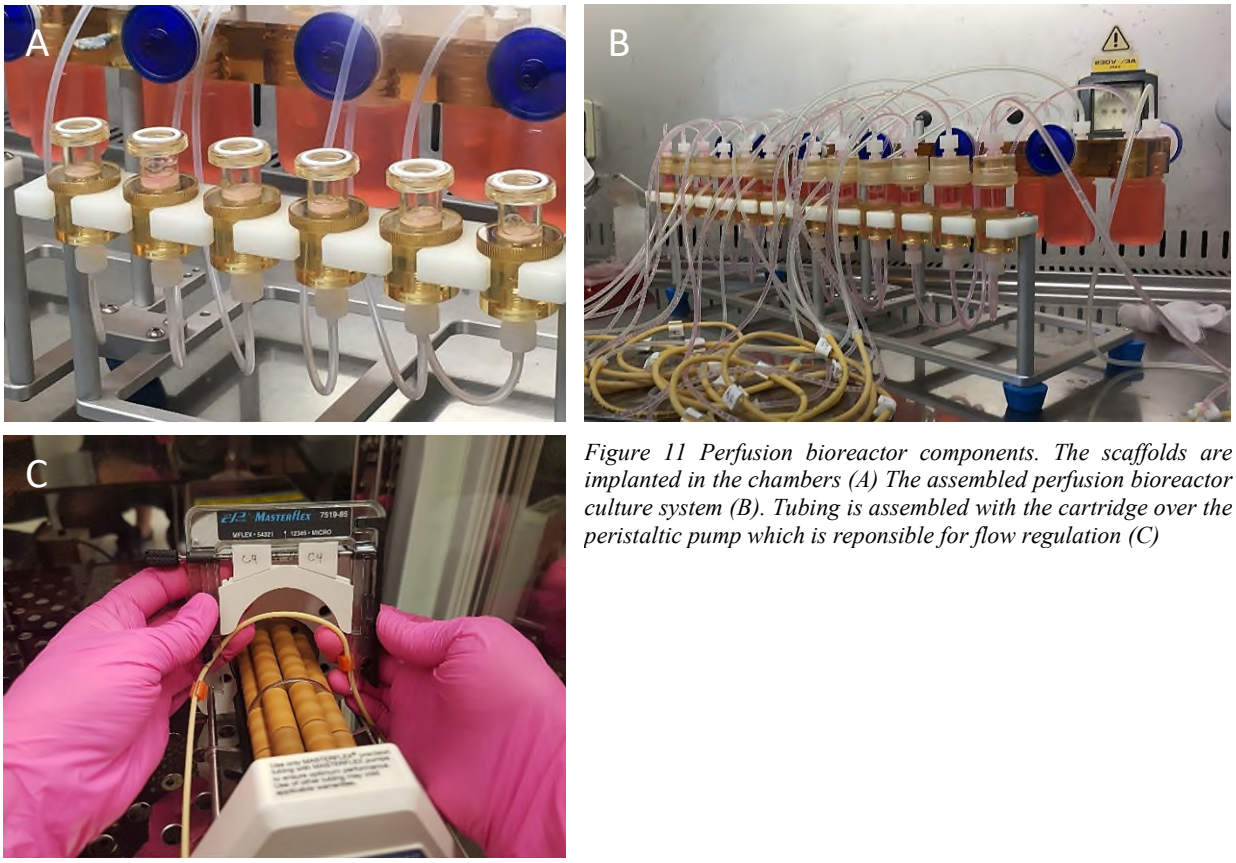

Figure 11 Perfusion bioreactor components. The scaffolds are implanted in the chambers (A) The assembled perfusion bioreactor culture system (B). Tubing is assembled with the cartridge over the peristaltic pump which is reponsible for flow regulation (C)

6.6 Colorimetric assay for assessing cell metabolic activity

MTS assay is an assay which uses a colorimetric method to measure metabolic activity of viable cells only. It is based on reduction of a tetrazolium salt (3-(4,5-dimethylthiazol-2-yl)-5-(3-carboxymethoxyphenyl)-2-(4-sulfophenyl)-2H-tetrazolium) to strongly coloured water-soluble formazan compound that has an absorbance maximum at 490 nm. The reduction is performed by mitochondrial NAD(P)H-dependent dehydrogenase enzymes in live, metabolically active cells (Dunigan et al. 1995). Dead cells lose the ability to convert the reagent to formazan salt, which is the basis of variety assay method estimating cell viability in a sample.

Metabolic activity of mitochondrial enzymes produced by live cells is proportional to the quantity of coloured formazan. It can be determined by measuring the absorbance of formazan delivered into the culture medium (Cory et al. 1991).

6.6.1 MTS assay protocol

The assay was performed on day 21 (last day) of the experiment. It is important to perform the assay in the dark and to cover test tubes with aluminium foil, because the substrate is light sensitive. The MTS substrate needs to be diluted with the culture medium in ration 1:5.
The reaction was performed in 48-well plates. In order for the adherent cells on the bottom of the well plate not to interfere with the assay and produce false positive results, the scaffolds were transferred and cultured under static conditions to new wells. The scaffolds dynamically cultured in the bioreactor were transferred in the clean wells of 48-well plate. Then, 480 μL of the diluted substrate was added to 3 different groups. The first group was the wells with the scaffolds. 4 scaffolds originated from static culture and other 4 originated from dynamic culture. The second group was 4 wells with hMSCs cultured on tissue culture plastic of the well, which were used as a control of the condition that the cells are in overall. The last group were 4 control wells for background subtraction. The incubation period is 2 hours long and is performed at 37°C and 5% CO_2. Aferwards, 100 μL of solution was taken from each well and added to empty wells of 96-well plate. The absorbance of samples was measured in a spectrophotometer Infinite 200 PRO NanoQuant at wave lengths of 490 nm and 690 nm. The reference values measured at 690 nm and the values measured from control wells with no cells were subtracted from the values measured at 490 nm.

6.7 Alkaline phosphatase assay

Elevated levels of ALP serve as an osteogenic marker as it is a calcification activity marker (Kadiyala et al. 1997). Measurement of ALP activity was performed in samples, both cultured in static and dynamic conditions. ALP substrate is *p*-Nitrophenyl phosphate (pNPP), a disodium salt. ALP reduces the colourless pNPP to p-nitrophenol, a yellow water-soluble product. This product absorbs light at 405 nm.

6.7.1 Alkaline phosphatase assay protocol

It is important to perform the assay in the dark and to cover the well plate, because the substrate is light sensitive. The assay was performed on day 21 (last day) of the experiment. The assay was performed on the scaffolds previously used for MTS assay, after washing them in PBS.

The reaction was performed in 48-well plates. 350 μL of ALP substrate was added to each well with the scaffolds and the same amount of the reaction substrate was added to 2 control wells

for background subtraction. The incubation period was 10 minutes at room temperature. After 10 minutes scaffolds were removed to Eppendorf tubes for DNA quantification and 175 µL 2M NaOH were added to the wells with ALP substrate to stop the reaction. NaOH stops the conversion of the substrate. 100 µL of the reaction mixture was transferred from each well to empty wells on 96-well plate. The absorbance of samples was measured in a spectrophotometer at wavelength of 405 nm using Infinite 200 PRO NanoQuant. The values measured for control wells were subtracted from the values measured at 405 nm.

6.8 Quantification of DNA

Since the MTS assay does not tell us precisely the number of viable cells, as cell can differ in their metabolic activity in different cell stages, DNA was quantified. The amount of the DNA present in static and dynamic cultures on the scaffolds was measured by the DNA quantitation assay using a fluorescent probe binding double-stranded DNA (dsDNA). Upon DNA binding, the fluorescence of complex DNA-probe enhances many fold, while the intrinsic fluorescence of free PicoGreen (PG) dye was negligible when excited at the same wavelength, around 500 nm (Pradeep et al. 2013). PG dye, of chemical structure 2-(n -bis-(3-dimethylaminopropyl)-amino)-4-(2,3-dihydro-3-methyl-(benzo-1,3-thiazol-2-yl)-methylidene)-1-phenyl-quinolinium, was immobilized by intercalation and electrostatic interactions with the DNA, which resulted in >1000-fold fluorescence enhancement (Dragan et al. 2010a) proportional to the quantity of DNA present (Dragan et al. 2010b).

6.8.1 PicoGreen assay protocol

The assay was performed on day 21 (last day) of the experiment with Quant-iT™ dsDNA Assay Kit per the instruction for use provided by the manufacturer. Scaffolds used in the ALP assay were washed in PBS twice. 400 µL of lysis buffer, consisting of 10mM tris(hydroxymethyl)aminomethan (Tris), 1mM EDTA, 0,2% Triton-X-100 were added separately into 1.5mL Eppendorf tubes. Scaffolds were immersed into the lysis buffer. These samples were stored in the freezer at -20°C and subsequently defrosted and frosted again three times. After each defrosting, the samples were vortexed. Quant-iT™ dsDNA HS Reagent was diluted in ratio 1:200 with Quant-iT™ dsDNA HS buffer. 200 µL of this working solution was added into each well of 96 well black polystyrene microplate corresponding to the number of samples to be measured. 10 µL of 8 DNA standards of bacteriophage lambda were added in duplet to the wells for calibration

curve calculation. 20 µL of the samples from cell lysates were added to the working solution in wells. The fluorescence of the PG reagent was measured in a microplate reader at excitation wavelength of 485 nm and emission wavelength 523 nm. The values measured for standards were used to determine the calibration curve and to subsequently calculate the DNA amount in samples.

6.9 RT-PCR analysis

Quantification of the expression of osteogenic biomarkers at the mRNA level was performed via real-time polymerase chain reaction (qPCR). qPCR is a method that is based on amplification of a specific DNA fragment *in vitro*. Three basic steps are performed and repeated: denaturation of the dsDNA by applying high temperature, hybridization of specific oligonucleotides called primers and DNA template strands and extension of primers. The aim was to test if osteogenic differentiation was induced in the hMSCs cultured on the scaffolds, so mRNA was isolated first, then reverse transcription was performed, making complementary DNA (cDNA) by using primers complementary to RNA. cDNA is used to perform qPCR reaction. RNA samples low in abundance can be detected and reversely transcribed this way and low copy genes can subsequently be amplified and detected. Genes with higher levels of expression in cells committed to osteogenic differentiation are RunX2, type I collagen, BSP and OCN, which the cells were tested for with PCR. RunX2 is associated with activation of osteogenic genes, and OCN and Col1 are bone ECM protein markers. Eukaryotic Translation Elongation Factor 1 Alpha 1 (EEF1A1) is a housekeeping gene serving for relative quantification of mRNA and was amplified by the qPCR as well.

In the course of this work, I have benefited from technical assistance from Mgr. Veronika Hefka Blahnová. She has performed, specifically, PCR analyses of all samples in the experiment run where 5 mL/min flow rate was applied in the perfusion bioreactor.

6.9.1 qPCR protocol

The culture medium was removed, and scaffolds were cut into tiny pieces using forceps and scissors. Then, the RNA was isolated using RNeasy Mini Kit. After the addition of 350 µL of RLT buffer the samples were vortexed and centrifuged at 12000 rpm for 5 minutes. Supernatant was separated and 350 µL of frozen 70% ethanol was added, which precipitates the RNA upon mild mixing. In the next steps a test tube with silica gel was used where the precipitated RNA binds. Firstly, the supernatant was transferred to these test tubes and centrifuged at 10000 rpm for

1 minute. After that, 700 µL of RW1 buffer was added and centrifuged again in the same manner. Then, 500 µL of RPE was added and centrifuged again in the same manner. After following addition of 500 µL of RPE, the samples were centrifuged at 10000 rpm for 2 minutes, and again after emptying the tube for 3 minutes at 12000 rpm. This helps to remove any alcohol that could interfere with PCR fragment production. The last step was releasing the RNA from silica gel, addition of 30 µL of RNA-ase free water and collecting the sample upon centrifugation at 10000 rpm for 1 minute. The samples were stored at -80°C until performed reverse transcription reaction was performed.

Before reverse transcription, RNA concentration of samples was measured. This was done using NanoQuant Plate and microplate reader, by adding 2 µL of samples to the plate and measuring the absorbance at wavelengths 260 nm and 280 nm. The ratio value was used in purity evaluation. RNA samples were diluted with RNA-ase free water, so they all had the maximum 1440 ng/11 µL concentration with regards to maximum amount of DNA being prepared for qPCR reaction. RevertAid First Strand cDNA Synthesis Kit was used to synthesize cDNA. 20 µL of the reaction mixture contained template 645,92-1433,52 ng RNA, 1 µL oligo $(dT)_{18}$ primer, nuclease-free water (12 µL after addition of RNA sample and primers), 4 µL of 5x Reaction buffer, 1 µL of RiboLock Rnase inhibitor and 2 µL of 10 mM dNTP mix. In the end 1 µL reverse transcriptase was added. Two control samples were prepared, one without reverse transcriptase and the other without any RNA sample. All samples were gently mixed and centrifuged. The mixture was incubated at 42°C for 60 minutes, then at 70°C for 5 minutes. The samples were stored at -20°C until qPCR was performed.

TaqMan™ Gene Expression Master Mix, PCR Grade Water and TaqMan Gene Expression Assay containing both primer and probe, depending on desired gene, were used to prepare the mixture for qPCR reaction, which was conducted in thermocycler. In the beginning there was one cycle of pre-incubation at 95°C for 10 minutes, which was followed by 45 cycles of the following amplification sequence: heating the mixture at 95°C for 10 seconds, at 60°C for 30 seconds and at 72°C for 1 second, finally cooling for one cycle at 40°C for 30 seconds. Each gene was evaluated relatively to expression of EEF1A1 using 2-ΔCp method.

6.10 Cell visualization

In order to visualize cell adhesion to the scaffolds, on the last day (21) of the experiment I dyes 3,3'-dihexyloxacarbocyanine iodide ($DiOC_6(3)$) were applied, which stains cell membrane structures at higher concentrations, and-propidium iodide (PI), which binds to dsDNA. DiOC6(3) had excitation wavelength at 488 nm and emission wavelength at 520 nm. PI had excitation wavelength at 560 nm and emission wavelength in the 610/620 nm bandpass.

Scaffolds were washed with PBS and fixed 10 minutes with methanol frosted at -20°C and washed with PBS again. DiOC6(3) was diluted with PBS to a final concentration 1 μg/mL and to each scaffold 500 μL of the working solution was added and incubated for 40 minutes in the dark at room temperature, since the dye is light sensitive. Then, all scaffolds were washed with PBS and PI was added, diluted with PBS as well, in ratio 1:200. The mixture was left to rest for 5 minutes at room temperature. All scaffolds were washed three times in PBS. Stained cells were visualized by confocal microscope LSM 5 DUO. All groups of images compared were acquired with the same settings. LSM Image browser was used to process the images into color-coded projections and to measure cell infiltration. Colour-coding on the images represents the depth of the scanned scaffold plane from which the cell infiltration depth can be determined.

6.11 Statistical analysis

All data are presented as mean values ± standard deviation (SD). Average values were calculated from 5 independent measurements for metabolic activity and quantitation of DNA, 3. independent measurements for ALP activity and 3 independent measurements for qPCR. Statistic values presented in Cell metabolic activity, PicoGreen DNA quantitation and ALP activity sections were evaluated statistically using One-Way Analysis of Variance (ANOVA) (SigmaStat 12.0, Systat, USA) with significance level 0.05. If ANOVA test finds statistically significant differences in the analysed group, Student-Newman-Keuls method was applied. However, in case this method did not find statistically significant differences in the analysed group Dunn or Tukey method was applied (Herve & Williams 2010). If ANOVA test fails, Kruskal-Wallis test by ranks was applied.

7 Results

7.1 Characterization of scaffolds

The melt-blown fibers had a mean diameter of 9.8 ± 5.9 µm. The microfibers formed the main 3D network of the scaffold. The electrospun nanofibers formed a looser network filling the pores in melt-blown fibers. The electrospun fibers had a mean diameter of 719 ± 118 nm. Fraction of nanofibers was ~ 50%. The mean pore size was 69.7 ± 31.1 µm^2. Larger pores reached up to 1450 µm^2 in some areas of the scaffold structure.

7.2 Cell metabolic activity

Cell metabolic activity was measured on the last day (21) of the experiment in all groups and bioreactor runs. The Graph 1 shows that the most metabolically active cells were those cultured statically on tissue culture plastic (further referred to as control) across all groups when compared to their counterparts from the same batch cultured statically on scaffolds (further referred to as static sample).

In the group cultured in the perfusion bioreactor under 1 mL/min flow rate (further referred to as dynamic sample) cells were also less metabolically active than the control group. Overall, the values resulting from dynamic samples are slightly higher than the values resulting from static ones. However, the only significant difference when comparing these 2 groups is observable for cells exposed to flow rate of 1 mL/min in favour of cells from dynamic samples. The differences

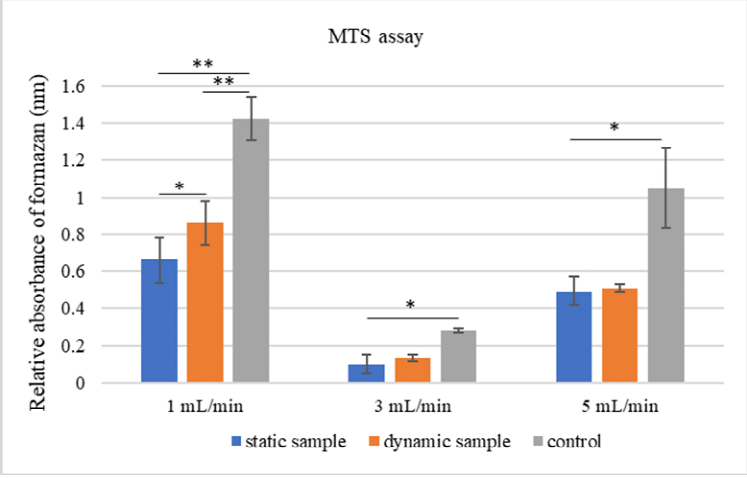

*Graph 1 Metabolic activity of cells evaluated by MTS assay in all 3 experiments. Groups that were evaluated were samples cultured in static conditions – static sample, samples cultured in perfusion bioreactor – dynamic sample, and cells cultured freely in the well plate – control. The absorbance was measured at wavelengths 490 nm and 690 nm and the values represented in the graph are relative. When the differences in the mean values among the treatment groups are greater than would be expected by chance and the statistically significant difference is P<0,001 it is marked by **. When the differences in the median values among the treatment groups are greater than would be expected by chance and the statistically significant difference is P<0,050 it is marked by *.*

in the median values among other groups are not great enough to exclude the possibility that the difference is due to random sampling variability.

7.3 ALP activity

ALP activity was measured on the last day (21) of the experiment in all groups and bioreactor runs. Graph 2 represents values of ALP activity measured in static and dynamic cultures.

In the group cultured in the perfusion bioreactor under 1 mL/min flow rate cells demonstrated a significantly higher activity of ALP than their static counterparts. Values measured for cells in the remaining experimental groups were comparable and the differences in their median values are not great enough to exclude the possibility that the difference is due to random sampling variability.

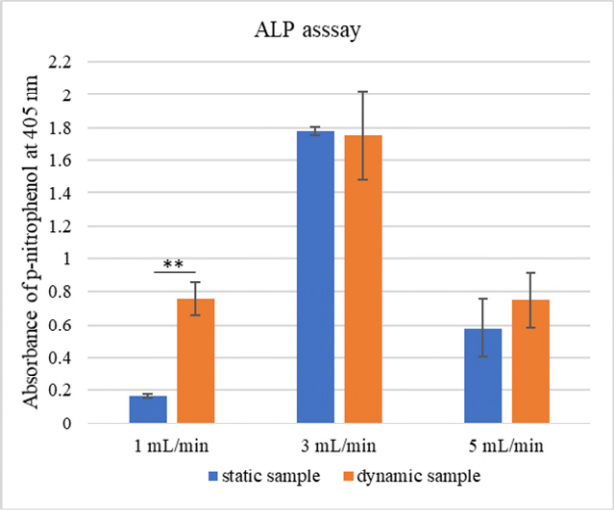

*Graph 2 ALP activity of cells from all 3 experiments. Groups that were evaluated were samples cultured in static conditions – static sample and samples cultured in perfusion bioreactor – dynamic sample. The absorbance was measured at wavelength 405 nm. When the differences in the mean values among the treatment groups are greater than would be expected by chance and the statistically significant difference is P<0,001 it is marked by **.*

7.4 PicoGreen DNA quantitation

DNA quantitation was measured on the last day (21) of the experiment in all groups and bioreactor runs. Graph 3Graph 2 represents values of DNA concentration in static and dynamic cultures calculated based on the PG reagent fluorescence.

In the group cultured in the perfusion bioreactor under 3 mL/min flow rate cells demonstrated a significantly higher DNA amount than their static counterparts. Taking in

consideration high variability of calculated values of DNA concentration in the remaining two experiments, other statistically significant differences were not observed.

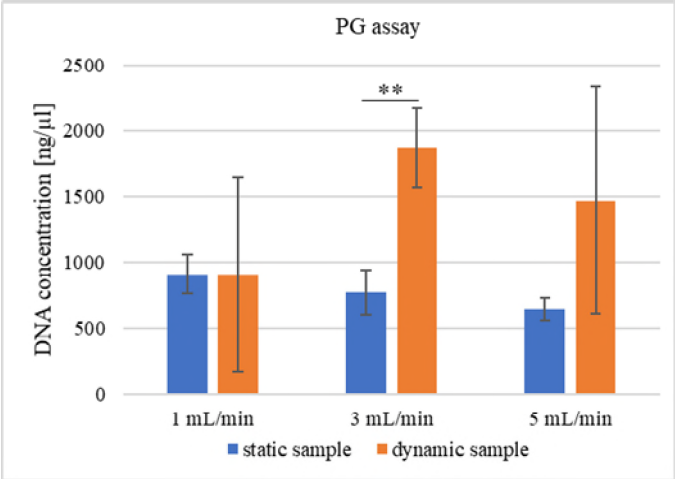

*Graph 3 Quantification of cell DNA from all 3 experiments. Groups that were evaluated were samples cultured in static conditions – static sample and samples cultured in perfusion bioreactor – dynamic sample. The absorbance was measured at wavelength 405 nm. When the differences in the mean values among the treatment groups are greater than would be expected by chance and the statistically significant difference is P<0,001 it is marked by **.*

7.5 qPCR quantification of gene expression

Osteogenic gene expression was measured on the last day (21) of the experiment in all groups and bioreactor runs. The following sections will cover results retrieved for 4 different osteogenic differentiation predictive marker genes levels.

7.5.1 RunX2

Graph 4 represents values of relative mRNA quantity for RunX2. The differences in the median values in other groups are not great enough to exclude the possibility that the difference is due to random sampling variability. There isn't a statistically significant difference.

7.5.2 Type I collagen

Graph 5 Relative expression of type I collagen from all 3 experiments. Groups that were evaluated were samples cultured in static conditions – static sample and samples cultured in perfusion bioreactor – dynamic sample. The quantitation was relativized to the amount of EEF1A1 mRNA and compared between different groups from the same experiment run. represents values of relative mRNA quantity for type I collagen. Significant differences in the median values are observable for several groups of cells.

Cells exposed to flow rate of 1 mL/min expressed higher level of type I collagen than their static counterparts. The differences in the median values in other groups are not great enough to exclude the possibility that the difference is due to random sampling variability.

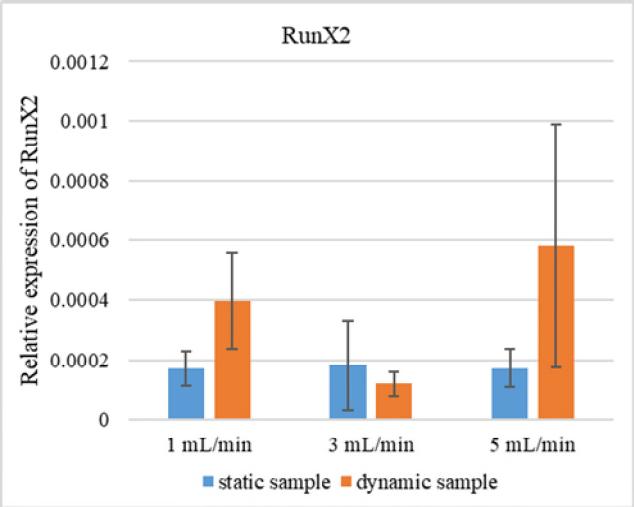

Graph 4 Relative expression of RunX2 from all 3 experiments. Groups that were evaluated were samples cultured in static conditions – static sample and samples cultured in perfusion bioreactor – dynamic sample. The quantitation was relativized to the amount of EEF1A1 mRNA and compared between different groups from the same experiment. The differences in the median values among the treatment groups are not great enough to exclude the possibility that the difference is due to random sampling variability; there isn't a statistically significant difference.

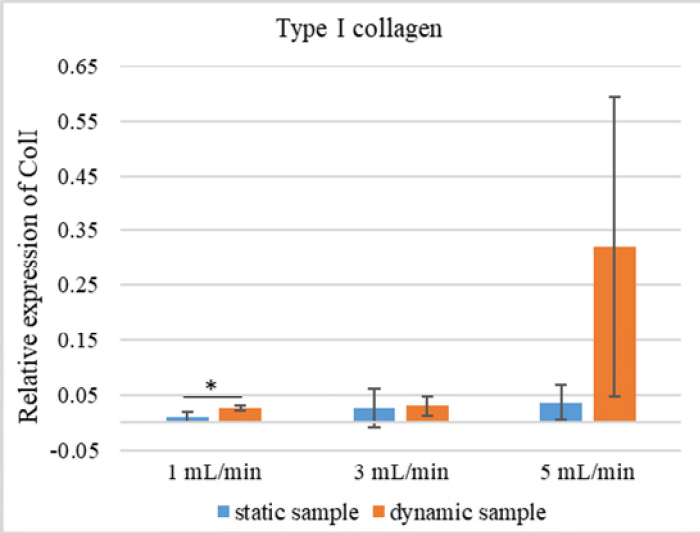

Graph 5 Relative expression of type I collagen from all 3 experiments. Groups that were evaluated were samples cultured in static conditions – static sample and samples cultured in perfusion bioreactor – dynamic sample. The quantitation was relativized to the amount of EEF1A1 mRNA and compared between different groups from the same experiment run. The differences in the median values among the treatment groups are greater than would be expected by chance; there is a statistically significant difference (P <0,050).

7.5.3 OCN

Graph 6 represent values of relative mRNA quantity for OCN. The differences in the median values in other groups are not great enough to exclude the possibility that the difference is due to random sampling variability. There isn't a statistically significant difference.

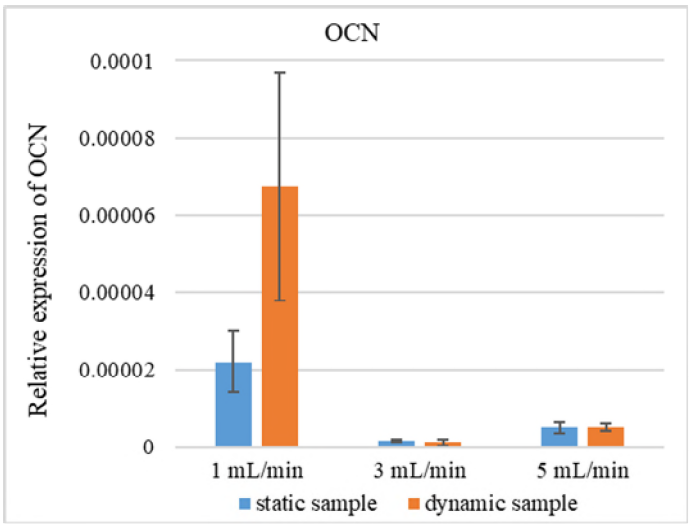

Graph 6 Relative expression of OCN from all 3 experiments. Groups that were evaluated were samples cultured in static conditions – static sample and samples cultured in perfusion bioreactor – dynamic sample. The quantitation was relativized to the amount of EEF1A1 mRNA and compared between different groups from the same experiment. The differences in the median values among the treatment groups are not great enough to exclude the possibility that the difference is due to random sampling variability; there isn't a statistically significant difference.

7.5.4 IBSP

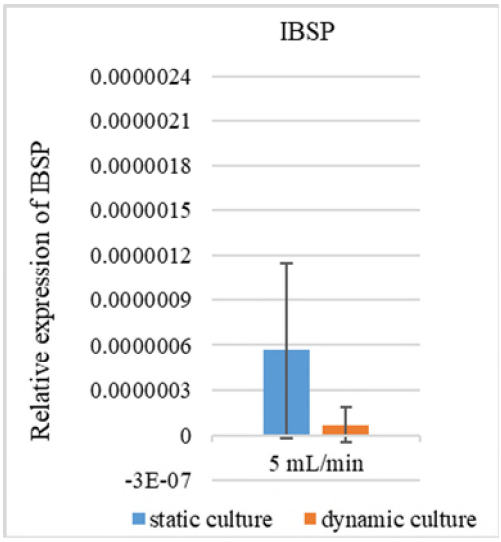

Graph 7 Relative expression IBSP mRNA from the experiment where perfusion bioreactor flow rate was set to 5 mL/min. Groups that were evaluated were samples cultured in static conditions – static sample and samples cultured in perfusion bioreactor – dynamic sample. The quantitation was relativized to the amount of EEF1A1 mRNA and compared between different groups from the same experiment. The differences in the median values among the treatment groups are not great enough to exclude the possibility that the difference is due to random sampling variability; there isn't a statistically significant difference.

Graph 7 represents values of relative mRNA quantity for IBSP. The only experiment where IBSP was possible to evaluate was where 5 mL/min flow rate was applied in the perfusion bioreactor. The differences in the median values between static and dynamic samples are not great enough to exclude the possibility that the difference is due to random sampling variability. In other

2 experiments there was only 1 detected and measurement in each sample type, which was not sufficient to perform statistical analysis.

7.6 Cell visualization

In order to verify cell adhesion, proliferation and infiltration on scaffolds for comparison purposes, confocal microscopy imaging was performed of the scaffolds cultured for 21 days.

7.6.1 Static sample vs dynamic sample 1 mL/min

As seen in Figure 12, the cells seem to adhere and are evenly distributed on the top side of scaffolds of both types of cultures. Top side is for the purposes of evaluation considered to be the side where the cells were seeded. However, from the colour signals that are visually possible to observe, the bottom side of the scaffolds show a difference. The cells seem to have proliferated more on the bottom side of the dynamic sample scaffold cultured in the bioreactor under 1 mL/min flow rate. This would be in agreement with the hypothesis.

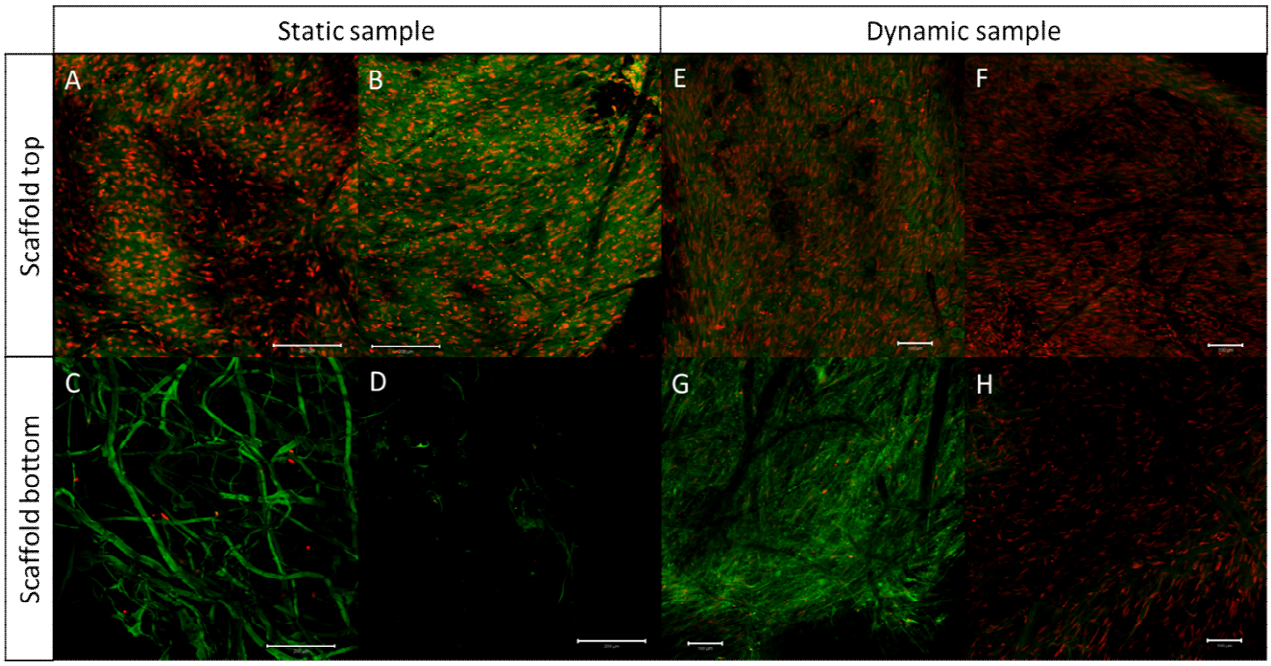

Figure 12 Visualization of cell adhesion and distribution on PCL scaffolds exposed to static and dynamic conditions (1 mL/min) using a confocal microscope. Cell nuclei were stained using PI (red colour) and cell membranes using DiOC6(3) (green colour). For images A, B, C, D magnification was 100 x, scale bar 100 µm. For images E, F, G, H magnification was 100 x, scale bar 200 µm.

Colour-coded projection in Figure 13 shows the depth of the cell infiltration into the scaffold. Both sides, top and bottom, were imaged. The highest value of infiltration from static samples is 100 µm. The highest values from dynamic sample is 90 µm. The values were overall similar in the group of the same sample type and among the groups.

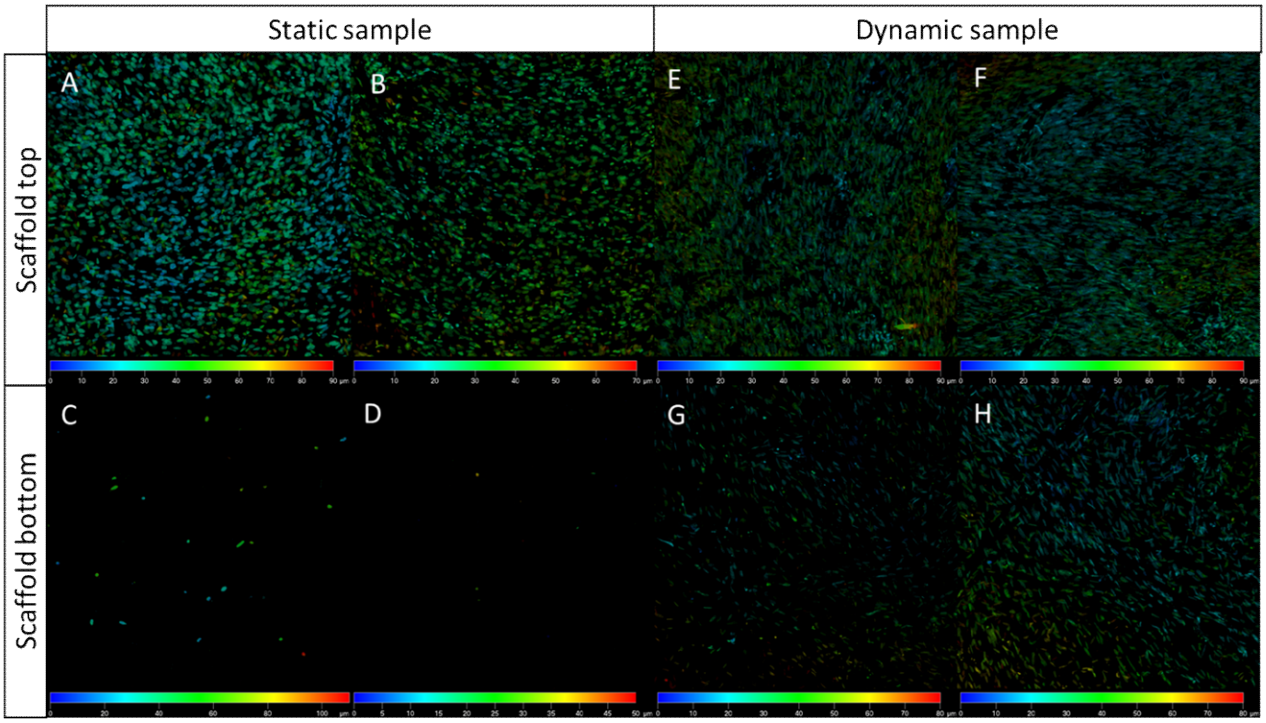

Figure 13 Visualization of the depth of cell infiltration into PCL scaffolds exposed to static and dynamic conditions (1 mL/min) using a confocal microscope. Colour-coding on the images represents the depth of cell infiltration.

7.6.2 Static sample vs dynamic sample 3 mL/min

As seen in Figure 14, the cells seem to adhere on the top side of scaffolds of both types of cultures. Top side of the static samples seems more confluent than the dynamic ones. However, from the colour signals that are visually possible to observe, the bottom side of the scaffolds show a difference. The cells seem to have proliferated more on the bottom side of the dynamic sample scaffold cultured in the bioreactor under 3 mL/min flow rate. This would be in agreement with the hypothesis.

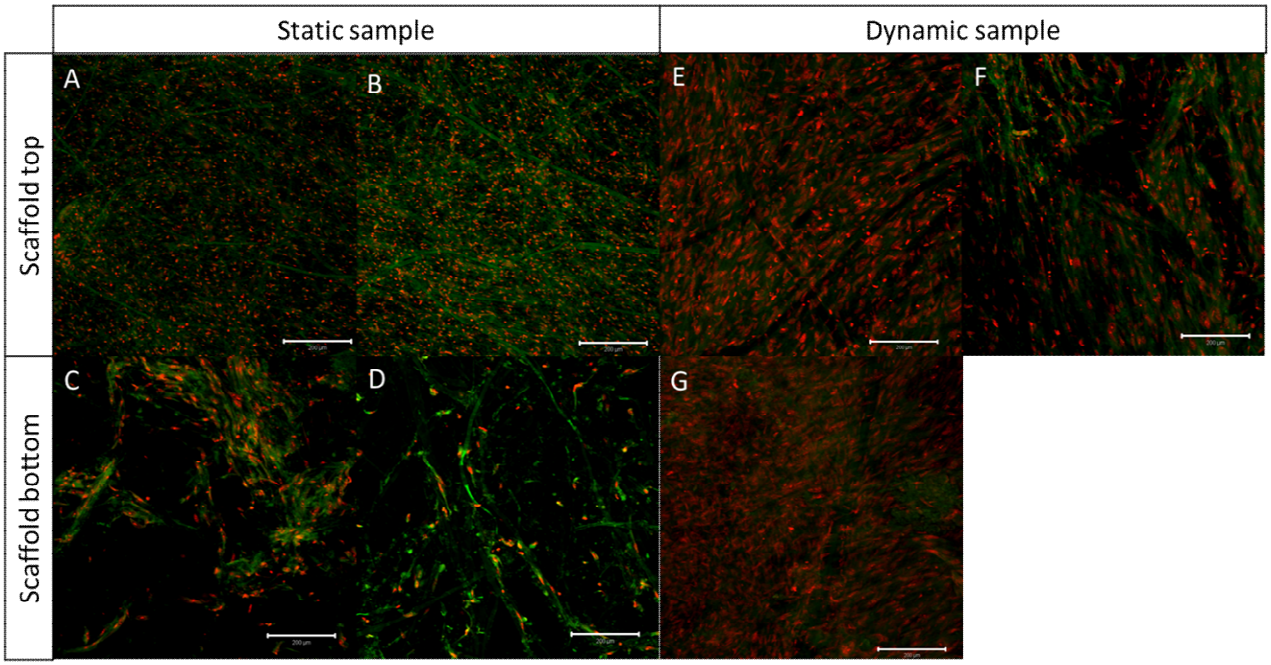

Figure 14 Visualization of cell adhesion and distribution on PCL scaffolds exposed to static and dynamic conditions (3 mL/min) using a confocal microscope. Cell nuclei were stained using PI (red colour) and cell membranes using DiOC6(3) (green colour. Magnification was 100 x, scale bar 200 µm.

Colour-coded projection in Figure 15 shows the depth of the cell infiltration into the scaffold. Both sides, top and bottom, were imaged. The highest value of infiltration from static

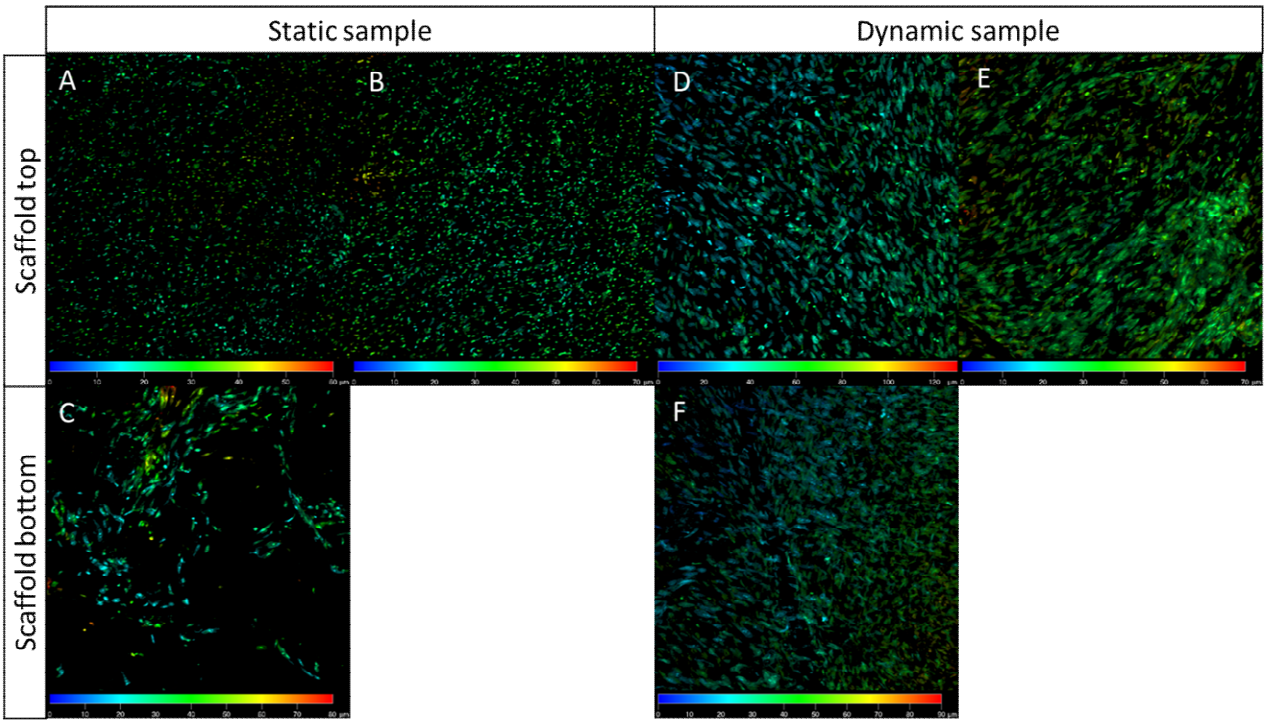

Figure 15 Visualization of the depth of cell infiltration into PCL scaffolds exposed to static and dynamic conditions (3 mL/min) using a confocal microscope. Colour-coding on the images represents the depth of cell infiltration.

samples is 70 µm. The highest values from dynamic sample is 120 µm and it is a result of infiltration of the cells from the top. The values for infiltration of cells from the bottom in both scaffold groups was similar (80-90 µm) This results is comparable with the result for the depth measurement from the group in the previous section Static sample vs dynamic sample 1 mL/min).

7.6.3 Static sample vs dynamic sample 5 mL/min

As seen in Figure 16, the cells seem to adhere and are evenly distributed on the top side of scaffolds of both types of samples. However, from the colour signals that are visually possible to observe, the bottom side of the scaffolds show a difference. The cells seem to have proliferated more on the bottom side of the dynamic sample scaffold cultured in the bioreactor under 5 mL/min flow rate. This would be in agreement with the hypothesis.

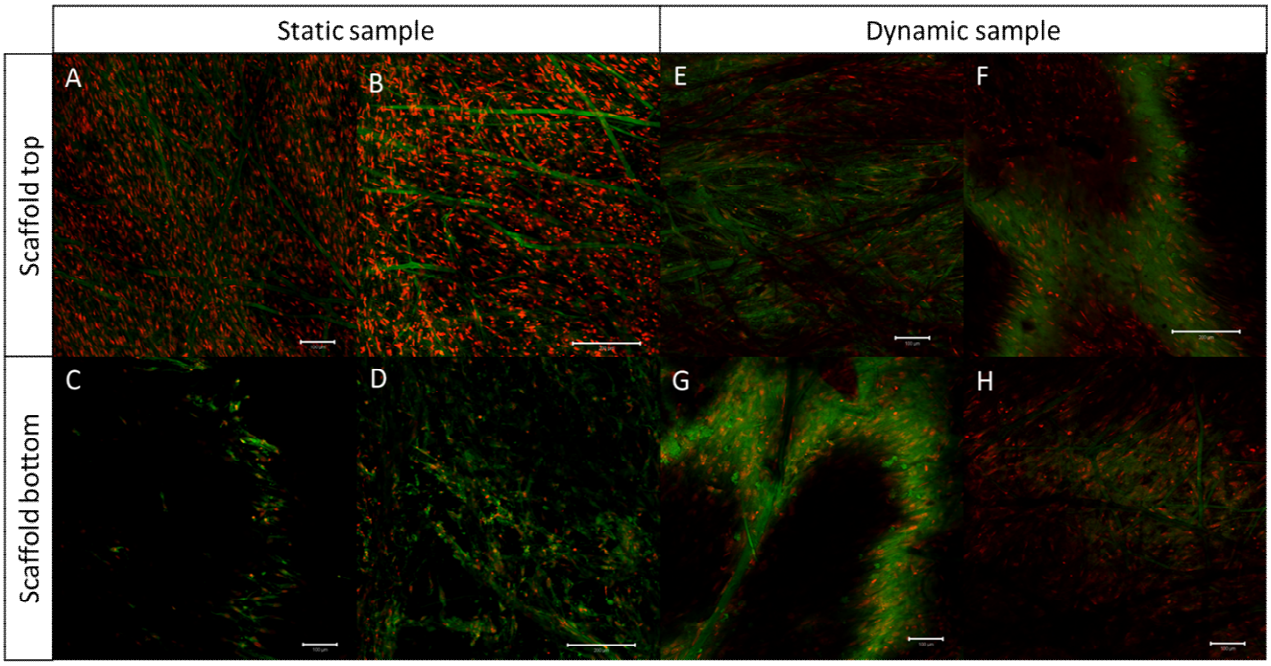

Figure 16 Visualization of cell adhesion and distribution on PCL scaffolds exposed to static and dynamic conditions (3 mL/min) using a confocal microscope. Cell nuclei were stained using PI (red colour) and cell membranes using DiOC6(3) (green colour). For images A,C, E, G and H magnification was 100 x, scale bar 100 µm. For images B, D and F magnification was 100 x, scale bar 200 µm.

Colour-coded projection in Figure 17 shows the depth of the cell infiltration into the scaffold. Both sides, top and bottom, were imaged. The highest value of infiltration from the top in static samples is 100 µm. The highest values of infiltration from the top in dynamic sample is 80 µm. These results are comparable to previous observation for all groups in all experiments. The highest value for infiltration of cells from the bottom is in the static sample and is 200 µm. The

values for the dynamic sample are similar to previous observations (80-100 µm) for the same type of sample regardless of the flow rate applied.

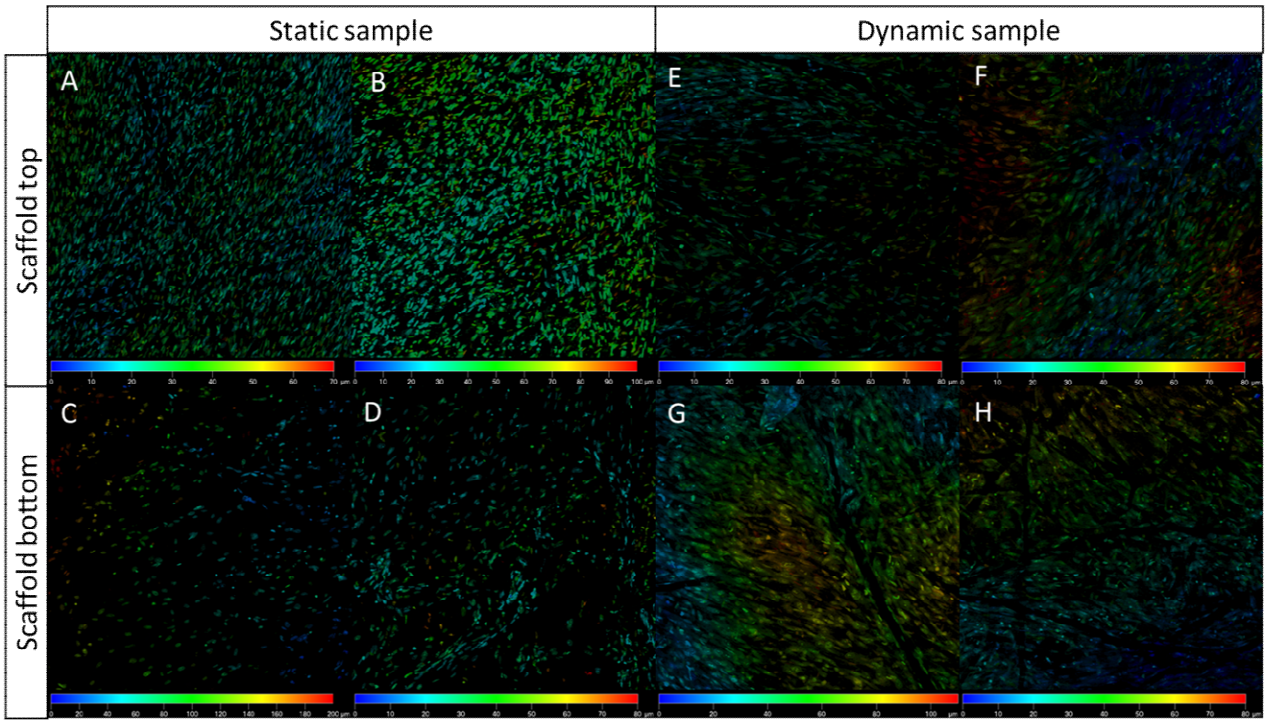

Figure 17 Visualization of the depth of cell infiltration into PCL scaffolds exposed to static and dynamic conditions (1 mL/min) using a confocal microscope. Colour-coding on the images represents the depth of cell infiltration.

8 Discussion

The goal of tissue engineering is to produce functional tissue implants. Not only are these implants supposed to support tissue healing and re-establishment of the damaged tissue function, but they should provide patients with a certain level of comfort during the treatment. This is ensured by testing growth and differentiation of cells on different types of biomaterials. These materials are supposed to provide cells with mechanical support and can be exposed to chemical and physical stimuli. Nowadays, stem cells have a big traction in the tissue engineering field, and it is possible to isolate and expand some types of stem cells to large quantities. In case of bone tissue engineering, the differentiation of stem cells into osteogenic progenitors is the key to regenerate bone defects (Bohner and Miron 2019). That is why MSCs and their differentiation into osteogenic lineage are strategically used to produce successful bone implants.

One of the strategies to achieve this, besides the use of a differentiation medium with osteoinductive properties, per the observation of Bancroft et al. (2002) and other authors (Gomes et al. 2006; Correia et al. 2013; Grayson et al. 2011; Volkmer et al. 2008; Kleinhans et al. 2015; Egger et al. 2017) , is the use of culture bioreactors in which cells are subjected to mechanical stress. Bone cells are continuously exposed to the fluid shear stress produced by the flow of the interstitial fluid flow in the lacunar-canalicular network. So, in order to target MSC differentiation into osteoblasts I used a perfusion bioreactor to mimic the interstitial flow, given that this is not something achievable in the classic culturing in static conditions. A convention on how to culture cells under dynamic conditions, especially for different dynamic systems, does not currently exist. For this reason, it was necessary to search for the optimal conditions with regards to the flow rate in which the cells would proliferate, differentiate, and infiltrate the 3D scaffold.

To obtain a sufficient amount of MSCs to perform several experiments it was necessary to expand them. However, sequential passage and the age of the donor can affect the characteristics of MSCs in terms of their proliferation rate, multipotency and surface marker expression (Muraglia et al. 2000; Prockop 2009; Stolzing et al. 2008). I could not use cells of the same origin for all bioreactor runs due to the configuration of the bioreactor and the length of the bioreactor run, samples in this work that were cultured under dynamic conditions were seeded with the same cells as the samples cultured under static conditions they were compared with. Different dynamic

sample groups were not compared against each other. The differences in MSC behaviour between the dynamic and static group can potentially reveal the direction that should be taken in order to improve the osteoinduction on 3D scaffolds such as PCL.

The effect of the static and dynamic culture of the MSCs seeded on scaffold was compared in the sense of cell penetration into the scaffolds, cell metabolic activity and proliferation, ALP activity and gene expression of four osteogenic markers. Based on the results retrieved from the cell metabolic activity assay, cells from all groups and experiments described in this paper showed some level of metabolic activity. Most metabolically active cells were the cells that were cultured only on tissue culture plastic. They showed superior metabolic activity over all static samples and the dynamic samples cultured under 1 mL/min flow rate. This is assumed to be related to the relatively undisturbed culturing process in the wells, as well as the duration of the experiment. These cells were receiving fresh medium at set intervals, the tissue culture plastic of the wells is coated for adherence and growth of cells. The cells did not have to infiltrate the scaffold, and there was no external force disrupting their attachment. They did, however, have a surface limitation especially taking into account that the cells were seeded in high density. Another factor that influenced this result is that 100% of the seeded cells remained in the tissue culture plastic samples. This is not the case with cells that were seeded on the scaffolds. First, usually not all seeded cells actually adhere to the scaffold and second, the scaffolds of the dynamic samples were moved from the well plate where the seeding was performed to the bioreactor. These factors that may have lowered the cell numbers on scaffolds, thereby impacting the results of the metabolic activity assay. As for the differences between static and dynamic samples - the only significant difference is observed for samples cultured under 1 mL/min. This rate had a supportive effect and resulted in an increase in the rate of metabolic activity, which is in agreement with findings by Egger et al. (2017) and Guyot et al. (2015). In case of samples that were exposed to 3 and 5 mL/min flow rate they had a statistically comparable level of cell metabolic activity as the respective control, however, they were not superior to the values measured in the static samples. Yaghoobi et al. (2019) investigated effect of perfusion flow at 2 and 4.5 mL/min on cells cultured on nanohydroxyapatite-PCL cellular multilayer electrospun scaffolds that were under and without perfusion flow and they also found no difference in cell metabolic activity between static and dynamic samples.

Because the cell metabolic activity is not necessarily proportional to the cell number, as their metabolic activity can differ besides examining the metabolic activity, DNA quantitation analysis was also performed. The results of this analysis demonstrate that almost all cells were proliferating comparably under all culturing conditions. Perfusion flow seemingly had a statistically significant impact in increasing the proliferation only when the cells were exposed to 3 mL/min flow rate ($P<0.001$). When compared to a study where to 0.3, 1 and 3 mL/min flow rates were examined (Bancroft et al. 2002), my result seems to be in a disagreement as 1 mL/min flow rate resulted in the highest proliferation rate. Two studies, one done with mouse osteoblasts-like MC 3T3-E1 cells seeded on porous tricalcium phosphate scaffold, and the other with rat bone marrow MSCs seeded on PCL fiber meshes have also tested 1 mL/min flow rate on the dynamic samples. In both cases it influenced the cells to proliferate more than the cell of the static cultures after 6 and 15 days respectively; however higher flow rates were not applied in these studies (Du et al. 2009; Gomes et al. 2006).

Cells exhibited normal morphology and established a monolayer on the top of all scaffolds spreading over the fibers as observed in the confocal microscope. Qualitative assessment of the bottom of the scaffolds demonstrates that cells were able to adhere to them and to proliferate to some extent in all conditions. These findings are consistent with positive cell metabolic activity measured for the samples by the MTS assay and cell proliferative activity measured by PG assay. Activity of the cells in the middle of 3D tissue scaffolds in static culture is usually lower than the activity on the periphery. This is a consequence of culture medium transport limitations. I expected also that cells would be infiltrating the scaffold when exposed to the medium flow and that a difference between the static and dynamic samples would be noticeable when visualized under the microscope based on a study performed by Rampichová et al. (2018), when the cells managed to penetrate the scaffold 250 μm. Bancroft et al. (2002) imaged the surface and cross-sections of 3D titanium mesh seeded with rat BMSCs. These scaffolds were cultured for 16 days under 0.3 mL/min, 1 mL/min and 3 mL/min. The most uniform distributions of cells was reached under the highest flow rate. Individual cells were seen lining the pores and scaffolds deeper than 120 μm, which was the maximum depth of migration noticed in the dynamic samples in my experiments. On the other hand, inhomogeneous cell distribution was found by Du et al. (2009) for unidirectional flow rate 1 mL/min after 6 days. The osteoblast-like cells showed penetration in the top 4 mm of the scaffold, however scaffold used in that study and here are not the same.

Taking into consideration the pore size of scaffolds it is possible that the density of cells upon seeding had an impact on their penetration. The proportion of nanofibers in the scaffolds I used was ~ 50%, whereas in the study (Rampichová et al. 2018) my assumption was based on the scaffold nanofiber proportion was much lower, it was 9%. It is possible that the proportion of the nanofibers in the scaffolds was too high and that it resulted in decreased pore sizes and subsequent low penetration. The cells might have interacted with each other and created on top of the scaffolds a cell layer thick enough to prevent further penetration to be heavily influenced by the perfusion.

To evaluate the osteoblast phenotype, I investigated the expression profile of mineralization-related marker genes - the OCN, ColI and IBSP, the osteogenic activation gene RunX2, and the activity of ALP. ALP activity of the cells in the scaffolds, an early marker of osteoblastic differentiation (Y. Chen et al. 2012), was significantly higher in dynamic samples cultured under flow rate 1 mL/min ($P<0.001$) than in the static samples. Higher flow rates did not show any significant effect on ALP activity when compared to their static counterparts, which is in agreement with Yaghoobi et al. (2019). They found that the samples cultured without mechanical stimulation under 2 and 4.5 mL/min flow rates did not demonstrate any difference in ALP activity between static and dynamic samples after 14 days. In another study by Yaghoobi et al. (2016), greater ALP activity was observed in the dynamic samples than that of the static culture in the compact nanohydroxyapatite-PCL cellular multilayer electrospun scaffolds cultured under flow rate 1 mL/min for 7 days. A difference in ALP activity across 16 days was noted by Bancroft et al. (2002). ALP of cells under all tested flow rates (0.3, 1 and 3 mL/min) was more active than in the static culture. On the contrary to the described findings, research has also shown a lack of difference between dynamic and static samples under flow rate 1 mL/min, however the cells and the scaffold material was different and culturing period was shorter to the ones I used (Du et al. 2009).

Actively proliferating cells committed to osteogenic lineage express collagen type I relatively early, which is followed by a period of down-regulation. Then the ALP is maximally expressed indicating the period of ECM maturation. Only after this expression sequence is the ECM competent for mineralization (Owen et al. 1990). As for RunX2, it appears earliest in osteoblastogenesis and remains present during cell maturation in varying levels (Marie 2008). Research showed that its expression peaks within the first 14 days of cell dynamic osteogenic

stimulation depending on cellular microenvironment and shear stress stimulation (Sellgren & Ma 2015; Yaghoobi et al. 2019; Kleinhans et al. 2015). This gene here was not expressed with a statistical significance in any of the samples across all groups. Results retrieved for ALP activity and gene expression of collagen type I for cells cultured under flow rate 1 mL/min were increased in comparison to their static counterparts. This suggests that these cells might have started differentiating into osteoblasts and that could be an explanation why RunX2 expression was not higher in the dynamic sample. Moreover, the activity of ALP over 21 days, which was the actual length of the experiment, points to osteogenic differentiation (Pittenger et al. 1999). OCN is a late-stage marker of osteogenic differentiation and its expression follows the onset of mineralization. This happens after the ALP concentration has peaked as ALP is most active and needed in preparation for mineralization (Owen et al. 1990; Li et al. 2009). ALP hydrolyses PPi allowing for formation of HA to which the OCN binds to (Pikner R et al. 2020). It is possible that the cells cultured under flow rate 1 mL/min haven't reached the stage of mature osteoblast and ECM mineralization because OCN was not yet expressed on a level of statistical significance in the duration of the experiment. It is also known that the ALP activity is associated with the end of proliferation (Owen et al. 1990), hence the result obtained from PG assay for this flow rate showing comparable proliferation between static and dynamic samples could be a consequence of the cells moving from proliferation to maturation phase. Lastly, the IBSP is observed in fully differentiated osteoblasts. In addition, IBSP detection, was successful only in 1 sample per culture group. Therefore, a meaningful assessment could not be performed. In order to detect the late-stage osteogenic markers, such as IBSP, the experiment duration might have been insufficient.

Whereas the flow rate 1 mL/min looks promising with regards to osteoblastogenesis, flow rate 3 mL/min was seen, in this case, only to increase cell proliferation. Cell proliferation and differentiation are mutually exclusive events; therefore, low levels of cell proliferation are not unpredictable once the cell are equipped with high differentiation stimuli (both biochemical and biomechanical). Similarly, in cells cultured under flow rate 5 mL/min none of the performed analysis showed any significantly superior result in comparison with static culture with regards to viability, proliferation or differentiation. It is possible that increasing flow rate was excessively high and that it leads to contact inhibition and detachment from the culture surface, which would keep these cells in different phases. To set in motion a cascade of events leading to commitment to osteogenic differentiation, the MSCs need the initial adhesion to the biomaterials (Chastain et

al. 2006). Therefore, cell cultured under flow rate 5 mL/min might have been detaching and perpetually trying to adhere. As for the flow rate 3 mL/min - it may be sufficient for the cells to adhere and thrive, however, not to differentiate.

The data available in published literature on the topic of cell proliferation and osteogenic differentiation in perfusion bioreactor is quite ambiguous. In addition, the data is scarce when taken into account that the perfusion bioreactors can differ and that the scaffold materials, cell types and flow rates used are diverse. That is why I cannot unequivocally confirm nor deny past findings. Yet, a trend can be observed for a range of flow rates that positively impact cells in proliferation and commitment to osteogenic lineage. The range falls between 0.2-3 mL/min as per the beforementioned observations of Bancroft et al. (2002), Gaspar et al. (2012) and Mehrian et al. (2018). In the bioreactor system used here the most beneficial out of the three examined flow rates to culture hMSCs on PCL with the intent to differentiate them into osteoblasts is 1 mL/min and the most beneficial to support cell proliferation is 3 mL/min.

The limitation of this study is, firstly, the fact that the scaffolds were tested *in vitro*. *In vivo* the hMSCs may behave in a different manner, and once introduced into the body it is possible they do not secrete the same cytokines or their concentrations that have been observed *in vitro*. Secondly the number of samples in dynamic conditions was a limiting factor due to the construct of the bioreactor. It was possible to culture cells on up to 12 scaffolds at the same time. Thus, it was necessary to strategize the use of the scaffolds in the post-experiment analyses. Higher number of samples would have resulted in a higher number of possible measurements per experiment. In my case this has proven to be restrictive especially in the RNA analysis of osteogenic gene markers, and it has had, to a certain extent, an impact on undertaken statistical tests.

Furthermore, cell seeding on 3D scaffold is a challenging task when creating optimal strategy for dynamic cell culturing (Vunjak-Novakovic et al. 1998), especially when cells are seeded in high concentration. The typical approach is static cell seeding to which there are dynamic alternatives encouraging the cells to infiltrate the scaffold more at the very beginning. Dynamic seeding techniques are reported to be highly efficient in seeding and even cell distribution. Those include seeding in the beforementioned spinner flasks in which the cells are a part of the suspension being stirred by a magnetic bar (Vunjak-Novakovic et al. 1998), or techniques using perfusion bioreactors and oscillation (Weinand et al. 2009; Alvarez-Barreto & Sikavitsas 2007; Du et al.

2009). Other techniques of dynamic cell seeding are centrifugal (Roh et al. 2007), beforementioned rotating cell seeding (Freed & Vunjak-Novakovic 1995), and agitation with an orbital shaker (B.-S. Kim et al. 1998). For successful seeding it is important of course to choose favourable parameters, such as material and architecture of the scaffold, source cells, etc. In this work cells were incubated for 2 hours on scaffolds after static seeding. Cells were seeded in high concentration to increase the proliferative capacity and confluence which induces osteogenic differentiation (Abo-Aziza & Zaki 2017). Per the images taken by the confocal microscope we could observe low cell infiltration which confirms that static seeding on 3D scaffolds has low efficiency (Fahimipour et al. 2019; Luo et al. 2013). This is the reason why I believe that an effort to improve cell seeding would increase the efficiency of cell migration and evenly distribute the cells in the interior of the scaffold, which could in turn lead to tissue formation.

Bone tissue formation in vivo happens under fluid shear stress. The fluid flow of the culture medium in the bioreactor not only continuously delivers the nutrients, but also exerts mechanical stress. However, the stress and the fluid flow rate are not directly proportional. Stress is a function of the flow rate, configuration of the bioreactor, medium viscosity, scaffold architecture and porosity (Hadida and Marchat 2020; Guyot et al. 2015). To make things more complex, with cell growth and new tissue formation the environment of the scaffold changes too. Therefore the estimation of the shear stress values experienced by cells in the beginning and throughout the experiment duration are not the same as proven by computational strategies (Guyot et al. 2015). During my experiments I have applied only one flow rate in the bioreactor runs. This was a limiting factor, per the observations of the bone formation and computational models, as it did not take into account the filling of the scaffolds over time and the need to re-adjust the system. It appears however the most important parameter in culturing in the perfusion bioreactor is to be aware of the shear stress values at all times and to control it. This was not a possibility for the bioreactor that I used. This leads to another valuable point, which is the limitations in the bioreactor design.

There are different perfusion bioreactor systems described in literature, some commercial some self-made. Apart from being different in the number of samples they are able to support, and the features available, such as valves, real-time cell observation and medium exchange, they can differ in the direction and type of applied flow and pressure. When comparing unidirectional perfusion and oscillatory flow tested on mouse osteo-blast-like MC 3T3-E1 cells research shows

the 3D ceramic scaffolds cultured by the oscillatory flow under 0.5 mL/min had a more uniform distribution of cells throughout in comparison to inhomogeneous distribution of cells grown in unidirectional perfusion under 1 mL/min. The ALP activity was higher in the oscillatory flow group in the 6 days of the experiment duration, but the proliferation was higher in the unidirectional flow group. Based on this study the continuous medium flow is better for cell proliferation, whereas the oscillatory perfusion is more meaningful in induction of osteogenesis (Du et al.2009). Another study compared continuous and intermittent pulsatile perfusion individually with the combination of both, with a duration of five weeks. The best osteogenic results were yielded when the human adipose stem cells cultured on porous 3D silk fibroin scaffolds were exposed not only to continuous or pulsatile flow but to their combination. Two weeks of continuous flow and three weeks of pulsatile flow produced the highest osteopontin and bone sialoprotein deposition and the corresponding gene expression, calcification and bone volume. It is important to note that those cells were first exposed to continuous flow to "pre-differentiate" them (Correia et al. 2013). Taking this into consideration, it may be interesting to test the continuous flow in combination with pulsatile or oscillatory, as it seems that it could lead to bone tissue formation in PCL scaffolds.

Another thing that could be beneficial to try, based on the bone marker gene expression results, is comparing not only different flow rates against the static culture, but also different durations of the bioreactor run against each other and static culture. Firstly, this could help to have an overview of gene expression levels over time. Secondly, late osteoblastogenesis markers, such as IBSP, could be detected. In order to confirm the findings of gene expression analysis, immunostaining OCN could be performed to visualize protein deposition in the scaffolds. As higher proteins deposition increases the shear stress in the scaffolds, the flow rates could be altered in a single bioreactor run as well. Lastly, since the flow rate 1 mL/min was the lowest used in my work, and it demonstrated positive results with regards to osteoblastogenesis, while the higher flow rate did not, administration of a lower flow could further characterize the conditions of osteogenic differentiation under perfusion flow.

9 Conclusion

A bone tissue engineering model consisting of hMSCs cultured on electrospun/melt-blown PCL scaffolds in a perfusion bioreactor with continuous flow of culture medium was used to investigate the effects of three different flow rates in comparison to static culture. My hypothesis was that the 3D environment of scaffold and mechanic stimulation will stimulate MSCs more, in comparison to the static culture, to proliferate and differentiate into osteoblasts. The results of my work suggest that the flow configuration in the bioreactor enables the creation of culture environment with re-distribution of medium and some mechanical stimulation for hMSC osteogenic differentiation. It was possible to direct cellular behaviour within 3D scaffolds via modulation of perfusion flow rate. Low perfusion flow rate of 1 mL/min improved differentiation, whereas higher flow rate of 3 mL/min increased the cell mass. In general, a positive effect on metabolic activity, proliferation and osteogenic differentiation of hMSCs in the presence of perfusion flow was proven. Cell migration was not effective under any of the chosen flow rates. It is expected that the use of dynamic seeding technique would further enhance cell distribution and infiltration in the scaffold and subsequent tissue formation.

Differences in the architecture and in the porosity of the scaffolds utilized in perfusion studies result in different shear stress values that cells are exposed to in the scaffold surfaces. I used a perfusion bioreactor system to describe if and how modifying the flow rate through 3D scaffold impacts influences cell viability, proliferation, distribution and expression of osteogenic markers. The flow rate of the medium remains an important operational factor and requires further investigation, in combination with the fluid shear stress. Longer term studies measuring the effect of perfusion are needed to further characterize hMSC behaviour in 3D environment and optimize perfusion systems to overcome limitations of in vitro diffusion into scaffolds, while applying appropriate mechanical stimuli.

10 References

Abbasi, N., Lee, R. S. B., Ivanovski, S., Love, R. M., & Hamlet, S. (2020). In vivo bone regeneration assessment of offset and gradient melt electrowritten (MEW) PCL scaffolds. Biomaterials Research, 24(1), 1–24. https://doi.org/10.1186/S40824-020-00196-1/FIGURES/15

Abdallah, B. M., and M. Kassem. 2007. "Human Mesenchymal Stem Cells: From Basic Biology to Clinical Applications." Gene Therapy 2008 15:2 15 (2): 109–16. https://doi.org/10.1038/sj.gt.3303067.

Abo-Aziza, Faten A.M., and A. A. Zaki. 2017. "The Impact of Confluence on Bone Marrow Mesenchymal Stem (BMMSC) Proliferation and Osteogenic Differentiation." International Journal of Hematology-Oncology and Stem Cell Research 11 (2): 121. /pmc/articles/PMC5575725/.

Aenlle, Kristina K., Kevin M. Curtis, Bernard A. Roos, and Guy A. Howard. 2014. "Hepatocyte Growth Factor and P38 Promote Osteogenic Differentiation of Human Mesenchymal Stem Cells." Molecular Endocrinology 28 (5): 722–30. https://doi.org/10.1210/ME.2013-1286.

Aerssens, J., S. Boonen, J. Joly, and J. Dequeker. 1997. "Variations in Trabecular Bone Composition with Anatomical Site and Age: Potential Implications for Bone Quality Assessment." The Journal of Endocrinology 155 (3): 411–21. https://doi.org/10.1677/JOE.0.1550411.

Aguilar-Reyes, E. A., C. A. León-Patiño, B. Jacinto-Díaz, E. Perdomo-Cervantes, and L. P. Lefebvre. 2010. "Synthesis of 45S5 Bioglass® Foams by a Powder Metallurgy Approach." Materials Science and Technology Conference and Exhibition 2010, MS and T'10 1: 70–77.

Aguilar-Reyes, E. A., León-Patiño, C. A., Jacinto-Díaz, B., Perdomo-Cervantes, E., & Lefebvre, L. P. (2010). Synthesis of 45S5 Bioglass® foams by a powder metallurgy approach. Materials Science and Technology Conference and Exhibition 2010, MS and T'10, 1, 70–77.

Ahmed, E. M. (2015). Hydrogel: Preparation, characterization, and applications: A review. Journal of advanced research, 6(2), 105-121.

Akter, F., and J. Ibanez. 2016. "Bone and Cartilage Tissue Engineering." Tissue Engineering Made Easy, January, 77–97. https://doi.org/10.1016/B978-0-12-805361-4.00008-4.

Al-Bari, Abdul Alim, and Abdullah Al Mamun. 2020. "Current Advances in Regulation of Bone Homeostasis." FASEB BioAdvances 2 (11): 668–79. https://doi.org/10.1096/FBA.2020-00058.

Ali, A. Afshan, Robert S. Weinstein, Scott A. Stewart, A. Michael Parfitt, Stavros C. Manolagas, and Robert L. Jilka. 2005. "Rosiglitazone Causes Bone Loss in Mice by Suppressing Osteoblast Differentiation and Bone Formation." Endocrinology 146 (3): 1226–35. https://doi.org/10.1210/EN.2004-0735.

Alvarez-Barreto, Jose F., and Vassilios I. Sikavitsas. 2007. "Improved Mesenchymal Stem Cell Seeding on RGD-Modified Poly(L-Lactic Acid) Scaffolds Using Flow Perfusion." Macromolecular Bioscience 7 (5): 579–88. https://doi.org/10.1002/MABI.200600280.

Andalib, M. N., Lee, J. S., Ha, L., Dzenis, Y., & Lim, J. Y. (2016). Focal adhesion kinase regulation in stem cell alignment and spreading on nanofibers. Biochemical and Biophysical Research Communications, 473(4), 920–925. https://doi.org/10.1016/J.BBRC.2016.03.151

Andalib, Mohammad Nahid, Jeong Soon Lee, Ligyeom Ha, Yuris Dzenis, and Jung Yul Lim. 2016. “Focal Adhesion Kinase Regulation in Stem Cell Alignment and Spreading on Nanofibers.” Biochemical and Biophysical Research Communications 473 (4): 920–25. https://doi.org/10.1016/J.BBRC.2016.03.151.

Anderson, H. Clarke. 2003. “Matrix Vesicles and Calcification.” Current Rheumatology Reports 2003 5:3 5 (3): 222–26. https://doi.org/10.1007/S11926-003-0071-Z.

Andrades, Jose A. 2013. “Regenerative Medicine and Tissue Engineering.” Regenerative Medicine and Tissue Engineering, May. https://doi.org/10.5772/46192.

Andrades, José A., B. Han, M. E. Nimni, D. C. Ertl, R. J. Simpkins, M. P. Arrabal, and J. Becerra. 2009. “A Modified RhTGF-B1 and RhBMP-2 Are Effective in Initiating a Chondro-Osseous Differentiation Pathway in Bone Marrow Cells Cultured In Vitro.” Http://Dx.Doi.Org/10.1080/03008200390229912 44 (3–4): 188–97. https://doi.org/10.1080/03008200390229912.

Atashi, Fatemeh, Ali Modarressi, and Michael S. Pepper. 2015. “The Role of Reactive Oxygen Species in Mesenchymal Stem Cell Adipogenic and Osteogenic Differentiation: A Review.” Stem Cells and Development 24 (10): 1150–63. https://doi.org/10.1089/SCD.2014.0484/ASSET/IMAGES/LARGE/FIGURE5.JPEG.

Athanasiou, K. A., Agrawal, C. M., Barber, F. A., & Burkhart, S. S. (1998). Orthopaedic applications for PLA-PGA biodegradable polymers. Arthroscopy: The Journal of Arthroscopic & Related Surgery, 14(7), 726-737.

Bai, Yan, Peipei Li, Guangfu Yin, Zhongbing Huang, Xiaoming Liao, Xianchun Chen, and Yadong Yao. 2013. “BMP-2, VEGF and BFGF Synergistically Promote the Osteogenic Differentiation of Rat Bone Marrow-Derived Mesenchymal Stem Cells.” Biotechnology Letters 35 (3): 301–8. https://doi.org/10.1007/S10529-012-1084-3/FIGURES/5.

Balogh, Enikő, György Paragh, and Viktória Jeney. 2018. “Influence of Iron on Bone Homeostasis.” Pharmaceuticals 2018, Vol. 11, Page 107 11 (4): 107. https://doi.org/10.3390/PH11040107.

Bancroft, Gregory N., Vassilios I. Sikavitsas, Juliette Van Den Dolder, Tiffany L. Sheffield, Catherine G. Ambrose, John A. Jansen, and Antonios G. Mikos. 2002. “Fluid Flow Increases Mineralized Matrix Deposition in 3D Perfusion Culture of Marrow Stromal Osteoblasts in a Dose-Dependent Manner.” Proceedings of the National Academy of Sciences of the United States of America 99 (20): 12600. https://doi.org/10.1073/PNAS.202296599.

Baron, Roland, and Michaela Kneissel. 2013. “WNT Signaling in Bone Homeostasis and Disease: From Human Mutations to Treatments.” Nature Medicine 2013 19:2 19 (2): 179–92. https://doi.org/10.1038/nm.3074.

Bartnikowski, M., Dargaville, T. R., Ivanovski, S., & Hutmacher, D. W. (2019). Degradation mechanisms of polycaprolactone in the context of chemistry, geometry and environment. Progress in Polymer Science, 96, 1–20. https://doi.org/10.1016/J.PROGPOLYMSCI.2019.05.004

Bartnikowski, Michal, Tim R. Dargaville, Sašo Ivanovski, and Dietmar W. Hutmacher. 2019. “Degradation Mechanisms of Polycaprolactone in the Context of Chemistry, Geometry and Environment.” Progress in Polymer Science 96 (September): 1–20. https://doi.org/10.1016/J.PROGPOLYMSCI.2019.05.004.

Becquart, P., M. Cruel, T. Hoc, L. Sudre, K. Pernelle, R. Bizios, D. Logeart-Avramoglou, H. Petite, and M. Bensidhoum. 2016. “Human Mesenchymal Stem Cell Responses to Hydrostatic Pressure and Shear Stress.” European Cells and Materials 31: 160–73. https://doi.org/10.22203/eCM.v031a11.

Bhat, Samatha, Pachaiyappan Viswanathan, Shashank Chandanala, S. Jyothi Prasanna, and Raviraja N. Seetharam. 2021. “Expansion and Characterization of Bone Marrow Derived Human Mesenchymal Stromal Cells in Serum-Free Conditions.” Scientific Reports 2021 11:1 11 (1): 1–18. https://doi.org/10.1038/s41598-021-83088-1.

Bianco, P., M. Riminucci, E. Bonucci, J. D. Termine, and P. G. Robey. 2017. “Bone Sialoprotein (BSP) Secretion and Osteoblast Differentiation: Relationship to Bromodeoxyuridine Incorporation, Alkaline Phosphatase, and Matrix Deposition.:” Http://Dx.Doi.Org/10.1177/41.2.8419458 41 (2): 183–91. https://doi.org/10.1177/41.2.8419458.

Bohner, M. (2010). Resorbable biomaterials as bone graft substitutes. Materials Today, 13(1-2), 24-30.

Bohner, Marc, and Richard J. Miron. 2019. “A Proposed Mechanism for Material-Induced Heterotopic Ossification.” Materials Today 22 (January): 132–41. https://doi.org/10.1016/J.MATTOD.2018.10.036.

Bölgen, N., Menceloğlu, Y. Z., Acatay, K., Vargel, I., & Pişkin, E. (2012). In vitro and in vivo degradation of non-woven materials made of poly(ε-caprolactone) nanofibers prepared by electrospinning under different conditions. Journal of Biomaterials Science, Polymer Edition, 16(12), 1537–1555. https://doi.org/10.1163/156856205774576655

Bonewald, Lynda F. 2011. “The Amazing Osteocyte.” Journal of Bone and Mineral Research 26 (2): 229–38. https://doi.org/10.1002/JBMR.320.

Bose, S., Tarafder, S., Banerjee, S. S., Davies, N. M., & Bandyopadhyay, A. (2011). Understanding in vivo response and mechanical property variation in MgO, SrO and SiO2 doped β-TCP. Bone, 48(6), 1282-1290.

Bosnakovski, Darko, Morimichi Mizuno, Gonhyung Kim, Satoshi Takagi, Masahiro Okumura, and Toru Fujinaga. 2006. “Chondrogenic Differentiation of Bovine Bone Marrow Mesenchymal Stem Cells (MSCs) in Different Hydrogels: Influence of Collagen Type II Extracellular Matrix on MSC Chondrogenesis.” Biotechnology and Bioengineering 93 (6): 1152–63. https://doi.org/10.1002/BIT.20828.

Bruder, Scott P, Neelam Jaiswal, and Stephen E Haynesworth. n.d. “Growth Kinetics, Self-Renewal, and the Osteogenic Potential of Purified Human Mesenchymal Stem Cells During Extensive Subcultivation and Following Cryopreservation.”

Cao, Xu, and Di Chen. 2005. “The BMP Signaling and in Vivo Bone Formation.” Gene 357 (1): 1–8. https://doi.org/10.1016/J.GENE.2005.06.017.

Capulli, Mattia, Riccardo Paone, and Nadia Rucci. 2014. “Osteoblast and Osteocyte: Games without Frontiers.” Archives of Biochemistry and Biophysics 561 (November): 3–12. https://doi.org/10.1016/J.ABB.2014.05.003.

Cardoso, Luis, Susannah P. Fritton, Gaffar Gailani, Mohammed Benalla, and Stephen C. Cowin. 2013. “A Review of Recent Advances in the Assessment of Bone Porosity, Permeability, and Interstitial Fluid Flow.” Journal of Biomechanics 46 (2): 253. https://doi.org/10.1016/J.JBIOMECH.2012.10.025.

Chan, Ariel W., Ralph A. Whitney, and Ronald J. Neufeld. 2008. “Kinetic Controlled Synthesis of PH-Responsive Network Alginate.” Biomacromolecules 9 (9): 2536–45. https://doi.org/10.1021/BM800594F.

Chastain, Sara R., Anup K. Kundu, Sanjay Dhar, Jay W. Calvert, and Andrew J. Putnam. 2006. "Adhesion of Mesenchymal Stem Cells to Polymer Scaffolds Occurs via Distinct ECM Ligands and Controls Their Osteogenic Differentiation." Journal of Biomedical Materials Research - Part A 78 (1): 73–85. https://doi.org/10.1002/JBM.A.30686.

Chen, Guiqian, Chuxia Deng, and Yi Ping Li. 2012. "TGF-β and BMP Signaling in Osteoblast Differentiation and Bone Formation." International Journal of Biological Sciences 8 (2): 272. https://doi.org/10.7150/IJBS.2929.

Chen, Q. Z. 2011. "Foaming Technology of Tissue Engineering Scaffolds - a Review." Bubble Science, Engineering and Technology 3 (2): 34–47. https://doi.org/10.1179/1758897911Y.0000000003.

Chen, Yan, Zhi Huang, Xiaoming Li, Songjian Li, Zhilai Zhou, Yichen Zhang, Qing Ling Feng, and Bo Yu. 2012. "In Vitro Biocompatibility and Osteoblast Differentiation of an Injectable Chitosan/Nano-Hydroxyapatite/Collagen Scaffold." Journal of Nanomaterials 2012 (January). https://doi.org/10.1155/2012/401084.

Christenson, E. M., Anseth, K. S., van den Beucken, J. J., Chan, C. K., Ercan, B., Jansen, J. A., ... & Ramakrishna, S. (2007). Nanobiomaterial applications in orthopedics. Journal of Orthopaedic Research, 25(1), 11-22.

Chu, Shijian, and Thomas J. Ferro. 2005. "Sp1: Regulation of Gene Expression by Phosphorylation." Gene 348 (1-2 SUPPL.): 1–11. https://doi.org/10.1016/J.GENE.2005.01.013.

Civitelli, Roberto, Fernando Lecanda, Niklas R. Jørgensen, and Thomas H. Steinberg. 2002. "Intercellular Junctions and Cell-Cell Communication in Bone." Principles of Bone Biology, January, 287–302. https://doi.org/10.1016/B978-012098652-1.50120-7.

Clarke, Bart. 2008. "Normal Bone Anatomy and Physiology." Clinical Journal of the American Society of Nephrology 3 (Supplement 3): S131–39. https://doi.org/10.2215/CJN.04151206.

Clegg, Andrew, John Young, Steve Iliffe, Marcel Olde Rikkert, and Kenneth Rockwood. 2013. "Frailty in Elderly People." The Lancet 381 (9868): 752–62. https://doi.org/10.1016/S0140-6736(12)62167-9.

Comazzetto, Stefano, Bo Shen, and Sean J. Morrison. 2021. "Niches That Regulate Stem Cells and Hematopoiesis in Adult Bone Marrow." Developmental Cell 56 (13): 1848–60. https://doi.org/10.1016/J.DEVCEL.2021.05.018.

Corcione, Anna, Federica Benvenuto, Elisa Ferretti, Debora Giunti, Valentina Cappiello, Francesco Cazzanti, Marco Risso, et al. 2006. "Human Mesenchymal Stem Cells Modulate B-Cell Functions." Blood 107 (1): 367–72. https://doi.org/10.1182/BLOOD-2005-07-2657.

Cornelissen, D. J., Faulkner-Jones, A., & Shu, W. (2017). Current developments in 3D bioprinting for tissue engineering. Current Opinion in Biomedical Engineering, 2, 76-82.

Correia, Cristina, Sarindr Bhumiratana, Rui A. Sousa, Rui L. Reis, and Gordana Vunjak-Novakovic. 2013. "Sequential Application of Steady and Pulsatile Medium Perfusion Enhanced the Formation of Engineered Bone." Https://Home.Liebertpub.Com/Tea 19 (9–10): 1244–54. https://doi.org/10.1089/TEN.TEA.2011.0701.

Correlo, V. M., Boesel, L. F., Bhattacharya, M., Mano, J. F., Neves, N. M., & Reis, R. L. (2005). Hydroxyapatite Reinforced Chitosan and Polyester Blends for Biomedical Applications. Macromolecular Materials and Engineering, 290(12), 1157–1165. https://doi.org/10.1002/MAME.200500163

Cory, A. H., T. C. Owen, J. A. Barltrop, and J. G. Cory. 1991. "Use of an Aqueous Soluble Tetrazolium/Formazan Assay for Cell Growth Assays in Culture." Cancer Communications 3 (7): 207–12. https://doi.org/10.3727/095535491820873191.

Cowin, Stephen C., and Luis Cardoso. 2015. "Blood and Interstitial Flow in the Hierarchical Pore Space Architecture of Bone Tissue." Journal of Biomechanics 48 (5): 842–54. https://doi.org/10.1016/J.JBIOMECH.2014.12.013.

Cunniffe, G. M., Dickson, G. R., Partap, S., Stanton, K. T., & O'Brien, F. J. (2010). Development and characterisation of a collagen nano-hydroxyapatite composite scaffold for bone tissue engineering. Journal of Materials Science: Materials in Medicine, 21(8), 2293-2298.)

Dallas, Sarah L., Matthew Prideaux, and Lynda F. Bonewald. 2013. "The Osteocyte: An Endocrine Cell … and More." Endocrine Reviews 34 (5): 658–90. https://doi.org/10.1210/ER.2012-1026.

Davies, Owen G., Liam M. Grover, Mark P. Lewis, and Yang Liu. 2018. "PDGF Is a Potent Initiator of Bone Formation in a Tissue Engineered Model of Pathological Ossification." Journal of Tissue Engineering and Regenerative Medicine 12 (1): e355. https://doi.org/10.1002/TERM.2320.

Deng, N., He, H., Yan, J., Zhao, Y., Ben Ticha, E., Liu, Y., Kang, W., & Cheng, B. (2019). One-step melt-blowing of multi-scale micro/nano fabric membrane for advanced air-filtration. Polymer, 165, 174–179. https://doi.org/10.1016/J.POLYMER.2019.01.035

Deng, Nanping, Hongsheng He, Jing Yan, Yixia Zhao, Eya Ben Ticha, Yong Liu, Weimin Kang, and Bowen Cheng. 2019. "One-Step Melt-Blowing of Multi-Scale Micro/Nano Fabric Membrane for Advanced Air-Filtration." Polymer 165 (February): 174–79. https://doi.org/10.1016/J.POLYMER.2019.01.035.

Devescovi, Valentina, Elisa Leonardi, Gabriela Ciapetti, Elisabetta Cenni, V Devescovi, E Leonardi, · G Ciapetti, and · E Cenni. 2008. "Growth Factors in Bone Repair." La Chirurgia Degli Organi Di Movimento 2008 92:3 92 (3): 161–68. https://doi.org/10.1007/S12306-008-0064-1.

Dhawan, Puneet, Xiaorong Peng, Amelia L. M. Sutton, Paul N. MacDonald, Colleen M. Croniger, Christian Trautwein, Michael Centrella, Thomas L. McCarthy, and Sylvia Christakos. 2005. " Functional Cooperation between CCAAT/Enhancer-Binding Proteins and the Vitamin D Receptor in Regulation of 25-Hydroxyvitamin D 3 24-Hydroxylase ." Molecular and Cellular Biology 25 (1): 472–87. https://doi.org/10.1128/MCB.25.1.472-487.2005/ASSET/F97E43A7-0CFF-4C2D-BA3D-233E5F5C9879/ASSETS/GRAPHIC/ZMB0010546730009.JPEG.

Dhingra, Sanjiv, Peng Li, Xi Ping Huang, Jian Guo, Jun Wu, Anton Mihic, Shu Hong Li, et al. 2013. "Preserving Prostaglandin E2 Level Prevents Rejection of Implanted Allogeneic Mesenchymal Stem Cells and Restores Postinfarction Ventricular Function." Circulation 128 (SUPPL.1). https://doi.org/10.1161/CIRCULATIONAHA.112.000324.

Doblaré, M., J. M. García, and M. J. Gómez. 2004. "Modelling Bone Tissue Fracture and Healing: A Review." Engineering Fracture Mechanics 71 (13–14): 1809–40. https://doi.org/10.1016/J.ENGFRACMECH.2003.08.003.

Dobreva, Gergana, Maria Chahrour, Marcel Dautzenberg, Laura Chirivella, Benoit Kanzler, Isabel Fariñas, Gerard Karsenty, and Rudolf Grosschedl. 2006. “SATB2 Is a Multifunctional Determinant of Craniofacial Patterning and Osteoblast Differentiation.” Cell 125 (5): 971–86. https://doi.org/10.1016/J.CELL.2006.05.012.

Dominici, M., K. Le Blanc, I. Mueller, I. Slaper-Cortenbach, F. C. Marini, D. S. Krause, R. J. Deans, A. Keating, D. J. Prockop, and E. M. Horwitz. 2006. “Minimal Criteria for Defining Multipotent Mesenchymal Stromal Cells. The International Society for Cellular Therapy Position Statement.” Cytotherapy 8 (4): 315–17. https://doi.org/10.1080/14653240600855905.

Dragan, A. I., E. S. Bishop, J. R. Casas-Finet, R. J. Strouse, M. A. Schenerman, and C. D. Geddes. 2010. “Metal-Enhanced PicoGreen Fluorescence: Application for Double-Stranded DNA Quantification.” Analytical Biochemistry 396 (1): 8–12. https://doi.org/10.1016/J.AB.2009.09.010.

Dragan, A. I., J. R. Casas-Finet, E. S. Bishop, R. J. Strouse, M. A. Schenerman, and C. D. Geddes. 2010. “Characterization of PicoGreen Interaction with DsDNA and the Origin of Its Fluorescence Enhancement upon Binding.” Biophysical Journal 99 (9): 3010–19. https://doi.org/10.1016/J.BPJ.2010.09.012.

Dramowski, Angela, Sheylyn Pillay, Adrie Bekker, Ilhaam Abrahams, Mark F. Cotton, Susan E. Coffin, and Andrew C. Whitelaw. 2021. “Impact of 1% Chlorhexidine Gluconate Bathing and Emollient Application on Bacterial Pathogen Colonization Dynamics in Hospitalized Preterm Neonates – A Pilot Clinical Trial.” EClinicalMedicine 37. https://doi.org/10.1016/j.eclinm.2021.100946.

Du, Dajiang, Katsuko S. Furukawa, and Takashi Ushida. 2009. “3D Culture of Osteoblast-like Cells by Unidirectional or Oscillatory Flow for Bone Tissue Engineering.” Biotechnology and Bioengineering 102 (6): 1670–78. https://doi.org/10.1002/BIT.22214.

Ducy, Patricia, Rui Zhang, Valérie Geoffroy, Amy L. Ridall, and Gérard Karsenty. 1997. “Osf2/Cbfa1: A Transcriptional Activator of Osteoblast Differentiation.” Cell 89 (5): 747–54. https://doi.org/10.1016/S0092-8674(00)80257-3.

Duncan, R. L., and C. H. Turner. 1995. “Mechanotransduction and the Functional Response of Bone to Mechanical Strain.” Calcified Tissue International 1995 57:5 57 (5): 344–58. https://doi.org/10.1007/BF00302070.

Dunigan, David D., Summer B. Waters, and Terence C. Owen. 1995. “Aqueous Soluble Tetrazolium/Formazan MTS as an Indicator of NADH-and NADPH-Dependent Dehydrogenase Activity.” Biotechniques 19 (4): 640–49.

Egger, Dominik, Sarah Spitz, Monica Fischer, Stephan Handschuh, Martin Glösmann, Benedikt Friemert, Monika Egerbacher, and Cornelia Kasper. 2017. “Application of a Parallelizable Perfusion Bioreactor for Physiologic 3D Cell Culture.” Cells, Tissues, Organs 203 (5): 316–26. https://doi.org/10.1159/000457792.

Ellison, C. J., Phatak, A., Giles, D. W., Macosko, C. W., & Bates, F. S. (2007). Melt blown nanofibers: Fiber diameter distributions and onset of fiber breakup. Polymer, 48(11), 3306–3316. https://doi.org/10.1016/J.POLYMER.2007.04.005

Ellison, Christopher J., Alhad Phatak, David W. Giles, Christopher W. Macosko, and Frank S. Bates. 2007. “Melt Blown Nanofibers: Fiber Diameter Distributions and Onset of Fiber Breakup.” Polymer 48 (11): 3306–16. https://doi.org/10.1016/J.POLYMER.2007.04.005.

Enterprises, Knowledge. 2006. “The Worldwide Orthopedic Market—2005-2006.” Chagrin Falls, Ohio, USA.

Eqtesadi, S., Motealleh, A., Pajares, A., Guiberteau, F., & Miranda, P. (2016). Improving mechanical properties of 13–93 bioactive glass robocast scaffold by poly (lactic acid) and poly (ε-caprolactone) melt infiltration. Journal of Non-Crystalline Solids, 432, 111-119.

Erben, J., Pilarova, K., Sanetrnik, F., Chvojka, J., Jencova, V., Blazkova, L., Havlicek, J., Novak, O., Mikes, P., Prosecka, E., Lukas, D., & Kuzelova Kostakova, E. (2015). The combination of meltblown and electrospinning for bone tissue engineering. Materials Letters, 143, 172–176. https://doi.org/10.1016/J.MATLET.2014.12.100

Erben, Jakub, Katerina Pilarova, Filip Sanetrnik, Jiri Chvojka, Vera Jencova, Lenka Blazkova, Jiri Havlicek, et al. 2015. “The Combination of Meltblown and Electrospinning for Bone Tissue Engineering.” Materials Letters 143 (March): 172–76. https://doi.org/10.1016/J.MATLET.2014.12.100.

Eshraghi, S., & Das, S. (2010). Mechanical and microstructural properties of polycaprolactone scaffolds with one-dimensional, two-dimensional, and three-dimensional orthogonally oriented porous architectures produced by selective laser sintering. Acta Biomaterialia, 6(7), 2467–2476. https://doi.org/10.1016/J.ACTBIO.2010.02.002

Fahimipour, Farahnaz, Erfan Dashtimoghadam, Mohammad Mahdi Hasani-Sadrabadi, Jessica Vargas, Daryoosh Vashaee, Douglas C. Lobner, Tahereh S. Jafarzadeh Kashi, Behnam Ghasemzadeh, and Lobat Tayebi. 2019. “Enhancing Cell Seeding and Osteogenesis of MSCs on 3D Printed Scaffolds through Injectable BMP2 Immobilized ECM-Mimetic Gel.” Dental Materials 35 (7): 990–1006. https://doi.org/10.1016/J.DENTAL.2019.04.004.

Fernández Vallone, V. B., M. A. Romaniuk, H. Choi, V. Labovsky, J. Otaegui, and N. A. Chasseing. 2013. “Mesenchymal Stem Cells and Their Use in Therapy: What Has Been Achieved?” Differentiation 85 (1–2): 1–10. https://doi.org/10.1016/J.DIFF.2012.08.004.

Fink, H A, S Litwack-Harrison, B C Taylor, D C Bauer, E S Orwoll, C G Lee, E Barrett-Connor, et al. 2016. “Clinical Utility of Routine Laboratory Testing to Identify Possible Secondary Causes in Older Men with Osteoporosis: The Osteoporotic Fractures in Men (MrOS) Study.” Osteoporosis International 27 (1): 331–38. https://doi.org/10.1007/s00198-015-3356-y.

Florencio-Silva, Rinaldo, Gisela Rodrigues Da Silva Sasso, Estela Sasso-Cerri, Manuel Jesus Simões, and Paulo Sérgio Cerri. 2015. “Biology of Bone Tissue: Structure, Function, and Factors That Influence Bone Cells.” BioMed Research International 2015. https://doi.org/10.1155/2015/421746.

Flynn, J. M. “Fracture Repair and Bone Grafting.” OKU 10: Orthopaedic Knowledge Update Rosemont, IL: American Academy of Orthopaedic Surgeons, 2011. 11-21.

Fratzl, P., H. S. Gupta, E. P. Paschalis, and P. Roschger. 2004. “Structure and Mechanical Quality of the Collagen–Mineral Nano-Composite in Bone.” Journal of Materials Chemistry 14 (14): 2115–23. https://doi.org/10.1039/B402005G.

Freed, L. E., and G. Vunjak-Novakovic. 1995. “Cultivation of Cell–Polymer Tissue Constructs in Simulated Microgravity.” Biotechnology and Bioengineering 46 (4): 306–13. https://doi.org/10.1002/BIT.260460403.

Freire, Marcelo O., Huyng Keun You, Joong Ki Kook, Jeong Ho Choi, and Homayoun H. Zadeh. 2011. "Antibody-Mediated Osseous Regeneration: A Novel Strategy for Bioengineering Bone by Immobilized Anti-Bone Morphogenetic Protein-2 Antibodies." Tissue Engineering. Part A 17 (23–24): 2911–18. https://doi.org/10.1089/TEN.TEA.2010.0584.

Fujisawa, Ryuichi, and Masato Tamura. 2012. "Acidic Bone Matrix Proteins and Their Roles in Calcification." Frontiers in Bioscience (Landmark Edition) 17 (5): 1891–1903. https://doi.org/10.2741/4026.

Gamsjaeger, Sonja, A. Masic, P. Roschger, M. Kazanci, J. W.C. Dunlop, K. Klaushofer, E. P. Paschalis, and P. Fratzl. 2010. "Cortical Bone Composition and Orientation as a Function of Animal and Tissue Age in Mice by Raman Spectroscopy." Bone 47 (2): 392–99. https://doi.org/10.1016/J.BONE.2010.04.608.

Gaspar, Diana Alves, Viviane Gomide, and Fernando Jorge Monteiro. 2012. "The Role of Perfusion Bioreactors in Bone Tissue Engineering." Biomatter 2 (4): 167. https://doi.org/10.4161/BIOM.22170.

Gattazzo, Francesca, Anna Urciuolo, and Paolo Bonaldo. 2014. "Extracellular Matrix: A Dynamic Microenvironment for Stem Cell Niche." Biochimica et Biophysica Acta (BBA) - General Subjects 1840 (8): 2506–19. https://doi.org/10.1016/J.BBAGEN.2014.01.010.

Geng, Xinying, Oh Hyeong Kwon, and Jinho Jang. 2005. "Electrospinning of Chitosan Dissolved in Concentrated Acetic Acid Solution." Biomaterials 26 (27): 5427–32. https://doi.org/10.1016/J.BIOMATERIALS.2005.01.066.

Gerstenfeld, Louis C., Dennis M. Cullinane, George L. Barnes, Dana T. Graves, and Thomas A. Einhorn. 2003. "Fracture Healing as a Post-Natal Developmental Process: Molecular, Spatial, and Temporal Aspects of Its Regulation." Journal of Cellular Biochemistry 88 (5): 873–84. https://doi.org/10.1002/JCB.10435.

Ghorbani, Ahmad, Seyed Amir Jalali, and Masoumeh Varedi. 2014. "Isolation of Adipose Tissue Mesenchymal Stem Cells without Tissue Destruction: A Non-Enzymatic Method." Tissue and Cell 46 (1): 54–58. https://doi.org/10.1016/J.TICE.2013.11.002.

Giannoudis, P. V., Dinopoulos, H., & Tsiridis, E. (2005). Bone substitutes: an update. Injury, 36(3), S20-S27.

Goldstein, Aaron S., Tiffany M. Juarez, Christopher D. Helmke, Michael C. Gustin, and Antonios G. Mikos. 2001. "Effect of Convection on Osteoblastic Cell Growth and Function in Biodegradable Polymer Foam Scaffolds." Biomaterials 22 (11): 1279–88. https://doi.org/10.1016/S0142-9612(00)00280-5.

Golub, Ellis E. 2009. "Role of Matrix Vesicles in Biomineralization." Biochimica et Biophysica Acta (BBA) - General Subjects 1790 (12): 1592–98. https://doi.org/10.1016/J.BBAGEN.2009.09.006.

Gomes, Manuela E., Heidi L. Holtorf, Rui L. Reis, and Antonios G. Mikos. 2006. "Influence of the Porosity of Starch-Based Fiber Mesh Scaffolds on the Proliferation and Osteogenic Differentiation of Bone Marrow Stromal Cells Cultured in a Flow Perfusion Bioreactor." Https://Home.Liebertpub.Com/Ten 12 (4): 801–9. https://doi.org/10.1089/TEN.2006.12.801.

Gong, J. K., J. S. Arnold, and S. H. Cohn. 1964. "COMPOSITION OF TRABECULAR AND CORTICAL BONE." The Anatomical Record 149 (3): 325–31. https://doi.org/10.1002/AR.1091490303.

Grayson, Warren L., Darja Marolt, Sarindr Bhumiratana, Mirjam Fröhlich, X. Edward Guo, and Gordana Vunjak-Novakovic. 2011. "Optimizing the Medium Perfusion Rate in Bone Tissue Engineering Bioreactors." Biotechnology and Bioengineering 108 (5): 1159–70. https://doi.org/10.1002/BIT.23024.

Guda, T., Appleford, M., Oh, S., & Ong, J. L. (2008). A cellular perspective to bioceramic scaffolds for bone tissue engineering: the state of the art. Current topics in medicinal chemistry, 8(4), 290-299.

Guvendiren, M., Molde, J., Soares, R. M., & Kohn, J. (2016). Designing biomaterials for 3D printing. ACS biomaterials science & engineering, 2(10), 1679-1693.

Guyot, Y., F. P. Luyten, J. Schrooten, I. Papantoniou, and L. Geris. 2015. "A Three-Dimensional Computational Fluid Dynamics Model of Shear Stress Distribution during Neotissue Growth in a Perfusion Bioreactor." Biotechnology and Bioengineering 112 (12): 2591–2600. https://doi.org/10.1002/BIT.25672.

Hadida, Mikhael, and David Marchat. 2020. "Strategy for Achieving Standardized Bone Models." Biotechnology and Bioengineering 117 (1): 251–71. https://doi.org/10.1002/BIT.27171.

Hadjidakis, Dimitrios J., and Ioannis I. Androulakis. 2006a. "Bone Remodeling." Annals of the New York Academy of Sciences 1092 (1): 385–96. https://doi.org/10.1196/ANNALS.1365.035.

Han, Younho, Yun Hye Jin, Jinah Yum, Hyung Min Jeong, Joong Kook Choi, Chang Yeol Yeo, and Kwang Youl Lee. 2011. "Protein Kinase A Phosphorylates and Regulates the Osteogenic Activity of Dlx5." Biochemical and Biophysical Research Communications 407 (3): 461–65. https://doi.org/10.1016/J.BBRC.2011.03.034.

Hass, Ralf, Cornelia Kasper, Stefanie Böhm, and Roland Jacobs. 2011. "Different Populations and Sources of Human Mesenchymal Stem Cells (MSC): A Comparison of Adult and Neonatal Tissue-Derived MSC." Cell Communication and Signaling 2011 9:1 9 (1): 1–14. https://doi.org/10.1186/1478-811X-9-12.

Hassan, Mohammad Q., Amjad Javed, Maria I. Morasso, Jeremy Karlin, Martin Montecino, Andre J. van Wijnen, Gary S. Stein, Janet L. Stein, and Jane B. Lian. 2004. "Dlx3 Transcriptional Regulation of Osteoblast Differentiation: Temporal Recruitment of Msx2, Dlx3, and Dlx5 Homeodomain Proteins to Chromatin of the Osteocalcin Gene." Molecular and Cellular Biology 24 (20): 9248–61. https://doi.org/10.1128/MCB.24.20.9248-9261.2004/ASSET/B6588B3C-51A0-43D0-8458-A83DC8FB726F/ASSETS/GRAPHIC/ZMB0200444610008.JPEG.

Hayrapetyan, Astghik, John A. Jansen, and Jeroen J.J.P. Van Den Beucken. 2014. "Signaling Pathways Involved in Osteogenesis and Their Application for Bone Regenerative Medicine." Https://Home.Liebertpub.Com/Teb 21 (1): 75–87. https://doi.org/10.1089/TEN.TEB.2014.0119.

Hench, L. L., Splinter, R. J., Allen, W. C. and Greenlee, T. K. (1971), Bonding mechanisms at the interface of ceramic prosthetic materials. J. Biomed. Mater. Res., 5: 117-141. doi:10.1002/jbm.820050611

Henriquez, Berta, Matias Hepp, Paola Merino, Hugo Sepulveda, Andre J. van Wijnen, Jane B. Lian, Gary S. Stein, Janet L. Stein, and Martin Montecino. 2011. "C/EBPβ Binds the P1 Promoter of the Runx2 Gene and up-Regulates Runx2 Transcription in Osteoblastic Cells." Journal of Cellular Physiology 226 (11): 3043–52. https://doi.org/10.1002/JCP.22652.

Herve, Abdi, and Lynne J. Williams. 2010. "Tukey's Honestly Signifcant Difference (HSD) Test." Encyclopedia of Research Design, 1–5. https://doi.org/10.4135/9781412961288.n181.

Houshyar, S., Kumar, G. S., Rifai, A., Tran, N., Nayak, R., Shanks, R. A., Padhye, R., Fox, K., & Bhattacharyya, A. (2019). Nanodiamond/poly-ε-caprolactone nanofibrous scaffold for wound management. Materials Science & Engineering. C, Materials for Biological Applications, 100, 378–387. https://doi.org/10.1016/J.MSEC.2019.02.110

Houshyar, Shadi, G. Sathish Kumar, Aaqil Rifai, Nhiem Tran, Rajkishore Nayak, Robert A. Shanks, Rajiv Padhye, Kate Fox, and Amitava Bhattacharyya. 2019. "Nanodiamond/Poly-ε-Caprolactone Nanofibrous Scaffold for Wound Management." Materials Science & Engineering. C, Materials for Biological Applications 100 (July): 378–87. https://doi.org/10.1016/J.MSEC.2019.02.110.

Huang HH. Electrochemical impedance spectroscopy study of strained titanium in fluoride media. Electrochim Acta 2002; 47: 2311–2318

Huang, Hayden, Roger D. Kamm, and Richard T. Lee. 2004. "Cell Mechanics and Mechanotransduction: Pathways, Probes, and Physiology." American Journal of Physiology - Cell Physiology 287 (1 56-1): 1–11. https://doi.org/10.1152/AJPCELL.00559.2003/ASSET/IMAGES/LARGE/ZH00070419951004.JPEG.

Huang, Her Hsiung. 2002. "Electrochemical Impedance Spectroscopy Study of Strained Titanium in Fluoride Media." Electrochimica Acta 47 (13–14): 2311–18. https://doi.org/10.1016/S0013-4686(02)00079-8.

Huang, Xia, Qiuman Chen, Wenping Luo, Mikhail Pakvasa, Yuxin Zhang, Liwen Zheng, Shuang Li, et al. 2020. "SATB2: A Versatile Transcriptional Regulator of Craniofacial and Skeleton Development, Neurogenesis and Tumorigenesis, and Its Applications in Regenerative Medicine." Genes & Diseases, October. https://doi.org/10.1016/J.GENDIS.2020.10.003.

Huang, Zheng Ming, Y. Z. Zhang, M. Kotaki, and S. Ramakrishna. 2003. "A Review on Polymer Nanofibers by Electrospinning and Their Applications in Nanocomposites." Composites Science and Technology 63 (15): 2223–53. https://doi.org/10.1016/S0266-3538(03)00178-7.

Huang, Zhinong, Pei Gen Ren, Ting Ma, R. Lane Smith, and Stuart B. Goodman. 2010. "Modulating Osteogenesis of Mesenchymal Stem Cells by Modifying Growth Factor Availability." Cytokine 51 (3): 305–10. https://doi.org/10.1016/J.CYTO.2010.06.002.

Hyuk Sang Yoo, Taek Gyoung Kim, Tae Gwan Park, Surface-functionalized electrospun nanofibers for tissue engineering and drug delivery, Advanced Drug Delivery Reviews, Volume 61, Issue 12, 2009, Pages 1033-1042, ISSN 0169-409X, https://doi.org/10.1016/j.addr.2009.07.007.

Jackson, Rebecca A., Victor Nurcombe, and Simon M. Cool. 2006. "Coordinated Fibroblast Growth Factor and Heparan Sulfate Regulation of Osteogenesis." Gene 379 (1–2): 79–91. https://doi.org/10.1016/J.GENE.2006.04.028.

James, Aaron W. 2013. "Review of Signaling Pathways Governing MSC Osteogenic and Adipogenic Differentiation." Scientifica 2013: 1–17. https://doi.org/10.1155/2013/684736.

Janssen, Frank W., Jaap Oostra, Arie Van Oorschot, and Clemens A. Van Blitterswijk. 2006. "A Perfusion Bioreactor System Capable of Producing Clinically Relevant Volumes of Tissue-Engineered Bone: In Vivo Bone Formation Showing Proof of Concept." Biomaterials 27 (3): 315–23. https://doi.org/(Volkmer et al. 2008.

Jia, Chang Chang, Tian Tian Wang, Wei Liu, Bin Sheng Fu, Xue Feng Hua, Guo Ying Wang, Tuan Jie Li, et al. 2013. "Cancer-Associated Fibroblasts from Hepatocellular Carcinoma Promote Malignant Cell

Proliferation by HGF Secretion." PLOS ONE 8 (5): e63243. https://doi.org/10.1371/JOURNAL.PONE.0063243.

Jin, H. J., Chen, J., Karageorgiou, V., Altman, G. H., & Kaplan, D. L. (2004). Human bone marrow stromal cell responses on electrospun silk fibroin mats. Biomaterials, 25(6), 1039-1047.

Kadiyala, S., R. G. Young, M. A. Thiede, and S. P. Bruder. 1997. "Culture Expanded Canine Mesenchymal Stem Cells Possess Osteochondrogenic Potential in Vivo and in Vitro." Cell Transplantation 6 (2): 125–34. https://doi.org/10.1016/S0963-6897(96)00279-5.

Karageorgiou, V., & Kaplan, D. (2005). Porosity of 3D biomaterial scaffolds and osteogenesis. Biomaterials, 26(27), 5474–5491. https://doi.org/10.1016/J.BIOMATERIALS.2005.02.002

Karin, M. 1990. "Too Many Transcription Factors: Positive and Negative Interactions." The New Biologist 2 (2): 126–31. https://europepmc.org/article/med/2128034.

Katz, Jordan M., Chandra Nataraj, Rebecca Jaw, Elizabeth Deigl, and Predrag Bursac. 2009. "Demineralized Bone Matrix as an Osteoinductive Biomaterial and in Vitro Predictors of Its Biological Potential." Journal of Biomedical Materials Research Part B: Applied Biomaterials 89B (1): 127–34. https://doi.org/10.1002/JBM.B.31195.

Kawane, Tetsuya, Hisato Komori, Wenguang Liu, Takeshi Moriishi, Toshihiro Miyazaki, Masako Mori, Yuki Matsuo, et al. 2014. "Dlx5 and Mef2 Regulate a Novel Runx2 Enhancer for Osteoblast-Specific Expression." Journal of Bone and Mineral Research 29 (9): 1960–69. https://doi.org/10.1002/JBMR.2240.

Kazemnejad, Somaieh, Abdolamir Allameh, Masoud Soleimani, Ahmad Gharehbaghian, Yousef Mohammadi, Naser Amirizadeh, and Maryam Jazayery. 2009. "Biochemical and Molecular Characterization of Hepatocyte-like Cells Derived from Human Bone Marrow Mesenchymal Stem Cells on a Novel Three-Dimensional Biocompatible Nanofibrous Scaffold." Journal of Gastroenterology and Hepatology 24 (2): 278–87. https://doi.org/10.1111/J.1440-1746.2008.05530.X.

Kempen, Diederik H.R., Lichun Lu, Andras Heijink, Theresa E. Hefferan, Laura B. Creemers, Avudaiappan Maran, Michael J. Yaszemski, and Wouter J.A. Dhert. 2009. "Effect of Local Sequential VEGF and BMP-2 Delivery on Ectopic and Orthotopic Bone Regeneration." Biomaterials 30 (14): 2816–25. https://doi.org/10.1016/J.BIOMATERIALS.2009.01.031.

Khosla, Sundeep, Merry Jo Oursler, and David G. Monroe. 2012. "Estrogen and the Skeleton." Trends in Endocrinology & Metabolism 23 (11): 576–81. https://doi.org/10.1016/J.TEM.2012.03.008.

Kiel, Mark J., Ömer H. Yilmaz, Toshihide Iwashita, Osman H. Yilmaz, Cox Terhorst, and Sean J. Morrison. 2005. "SLAM Family Receptors Distinguish Hematopoietic Stem and Progenitor Cells and Reveal Endothelial Niches for Stem Cells." Cell 121 (7): 1109–21. https://doi.org/10.1016/J.CELL.2005.05.026.

Kikuchi M, Itoh S, Ichinose S, et al. 2001. Self-organization mechanism in a bone-like hydroxyapatite/collagen nano- composite synthesized in vitro and its biological reaction in vivo. Biomaterials 22:1705 – 1711.

Kim, Byung-Soo, Andrew J Putnam, Thomas J Kulik, and David J Mooney. 1998. "Optimizing Seeding and Culture Methods to Engineer Smooth Muscle Tissue on Biodegradable Polymer Matrices." https://doi.org/10.1002/(SICI)1097-0290(19980105)57:1.

Kim, J., Kim, I. S., Cho, T. H., Lee, K. B., Hwang, S. J., Tae, G., ... & Sun, K. (2007). Bone regeneration using hyaluronic acid-based hydrogel with bone morphogenic protein-2 and human mesenchymal stem cells. Biomaterials, 28(10), 1830-1837.

Kim, Tae Hyun, Meeju Kim, Mohamed Eltohamy, Ye Rang Yun, Jun Hyeog Jang, and Hae Won Kim. 2013. "Efficacy of Mesoporous Silica Nanoparticles in Delivering BMP-2 Plasmid DNA for in Vitro Osteogenic Stimulation of Mesenchymal Stem Cells." Journal of Biomedical Materials Research Part A 101A (6): 1651–60. https://doi.org/10.1002/JBM.A.34466.

Kirkham, Glen R., Anna Lovrics, Helen M. Byrne, Oliver E. Jensen, John R. King, Kevin M. Shakesheff, and Lee D.K. Buttery. 2012. "Early Gene Regulation of Osteogenesis in Embryonic Stem Cells." Integrative Biology 4 (12): 1470–77. https://doi.org/10.1039/C2IB20164J.

Kleinhans, Claudia, Ramkumar Ramani Mohan, Gabriele Vacun, Thomas Schwarz, Barbara Haller, Yang Sun, Alexander Kahlig, et al. 2015. "A Perfusion Bioreactor System Efficiently Generates Cell-Loaded Bone Substitute Materials for Addressing Critical Size Bone Defects." Biotechnology Journal 10 (11): 1727–38. https://doi.org/10.1002/BIOT.201400813.

Kobolak, Julianna, Andras Dinnyes, Adnan Memic, Ali Khademhosseini, and Ali Mobasheri. 2016. "Mesenchymal Stem Cells: Identification, Phenotypic Characterization, Biological Properties and Potential for Regenerative Medicine through Biomaterial Micro-Engineering of Their Niche." Methods 99 (April): 62–68. https://doi.org/10.1016/J.YMETH.2015.09.016.

Kolf, Catherine M., Elizabeth Cho, and Rocky S. Tuan. 2007. "Mesenchymal Stromal Cells. Biology of Adult Mesenchymal Stem Cells: Regulation of Niche, Self-Renewal and Differentiation." Arthritis Research and Therapy 9 (1): 1–10. https://doi.org/10.1186/AR2116/FIGURES/3.

Kuo, Catherine K., and Rocky S. Tuan. 2003. "Tissue Engineering with Mesenchymal Stem Cells." IEEE Engineering in Medicine and Biology Magazine 22 (5): 51–56. https://doi.org/10.1109/MEMB.2003.1256272.

Kuo, Tsung Rong, and Chih Hwa Chen. 2017. "Bone Biomarker for the Clinical Assessment of Osteoporosis: Recent Developments and Future Perspectives." Biomarker Research 5 (1): 1–9. https://doi.org/10.1186/S40364-017-0097-4/TABLES/1.

Kweon, Hae Yong, Mi Kyong Yoo, In Kyu Park, Tae Hee Kim, Hyun Chul Lee, Hyun Sook Lee, Jong Suk Oh, Toshihiro Akaike, and Chong Su Cho. 2003. "A Novel Degradable Polycaprolactone Networks for Tissue Engineering." Biomaterials 24 (5): 801–8. https://doi.org/10.1016/S0142-9612(02)00370-8.

Lai, Y. and Baccei, L. J. (1991), Novel polyurethane hydrogels for biomedical applications. J. Appl. Polym. Sci., 42: 3173-3179. doi:10.1002/app.1991.070421210

Langlois, Jean A., Clifford J. Rosen, Marjolein Visser, Marian T. Hannan, Tamara Harris, Peter W. F. Wilson, and Douglas P. Kiel. 1998. "Association Between Insulin-Like Growth Factor I and Bone Mineral Density in Older Women and Men: The Framingham Heart Study." The Journal of Clinical Endocrinology & Metabolism 83 (12): 4257–62. https://doi.org/10.1210/JCEM.83.12.5308.

Lasorella, Anna, Robert Benezra, and Antonio Iavarone. 2014. "The ID Proteins: Master Regulators of Cancer Stem Cells and Tumour Aggressiveness." Nature Reviews Cancer 2014 14:2 14 (2): 77–91. https://doi.org/10.1038/nrc3638.

Lee, S.-H., Lee, J. H., & Cho, Y.-S. (2014). Analysis of Degradation Rate for Dimensionless Surface Area of Well-Interconnected PCL Scaffold Via in-vitro Accelerated Degradation Experiment. Tissue Engineering and Regenerative Medicine, 11(6), 446–452. https://doi.org/10.1007/s13770-014-0067-y

Lee, Se-Hwan, Jun Hee Lee, and Young-Sam Cho. 2014. "Analysis of Degradation Rate for Dimensionless Surface Area of Well-Interconnected PCL Scaffold Via in-Vitro Accelerated Degradation Experiment." Tissue Engineering and Regenerative Medicine 11 (6): 446–52. https://doi.org/10.1007/s13770-014-0067-y.

Legate, Kyle R., Sara A. Wickström, and Reinhard Fässler. 2009. "Genetic and Cell Biological Analysis of Integrin Outside-in Signaling." Genes & Development 23 (4): 397–418. https://doi.org/10.1101/GAD.1758709.

Li, D., & Xia, Y. (2004). Electrospinning of Nanofibers: Reinventing the Wheel? Advanced Materials, 16(14), 1151–1170. https://doi.org/10.1002/ADMA.200400719

Li, Deqiang, Tingting Tang, Jianxi Lu, and Kerong Dai. 2009. "Effects of Flow Shear Stress and Mass Transport on the Construction of a Large-Scale Tissue-Engineered Bone in a Perfusion Bioreactor." Https://Home.Liebertpub.Com/Tea 15 (10): 2773–83. https://doi.org/10.1089/TEN.TEA.2008.0540.

Li, Jiao Jiao, Yao Yao Yang, Deng Guang Yu, Qing Du, and Xiang Liang Yang. 2018. "Fast Dissolving Drug Delivery Membrane Based on the Ultra-Thin Shell of Electrospun Core-Shell Nanofibers." European Journal of Pharmaceutical Sciences 122 (September): 195–204. https://doi.org/10.1016/J.EJPS.2018.07.002.

Li, Ming, and Susumu Ikehara. 2013. "Immunomodulatory Properties and Therapeutic Application of Bone Marrow Derived-Mesenchymal Stem Cells." J Bone Marrow Res 1: 131. https://doi.org/10.4172/2329-8820.1000131.

Li, Na, and Jinlian Hua. 2017. "Interactions between Mesenchymal Stem Cells and the Immune System." Cellular and Molecular Life Sciences 74: 2345–60. https://doi.org/10.1007/s00018-017-2473-5.

Li, W. J., Cooper Jr, J. A., Mauck, R. L., & Tuan, R. S. (2006). Fabrication and characterization of six electrospun poly (α-hydroxy ester)-based fibrous scaffolds for tissue engineering applications. Acta biomaterialia, 2(4), 377-385.

Li, W. J., Danielson, K. G., Alexander, P. G., & Tuan, R. S. (2003). Biological response of chondrocytes cultured in three-dimensional nanofibrous poly(epsilon-caprolactone) scaffolds. Journal of Biomedical Materials Research. Part A, 67(4), 1105–1114. https://doi.org/10.1002/JBM.A.10101

Li, W. J., Laurencin, C. T., Caterson, E. J., Tuan, R. S., & Ko, F. K. (2002). Electrospun nanofibrous structure: a novel scaffold for tissue engineering. Journal of Biomedical Materials Research: An Official Journal of The Society for Biomaterials, The Japanese Society for Biomaterials, and The Australian Society for Biomaterials and the Korean Society for Biomaterials, 60(4), 613-621.

Li, W. J., Tuli, R., Okafor, C., Derfoul, A., Danielson, K. G., Hall, D. J., & Tuan, R. S. (2005). A three-dimensional nanofibrous scaffold for cartilage tissue engineering using human mesenchymal stem cells. Biomaterials, 26(6), 599-609.

Li, Wan Ju, Keith G. Danielson, Peter G. Alexander, and Rocky S. Tuan. 2003. "Biological Response of Chondrocytes Cultured in Three-Dimensional Nanofibrous Poly(Epsilon-Caprolactone) Scaffolds." Journal of Biomedical Materials Research. Part A 67 (4): 1105–14. https://doi.org/10.1002/JBM.A.10101.

Li, Wan Ju, Richard Tuli, Xiaoxue Huang, Patrice Laquerriere, and Rocky S. Tuan. 2005. “Multilineage Differentiation of Human Mesenchymal Stem Cells in a Three-Dimensional Nanofibrous Scaffold.” Biomaterials 26 (25): 5158–66. https://doi.org/10.1016/J.BIOMATERIALS.2005.01.002.

Li, Yanhong, Di Zhang, Ling Xu, Lin Dong, Ji Zheng, Yikong Lin, Jiefang Huang, et al. 2019. “Cell–Cell Contact with Proinflammatory Macrophages Enhances the Immunotherapeutic Effect of Mesenchymal Stem Cells in Two Abortion Models.” Cellular & Molecular Immunology 2019 16:12 16 (12): 908–20. https://doi.org/10.1038/s41423-019-0204-6.

Liang, D., Hsiao, B. S., & Chu, B. (2007). Functional electrospun nanofibrous scaffolds for biomedical applications. Advanced drug delivery reviews, 59(14), 1392-1412.

Ling, Ling, Christian Dombrowski, Kin Mun Foong, Larisa M. Haupt, Gary S. Stein, Victor Nurcombe, Andre J. Van Wijnen, and Simon M. Cool. 2010. “Synergism between Wnt3a and Heparin Enhances Osteogenesis via a Phosphoinositide 3-Kinase/Akt/RUNX2 Pathway.” Journal of Biological Chemistry 285 (34): 26233–44. https://doi.org/10.1074/JBC.M110.122069/ATTACHMENT/38088AB0-DFF5-402D-B299-199F4F095BA1/MMC1.PDF.

Linh, N. T. B., Mondal, D., & Lee, B. T. (2014). In vitro study of CaTiO3–hydroxyapatite composites for bone tissue engineering. Asaio Journal, 60(6), 722-729.

Liu, Qian, Mao Li, Shiyi Wang, Zhousheng Xiao, Yuanyuan Xiong, and Guangwei Wang. 2020. “Recent Advances of Osterix Transcription Factor in Osteoblast Differentiation and Bone Formation.” Frontiers in Cell and Developmental Biology 8 (December): 1575. https://doi.org/10.3389/FCELL.2020.601224/BIBTEX.

Luo, Fei, Tian Yong Hou, Ze Hua Zhang, Zhao Xie, Xue Hui Wu, and Jian Zhong Xu. 2013. “Effects of Initial Cell Density and Hydrodynamic Culture on Osteogenic Activity of Tissue-Engineered Bone Grafts.” PLOS ONE 8 (1): e53697. https://doi.org/10.1371/JOURNAL.PONE.0053697.

M. M. Stevens, “Biomaterials for bone tissue engineering,” Materials Today, vol. 11, no. 5, pp. 18–25, 2008.

Mailoo, Venthan Jeyaratnam, Vidya Srinivas, Jeremy Turner, and William Duncan Fraser. 2019. “Case Report: Beware of Bone Pain with Bisphosphonates.” BMJ Case Reports 12 (3): 225385. https://doi.org/10.1136/BCR-2018-225385.

Malaval, Luc, Fina Liu, Patricia Roche, and Jane E Aubin. 1999. “Kinetics of Osteoprogenitor Proliferation and Osteoblast Differentiation In Vitro.” J. Cell. Biochem 74: 616–27. https://doi.org/10.1002/(SICI)1097-4644(19990915)74:4.

Manolagas, Stavros C. 2006. “Choreography from the Tomb: An Emerging Role of Dying Osteocytes in the Purposeful, and Perhaps Not so Purposeful, Targeting of Bone Remodeling.” BoneKEy-Osteovision 3 (1): 5–14. https://doi.org/10.1138/20060193.

Marie, Pierre J. 2008. “Transcription Factors Controlling Osteoblastogenesis.” Archives of Biochemistry and Biophysics 473 (2): 98–105. https://doi.org/10.1016/J.ABB.2008.02.030.

Marla, V. T., & Shambaugh, R. L. (2003). Three-Dimensional Model of the Melt-Blowing Process. Industrial and Engineering Chemistry Research, 42(26), 6993–7005. https://doi.org/10.1021/IE030517U

Marla, Vishnu T., and Robert L. Shambaugh. 2003. “Three-Dimensional Model of the Melt-Blowing Process.” Industrial and Engineering Chemistry Research 42 (26): 6993–7005. https://doi.org/10.1021/IE030517U.

Massagué, Joan, Liliana Attisano, and Jeffrey L. Wrana. 1994. “The TGF-β Family and Its Composite Receptors.” Trends in Cell Biology 4 (5): 172–78. https://doi.org/10.1016/0962-8924(94)90202-X.

Mattar, Philipp, and Karen Bieback. 2015. “Comparing the Immunomodulatory Properties of Bone Marrow, Adipose Tissue, and Birth-Associated Tissue Mesenchymal Stromal Cells.” Frontiers in Immunology 6 (NOV): 560. https://doi.org/10.3389/FIMMU.2015.00560/BIBTEX.

McBeath, Rowena, Dana M. Pirone, Celeste M. Nelson, Kiran Bhadriraju, and Christopher S. Chen. 2004. “Cell Shape, Cytoskeletal Tension, and RhoA Regulate Stem Cell Lineage Commitment.” Developmental Cell 6 (4): 483–95. https://doi.org/10.1016/S1534-5807(04)00075-9.

McComb, Robert B., George N. Bowers, and Solomon Posen. 1979. “Alkaline Phosphatase.” https://doi.org/10.1007/978-1-4613-2970-1.

McKee, M. G., Layman, J. M., Cashion, M. P., & Long, T. E. (2006). Phospholipid nonwoven electrospun membranes. Science, 311(5759), 353-355.

Mehrian, Mohammad, Yann Guyot, Ioannis Papantoniou, Simon Olofsson, Maarten Sonnaert, Ruth Misener, and Liesbet Geris. 2018. “Maximizing Neotissue Growth Kinetics in a Perfusion Bioreactor: An in Silico Strategy Using Model Reduction and Bayesian Optimization.” Biotechnology and Bioengineering 115 (3): 617–29. https://doi.org/10.1002/BIT.26500.

Meisel, Roland, Andree Zibert, Maurice Laryea, Ulrich Göbel, Walter Däubener, and Dagmar Dilloo. 2004. “Human Bone Marrow Stromal Cells Inhibit Allogeneic T-Cell Responses by Indoleamine 2,3-Dioxygenase–Mediated Tryptophan Degradation.” Blood 103 (12): 4619–21. https://doi.org/10.1182/BLOOD-2003-11-3909.

Mikos, Antonios G., and Johnna S. Temenoff. 2000. “Formation of Highly Porous Biodegradable Scaffolds for Tissue Engineering.” Electronic Journal of Biotechnology 3 (2): 23–24. http://www.scielo.cl/scielo.php?script=sci_arttext&pid=S0717-34582000000200003&lng=es&nrm=iso&tlng=en.

Miura, Masako, Stan Gronthos, Mingrui Zhao, Bai Lu, Larry W. Fisher, Pamela Gehron Robey, and Songtao Shi. 2003. “SHED: Stem Cells from Human Exfoliated Deciduous Teeth.” Proceedings of the National Academy of Sciences 100 (10): 5807–12. https://doi.org/10.1073/PNAS.0937635100.

Mo, X. M., Xu, C. Y., Kotaki, M., & Ramakrishna, S. (2004). Electrospun P(LLA-CL) nanofiber: a biomimetic extracellular matrix for smooth muscle cell and endothelial cell proliferation. Biomaterials, 25(10), 1883–1890. https://doi.org/10.1016/J.BIOMATERIALS.2003.08.042

Mochane, Mokgaotsa Jonas, Teboho Simon Motsoeneng, Emmanuel Rotimi Sadiku, Teboho Clement Mokhena, and Jeremia Shale Sefadi. 2019. “Morphology and Properties of Electrospun PCL and Its Composites for Medical Applications: A Mini Review.” Applied Sciences 2019, Vol. 9, Page 2205 9 (11): 2205. https://doi.org/10.3390/APP9112205.

Moreira, Carolina A, David W Dempster, and Roland Baron. 2019. “Anatomy and Ultrastructure of Bone – Histogenesis, Growth and Remodeling.” Endotext, June. https://www.ncbi.nlm.nih.gov/books/NBK279149/.

Mueller, Stefan M., Shuichi Mizuno, Louis C. Gerstenfeld, and Julie Glowacki. 1999. “Medium Perfusion Enhances Osteogenesis by Murine Osteosarcoma Cells in Three-Dimensional Collagen Sponges.” Journal of Bone and Mineral Research 14 (12): 2118–26. https://doi.org/10.1359/JBMR.1999.14.12.2118.

Mullender, M. G., D. D. Van Der Meer, R. Huiskes, and P. Lips. 1996. “Osteocyte Density Changes in Aging and Osteoporosis.” Bone 18 (2): 109–13. https://doi.org/10.1016/8756-3282(95)00444-0.

Muraglia, Anita, Ranieri Cancedda, and Rodolfo Quarto. 2000. “Clonal Mesenchymal Progenitors from Human Bone Marrow Differentiate in Vitro According to a Hierarchical Model.” Journal of Cell Science 113 (7): 1161–66. https://doi.org/10.1242/JCS.113.7.1161.

Mushahary, Dolly, Andreas Spittler, Cornelia Kasper, Viktoria Weber, and Verena Charwat. 2018. “Isolation, Cultivation, and Characterization of Human Mesenchymal Stem Cells.” Cytometry Part A 93 (1): 19–31. https://doi.org/10.1002/CYTO.A.23242.

Nagata, T., V. Gupta, D. Sorce, W. Y. Kim, A. Sali, B. T. Chait, K. Shigesada, Y. Ito, and M. H. Werner. 1999. “Immunoglobulin Motif DNA Recognition and Heterodimerization of the PEBP2/CBF Runt Domain.” Nature Structural Biology 6 (7): 615–19. https://doi.org/10.1038/10658.

Nakashima, Kazuhisa, Xin Zhou, Gary Kunkel, Zhaoping Zhang, Jian Min Deng, Richard R. Behringer, and Benoit De Crombrugghe. 2002. “The Novel Zinc Finger-Containing Transcription Factor Osterix Is Required for Osteoblast Differentiation and Bone Formation.” Cell 108 (1): 17–29. https://doi.org/10.1016/S0092-8674(01)00622-5.

Nauta, Alma J., and Willem E. Fibbe. 2007. “Immunomodulatory Properties of Mesenchymal Stromal Cells.” Blood 110 (10): 3499–3506. https://doi.org/10.1182/BLOOD-2007-02-069716.

Noël, Danièle, Dan Gazit, Celine Bouquet, Florence Apparailly, Claire Bony, Pascale Plence, Virginie Millet, et al. 2004. “Short-Term BMP-2 Expression Is Sufficient for In Vivo Osteochondral Differentiation of Mesenchymal Stem Cells.” Stem Cells 22 (1): 74–85. https://doi.org/10.1634/STEMCELLS.22-1-74.

O'Brien, F. J. (2011). Biomaterials & scaffolds for tissue engineering. Materials today, 14(3), 88-95.

Ohkawa, K., Kim, H., Lee, K., & Yamamoto, H. (2004, September). Electrospun Non-Woven Fabrics of Poly (ϵ-caprolactone) and Their Biodegradation by Pure Cultures of Soil Filamentous Fungi. In Macromolecular Symposia (Vol. 216, No. 1, pp. 301-306). Weinheim: WILEY-VCH Verlag.

Otsuru, Satoru, Ted J. Hofmann, Timothy S. Olson, Massimo Dominici, and Edwin M. Horwitz. 2013. “Improved Isolation and Expansion of Bone Marrow Mesenchymal Stromal Cells Using a Novel Marrow Filter Device.” Cytotherapy 15 (2): 146–53. https://doi.org/10.1016/J.JCYT.2012.10.012.

Ouhadi, T., C. Stevens, and Ph Teyssié. 1976. “Study of Poly-ϵ-Caprolactone Bulk Degradation.” Journal of Applied Polymer Science 20 (11): 2963–70. https://doi.org/10.1002/APP.1976.070201104.

Owen, Thomas A., Michael Aronow, Victoria Shalhoub, Leesa M. Barone, Laurens Wilming, Melissa S. Tassinari, Mary Beth Kennedy, Shirwin Pockwinse, Jane B. Lian, and Gary S. Stein. 1990. “Progressive Development of the Rat Osteoblast Phenotype in Vitro: Reciprocal Relationships in Expression of Genes Associated with Osteoblast Proliferation and Differentiation during Formation of the Bone Extracellular Matrix.” Journal of Cellular Physiology 143 (3): 420–30. https://doi.org/10.1002/JCP.1041430304.

Park SA, Kim GH, Jeon YC, Koh YH, Kim WD. 3D polycaprolactone scaffolds with controlled pore structure using a rapid prototyping system. J Mater Sci Mater Med 2009; 20: 229–234.

Park, S. H., Park, D. S., Shin, J. W., Kang, Y. G., Kim, H. K., Yoon, T. R., & Shin, J. W. (2012). Scaffolds for bone tissue engineering fabricated from two different materials by the rapid prototyping technique: PCL versus PLGA. Journal of Materials Science. Materials in Medicine, 23(11), 2671–2678. https://doi.org/10.1007/S10856-012-4738-8

Parker, Kevin K, and Donald E Ingber. 2007. "Extracellular Matrix, Mechanotransduction and Structural Hierarchies in Heart Tissue Engineering." Philosophical Transactions of the Royal Society B: Biological Sciences 362 (1484): 1267–79. https://doi.org/10.1098/RSTB.2007.2114.

Pederson, Larry, Ming Ruan, Jennifer J. Westendorf, Sundeep Khosla, and Merry Jo Oursler. 2008. "Regulation of Bone Formation by Osteoclasts Involves Wnt/BMP Signaling and the Chemokine Sphingosine-1-Phosphate." Proceedings of the National Academy of Sciences of the United States of America 105 (52): 20764–69. https://doi.org/10.1073/PNAS.0805133106.

Peng, Ying, Quan Kang, Qing Luo, Wei Jiang, Weike Si, Bernard A. Liu, Hue H. Luu, et al. 2004. "Inhibitor of DNA Binding/Differentiation Helix-Loop-Helix Proteins Mediate Bone Morphogenetic Protein-Induced Osteoblast Differentiation of Mesenchymal Stem Cells *." Journal of Biological Chemistry 279 (31): 32941–49. https://doi.org/10.1074/JBC.M403344200.

Pérez-Campo, Flor M., Ana Santurtún, Carmen García-Ibarbia, María A. Pascual, Carmen Valero, Carlos Garcés, Carolina Sañudo, María T. Zarrabeitia, and José A. Riancho. 2016. "Osterix and RUNX2 Are Transcriptional Regulators of Sclerostin in Human Bone." Calcified Tissue International 99 (3): 302–9. https://doi.org/10.1007/S00223-016-0144-4/TABLES/1.

PetitClerc, C. 1976. "Quantitative Fractionation of Alkaline Phosphatase Isoenzymes According to Their Thermostability." Clinical Chemistry 22 (1): 42–48. https://doi.org/10.1093/CLINCHEM/22.1.42.

Pikner R, Palička V, Rosa J, Zikán V, Švagera Z, Racek J, Friedecký B, Kratochvíla J, and Zima T. 2020. "Markery Kostního Obratu u Osteoporózy-Společné Stanovisko k Jejich Využití Společnosti pro Metabolická Onemocnění Skeletu (SMOS) ČLS JEP a České Společnosti Klinické Biochemie (ČSKB) ČLS JEP." Biochem. Metab 28 (49): 48–63.

Piryaei, Abbas, Mojtaba Rezazadeh Valojerdi, Mansoureh Shahsavani, and Hossein Baharvand. 2010. "Differentiation of Bone Marrow-Derived Mesenchymal Stem Cells into Hepatocyte-like Cells on Nanofibers and Their Transplantation into a Carbon Tetrachloride-Induced Liver Fibrosis Model." Stem Cell Reviews and Reports 2010 7:1 7 (1): 103–18. https://doi.org/10.1007/S12015-010-9126-5.

Pitt, G. G., Gratzl, M. M., Kimmel, G. L., Surles, J., & Sohindler, A. (1981). Aliphatic polyesters II. The degradation of poly (DL-lactide), poly (ε-caprolactone), and their copolymers in vivo. Biomaterials, 2(4), 215-220.

Pittenger, Mark F., Alastair M. Mackay, Stephen C. Beck, Rama K. Jaiswal, Robin Douglas, Joseph D. Mosca, Mark A. Moorman, Donald W. Simonetti, Stewart Craig, and Daniel R. Marshak. 1999. "Multilineage Potential of Adult Human Mesenchymal Stem Cells." Science 284 (5411): 143–47. https://doi.org/10.1126/SCIENCE.284.5411.143/SUPPL_FILE/983855S5_THUMB.GIF.

Pradeep, C, S Mathew, B Nithyaja, P Radhakrishnan, and V P N Nampoori. 2013. "Nonlinear Optical Properties of PicoGreen Dye : DNA System." In National Laser Symposium, 3–6. Bhabha Atomic Research Centre, Trombay, Mumbai, India.

Prockop, Darwin J. 1997. "Marrow Stromal Cells as Stem Cells for Nonhematopoietic Tissues." Science 276 (5309): 71–74. https://doi.org/10.1126/SCIENCE.276.5309.71.

Prockop, Darwin J., and Joo Youn Oh. 2012. “Mesenchymal Stem/Stromal Cells (MSCs): Role as Guardians of Inflammation.” Molecular Therapy 20 (1): 14–20. https://doi.org/10.1038/MT.2011.211.

Qu, Shuang, Jiahui Wu, Qianyi Bao, Bing Yao, Rui Duan, Xiang Chen, Lingyun Li, Hongyan Yuan, Yucui Jin, and Changyan Ma. 2019. “Osterix Promotes the Migration and Angiogenesis of Breast Cancer by Upregulation of S100A4 Expression.” Journal of Cellular and Molecular Medicine 23 (2): 1116–27. https://doi.org/10.1111/JCMM.14012.

Quirici, Nadia, Davide Soligo, Patrizia Bossolasco, Federica Servida, Cristina Lumini, and Giorgio Lambertenghi Deliliers. 2002. “Isolation of Bone Marrow Mesenchymal Stem Cells by Anti-Nerve Growth Factor Receptor Antibodies.” Experimental Hematology 30 (7): 783–91. https://doi.org/10.1016/S0301-472X(02)00812-3.

Rahaman, M. N., Day, D. E., Bal, B. S., Fu, Q., Jung, S. B., Bonewald, L. F., & Tomsia, A. P. (2011). Bioactive glass in tissue engineering. Acta biomaterialia, 7(6), 2355-2373.

Rampichová, M., Chvojka, J., Jenčová, V., Kubíková, T., Tonar, Z., Erben, J., Buzgo, M., Daňková, J., Litvinec, A., Vocetková, K., Plencner, M., Prosecká, E., Sovková, V., Lukášová, V., Králíčková, M., Lukáš, D., & Amler, E. (2018). The combination of nanofibrous and microfibrous materials for enhancement of cell infiltration and in vivo bone tissue formation. Biomedical Materials (Bristol), 13(2). https://doi.org/10.1088/1748-605X/aa9717

Rampichová, M., J. Chvojka, V. Jenčová, T. Kubíková, Z. Tonar, J. Erben, M. Buzgo, et al. 2018. “The Combination of Nanofibrous and Microfibrous Materials for Enhancement of Cell Infiltration and in Vivo Bone Tissue Formation.” Biomedical Materials (Bristol) 13 (2). https://doi.org/10.1088/1748-605X/aa9717.

Rho, Jae Young, Liisa Kuhn-Spearing, and Peter Zioupos. 1998. “Mechanical Properties and the Hierarchical Structure of Bone.” Medical Engineering & Physics 20 (2): 92–102. https://doi.org/10.1016/S1350-4533(98)00007-1.

Robling, Alexander G., Alesha B. Castillo, and Charles H. Turner. 2006. “Biomechanical and Molecular Regulation of Bone Remodeling.” Annual Review of Biomedical Engineering 8: 455–98. https://doi.org/10.1146/ANNUREV.BIOENG.8.061505.095721.

Robling, Alexander G., and Lynda F. Bonewald. 2020. “The Osteocyte: New Insights.” Https://Doi.Org/10.1146/Annurev-Physiol-021119-034332 82 (February): 485–506. https://doi.org/10.1146/ANNUREV-PHYSIOL-021119-034332.

Rochefort, G. Y., S. Pallu, and C. L. Benhamou. 2010. “Osteocyte: The Unrecognized Side of Bone Tissue.” Osteoporosis International 2010 21:9 21 (9): 1457–69. https://doi.org/10.1007/S00198-010-1194-5.

Rodan, G. A. 1998. “Bone Homeostasis.” Proceedings of the National Academy of Sciences of the United States of America 95 (23): 13361–62. https://doi.org/10.1073/PNAS.95.23.13361.

Roh, Jason D., Gregory N. Nelson, Brooks V. Udelsman, Matthew P. Brennan, Britt Lockhart, Peter M. Fong, Reynold I. Lopez-Soler, W. Mark Saltzman, and Christopher K. Breuer. 2007. “Centrifugal Seeding Increases Seeding Efficiency and Cellular Distribution of Bone Marrow Stromal Cells in Porous Biodegradable Scaffolds.” Https://Home.Liebertpub.Com/Ten 13 (11): 2743–49. https://doi.org/10.1089/TEN.2007.0171.

Rosier, Randy N., Regis J. O'Keefe, and David G. Hicks. 1998. "The Potential Role of Transforming Growth Factor Beta in Fracture Healing." Clinical Orthopaedics and Related Research 355 (355 Suppl). https://doi.org/10.1097/00003086-199810001-00030.

Ross, R., D. F. Bowen-Pope, and E. W. Raines. 1990. "Platelet-Derived Growth Factor and Its Role in Health and Disease." Philosophical Transactions of the Royal Society of London. B, Biological Sciences 327 (1239): 155–69. https://doi.org/10.1098/RSTB.1990.0051.

Rydz, Joanna, Wanda Sikorska, Mariya Kyulavska, and Darinka Christova. 2014. "Polyester-Based (Bio)Degradable Polymers as Environmentally Friendly Materials for Sustainable Development." International Journal of Molecular Sciences 2015, Vol. 16, Pages 564-596 16 (1): 564–96. https://doi.org/10.3390/IJMS16010564.

Sadat-Shojai, Mehdi, Mohammad Taghi Khorasani, Ehsan Dinpanah-Khoshdargi, and Ahmad Jamshidi. 2013. "Synthesis Methods for Nanosized Hydroxyapatite with Diverse Structures." Acta Biomaterialia 9 (8): 7591–7621. https://doi.org/10.1016/J.ACTBIO.2013.04.012.

Samavedi, S., Whittington, A. R., & Goldstein, A. S. (2013). Calcium phosphate ceramics in bone tissue engineering: a review of properties and their influence on cell behavior. Acta biomaterialia, 9(9), 8037-8045.

Schindeler, Aaron, Michelle M. McDonald, Paul Bokko, and David G. Little. 2008. "Bone Remodeling during Fracture Repair: The Cellular Picture." Seminars in Cell & Developmental Biology 19 (5): 459–66. https://doi.org/10.1016/J.SEMCDB.2008.07.004.

Schofield, R. 1978. "The Relationship between the Spleen Colony-Forming Cell and the Haemopoietic Stem Cell." Blood Cells 4 (1–2): 7–25. https://europepmc.org/article/med/747780.

See, Constantin Von, Nils Claudius Gellrich, Ulrike Jachmann, Matthias W. Laschke, Kai Hendrik Bormann, and Martin Rücker. 2010. "Bone Augmentation after Soft-Tissue Expansion Using Hydrogel Expanders: Effects on Microcirculation and Osseointegration." Clinical Oral Implants Research 21 (8): 842–47. https://doi.org/10.1111/J.1600-0501.2009.01847.X.

Sellgren, Katelyn L., and Teng Ma. 2015. "Effects of Flow Configuration on Bone Tissue Engineering Using Human Mesenchymal Stem Cells in 3D Chitosan Composite Scaffolds." Journal of Biomedical Materials Research - Part A 103 (8): 2509–20. https://doi.org/10.1002/JBM.A.35386.

Shastri, V. P., Martin, I., & Langer, R. (2000). Macroporous polymer foams by hydrocarbon templating. Proceedings of the National Academy of Sciences, 97(5), 1970-1975.

Shbeh, M., Wally, Z. J., Elbadawi, M., Mosalagae, M., Al-Alak, H., Reilly, G. C., & Goodall, R. (2019). Incorporation of HA into porous titanium to form Ti-HA biocomposite foams. Journal of the mechanical behavior of biomedical materials, 96, 193-203.

Shetty, Sahana, Nitin Kapoor, Joseph Bondu, Nihal Thomas, and Thomas Paul. 2016. "Bone Turnover Markers: Emerging Tool in the Management of Osteoporosis." Indian Journal of Endocrinology and Metabolism 20 (6): 846. https://doi.org/10.4103/2230-8210.192914.

Shi, M., Z. W. Liu, and F. S. Wang. 2011. "Immunomodulatory Properties and Therapeutic Application of Mesenchymal Stem Cells." Clinical & Experimental Immunology 164 (1): 1–8. https://doi.org/10.1111/J.1365-2249.2011.04327.X.

Shi, Songtao, and Stan Gronthos. 2003. “Perivascular Niche of Postnatal Mesenchymal Stem Cells in Human Bone Marrow and Dental Pulp.” Journal of Bone and Mineral Research 18 (4): 696–704. https://doi.org/10.1359/JBMR.2003.18.4.696.

Shi, Xuetao, Yingjun Wang, Rohan R. Varshney, Li Ren, Yihong Gong, and Dong An Wang. 2010. “Microsphere-Based Drug Releasing Scaffolds for Inducing Osteogenesis of Human Mesenchymal Stem Cells in Vitro.” European Journal of Pharmaceutical Sciences 39 (1–3): 59–67. https://doi.org/10.1016/J.EJPS.2009.10.012.

Shi, Yigong, and Joan Massagué. 2003. “Mechanisms of TGF-β Signaling from Cell Membrane to the Nucleus.” Cell 113 (6): 685–700. https://doi.org/10.1016/S0092-8674(03)00432-X.

Shibuya, Masabumi. 2006. “Differential Roles of Vascular Endothelial Growth Factor Receptor-1 and Receptor-2 in Angiogenesis.” BMB Reports 39 (5): 469–78. https://doi.org/10.5483/BMBREP.2006.39.5.469.

Shin, Michael, Hiroshi Yoshimoto, and Joseph P. Vacanti. 2004. “In Vivo Bone Tissue Engineering Using Mesenchymal Stem Cells on a Novel Electrospun Nanofibrous Scaffold.” Tissue Engineering 10 (1–2): 33–41. https://doi.org/10.1089/107632704322791673.

Shirakawa, Ken, Shingo Maeda, Tomomi Gotoh, Makoto Hayashi, Kenichi Shinomiya, Shogo Ehata, Riko Nishimura, et al. 2006. “CCAAT/Enhancer-Binding Protein Homologous Protein (CHOP) Regulates Osteoblast Differentiation.” Molecular and Cellular Biology 26 (16): 6105–16. https://doi.org/10.1128/MCB.02429-05/ASSET/E1AACE3A-F539-4A91-A8B7-D1FD9B381548/ASSETS/GRAPHIC/ZMB0160661410008.JPEG.

Sikavitsas, Vassilios I., Gregory N. Bancroft, and Antonios G. Mikos. 2002. “Formation of Three-Dimensional Cell/Polymer Constructs for Bone Tissue Engineering in a Spinner Flask and a Rotating Wall Vessel Bioreactor.” Journal of Biomedical Materials Research 62 (1): 136–48. https://doi.org/10.1002/JBM.10150.

Siller, Alejandro F., and Michael P. Whyte. 2018. “Alkaline Phosphatase: Discovery and Naming of Our Favorite Enzyme.” Journal of Bone and Mineral Research 33 (2): 362–64. https://doi.org/10.1002/JBMR.3225.

Simmons, P. J., and B. Torok-Storb. 1991. “Identification of Stromal Cell Precursors in Human Bone Marrow by a Novel Monoclonal Antibody, STRO-1.” Blood 78 (1): 55–62. https://doi.org/10.1182/BLOOD.V78.1.55.55.

Sinha-Ray, S., A. L. Yarin, and B. Pourdeyhimi. 2013. “Prediction of Angular and Mass Distribution in Meltblown Polymer Lay-Down.” Polymer 54 (2): 860–72. https://doi.org/10.1016/J.POLYMER.2012.11.061.

Sinha-Ray, S., A.L. Yarin, and B. Pourdeyhimi. 2014. “Meltblown Fiber Mats and Their Tensile Strength.” Polymer 55 (16): 4241–47. https://doi.org/10.1016/j.polymer.2014.05.025.

Sinha-Ray, S., Yarin, A. L., & Pourdeyhimi, B. 2013. Prediction of angular and mass distribution in meltblown polymer lay-down. Polymer, 54(2), 860–872.

Sivalingam, G., S. Chattopadhyay, and G. Madras. 2003. “Enzymatic Degradation of Poly (ε-Caprolactone), Poly (Vinyl Acetate) and Their Blends by Lipases.” Chemical Engineering Science 58 (13): 2911–19. https://doi.org/10.1016/S0009-2509(03)00155-6.

Smalt, Rolf, Fred T. Mitchell, Ron L. Howard, and Timothy J. Chambers. 1997. “Mechanotransduction in Bone Cells: Induction of Nitric Oxide and Prostaglandin Synthesis by Fluid Shear Stress, but Not by Mechanical Strain.” Advances in Experimental Medicine and Biology 433: 311–14. https://doi.org/10.1007/978-1-4899-1810-9_66.

Štěpán, J., V. Volek, and J. KoláŘ. 1976. “A Modified Inactivation - Inhibition Method for Determining the Serum Activity of Alkaline Phosphatase Isoenzymes.” Clinica Chimica Acta 69 (1): 1–9. https://doi.org/10.1016/0009-8981(76)90465-4.

Stolzing, A., E. Jones, D. McGonagle, and A. Scutt. 2008. “Age-Related Changes in Human Bone Marrow-Derived Mesenchymal Stem Cells: Consequences for Cell Therapies.” Mechanisms of Ageing and Development 129 (3): 163–73. https://doi.org/10.1016/J.MAD.2007.12.002.

Subbiah, T., Bhat, G. S., Tock, R. W., Parameswaran, S., & Ramkumar, S. S. (2005). Electrospinning of nanofibers. Journal of applied polymer science, 96(2), 557-569.

Sumanasinghe, Ruwan D., T. Wayne Pfeiler, Nancy A. Monteiro-Riviere, and Elizabeth G. Loboa. 2009. “Expression of Proinflammatory Cytokines by Human Mesenchymal Stem Cells in Response to Cyclic Tensile Strain.” Journal of Cellular Physiology 219 (1): 77–83. https://doi.org/10.1002/JCP.21653.

Sun, Hongfan, Lin Mei, Cunxian Song, Xiumin Cui, and Pengyan Wang. 2006. “The in Vivo Degradation, Absorption and Excretion of PCL-Based Implant.” Biomaterials 27 (9): 1735–40. https://doi.org/10.1016/J.BIOMATERIALS.2005.09.019.

Sur, S., Tantakitti, F., Matson, J. B., & Stupp, S. I. (2015). Epitope topography controls bioactivity in supramolecular nanofibers. Biomaterials science, 3(3), 520-532.

Tabriz, A. G., Hermida, M. A., Leslie, N. R., & Shu, W. (2015). Three-dimensional bioprinting of complex cell laden alginate hydrogel structures. Biofabrication, 7(4), 045012.

Takamizawa, Shinji, Yojiro Maehata, Katsuyuki Imai, Haruki Senoo, Sadao Sato, and Ryu Ichiro Hata. 2004. “Effects of Ascorbic Acid and Ascorbic Acid 2-Phosphate, a Long-Acting Vitamin C Derivative, on the Proliferation and Differentiation of Human Osteoblast-like Cells.” Cell Biology International 28 (4): 255–65. https://doi.org/10.1016/J.CELLBI.2004.01.010.

Takayanagi, Hiroshi. 2007. “Osteoimmunology: Shared Mechanisms and Crosstalk between the Immune and Bone Systems.” Nature Reviews Immunology 2007 7:4 7 (4): 292–304. https://doi.org/10.1038/nri2062.

Takemoto M, Fujibayashi S, Neo M, Suzuki J, Kokubo T, Nakamura T. Mechanical properties and osteoconductivity of porous bioactive titanium. Biomaterials 2005; 26: 6014–6023.

Taner, Timucin, Nitin Abrol, Walter D. Park, Michael J. Hansen, Michael P. Gustafson, Lilach O. Lerman, Andre J. van Wijnen, Allan B. Dietz, Gregory J. Gores, and Mark D. Stegall. 2020. “Phenotypic, Transcriptional, and Functional Analysis of Liver Mesenchymal Stromal Cells and Their Immunomodulatory Properties.” Liver Transplantation 26 (4): 549–63. https://doi.org/10.1002/LT.25718.

Teitelbaum, Steven L., and F. Patrick Ross. 2003. “Genetic Regulation of Osteoclast Development and Function.” Nature Reviews. Genetics 4 (8): 638–49. https://doi.org/10.1038/NRG1122.

Thavornyutikarn, Boonlom, Nattapon Chantarapanich, Kriskrai Sitthiseripratip, George A. Thouas, and Qizhi Chen. 2014. “Bone Tissue Engineering Scaffolding: Computer-Aided Scaffolding Techniques.” Progress in Biomaterials 2014 3:2 3 (2): 61–102. https://doi.org/10.1007/S40204-014-0026-7.

Vater, Corina, Philip Kasten, and Maik Stiehler. 2011. “Culture Media for the Differentiation of Mesenchymal Stromal Cells.” Acta Biomaterialia 7 (2): 463–77. https://doi.org/10.1016/J.ACTBIO.2010.07.037.

Verwilghen, C., Chkir, M., Rio, S., Nzihou, A., Sharrock, P., & Depelsenaire, G. (2009). Convenient conversion of calcium carbonate to hydroxyapatite at ambient pressure. Materials Science and Engineering: C, 29(3), 771-773.

Vimalraj, Selvaraj. 2020. “Alkaline Phosphatase: Structure, Expression and Its Function in Bone Mineralization.” Gene 754 (September): 144855. https://doi.org/10.1016/J.GENE.2020.144855.

Volkmer, Elias, Inga Drosse, Sven Otto, Achim Stangelmayer, Michael Stengele, Bobby Cherian Kallukalam, Wolf Mutschler, and Matthias Schieker. 2008. “Hypoxia in Static and Dynamic 3D Culture Systems for Tissue Engineering of Bone.” Https://Home.Liebertpub.Com/Tea 14 (8): 1331–40. https://doi.org/10.1089/TEN.TEA.2007.0231.

Von See, C., Gellrich, N. C., Jachmann, U., Laschke, M. W., Bormann, K. H., & Rücker, M. (2010). Bone augmentation after soft-tissue expansion using hydrogel expanders: effects on microcirculation and osseointegration. Clinical Oral Implants Research, 21(8), 842–847. https://doi.org/10.1111/J.1600-0501.2009.01847.X

Vunjak-Novakovic, Gordana, Bojana Obradovic, Ivan Martin, Predrag M. Bursac, Robert Langer, and Lisa E. Freed. 1998. “Dynamic Cell Seeding of Polymer Scaffolds for Cartilage Tissue Engineering.” Biotechnology Progress 14 (2): 193–202. https://doi.org/10.1021/BP970120J.

Wagner, Wolfgang, Frederik Wein, Anja Seckinger, Maria Frankhauser, Ute Wirkner, Ulf Krause, Jonathon Blake, et al. 2005. “Comparative Characteristics of Mesenchymal Stem Cells from Human Bone Marrow, Adipose Tissue, and Umbilical Cord Blood.” Experimental Hematology 33 (11): 1402–16. https://doi.org/10.1016/J.EXPHEM.2005.07.003.

Wang, Chih Hsiang, Ting Ming Wang, Tai Horng Young, Yiu Kay Lai, and Men Luh Yen. 2013. “The Critical Role of ECM Proteins within the Human MSC Niche in Endothelial Differentiation.” Biomaterials 34 (17): 4223–34. https://doi.org/10.1016/J.BIOMATERIALS.2013.02.062.

Wang, H., Zhang, Y., Gao, H., Jin, X., & Xie, X. (2016). Composite melt-blown nonwoven fabrics with large pore size as Li-ion battery separator. International Journal of Hydrogen Energy, 41(1), 324–330. https://doi.org/10.1016/J.IJHYDENE.2015.09.130

Wang, Hong, Yao Zhang, Huipu Gao, Xiangyu Jin, and Xiaohua Xie. 2016. “Composite Melt-Blown Nonwoven Fabrics with Large Pore Size as Li-Ion Battery Separator.” International Journal of Hydrogen Energy 41 (1): 324–30. https://doi.org/10.1016/J.IJHYDENE.2015.09.130.

Wang, Hwai-Shi, Shih-Chieh Hung, Shu-Tine Peng, Chun-Chieh Huang, Hung-Mu Wei, Yi-Jhih Guo, Yu-Show Fu, Mei-Chun Lai, and Chin-Chang Chen. 2004. “Mesenchymal Stem Cells in the Wharton’s Jelly of the Human Umbilical Cord.” STEM CELLS 22 (7): 1330–37. https://doi.org/10.1634/STEMCELLS.2004-0013.

Wang, J. J., & Li, X. S. (2010). Improved oxygen permeability and mechanical strength of silicone hydrogels with interpenetrating network structure. Chinese Journal of Polymer Science, 28(6), 849-857.

Wang, P., Liu, P., Xu, F., Fan, X., Yuan, H., Li, H., & Yan, Y. (2018). Controlling the degradation of dicalcium phosphate/calcium sulfate/poly (amino acid) biocomposites for bone regeneration. Polymer Composites, 39, E122-E131.

Wang, Sainan, Jinquan Mu, Zhipeng Fan, Yan Yu, Ming Yan, Gang Lei, Chunbo Tang, et al. 2012. "Insulin-like Growth Factor 1 Can Promote the Osteogenic Differentiation and Osteogenesis of Stem Cells from Apical Papilla." Stem Cell Research 8 (3): 346–56. https://doi.org/10.1016/J.SCR.2011.12.005.

Wang, Yongmei, Shigeki Nishida, Takeshi Sakata, Hashem Z. Elalieh, Wenhan Chang, Bernard P. Halloran, Steven B. Doty, and Daniel D. Bikle. 2006. "Insulin-Like Growth Factor-I Is Essential for Embryonic Bone Development." Endocrinology 147 (10): 4753–61. https://doi.org/10.1210/EN.2006-0196.

Weinand, Christian, Wei Xu Jian, Giuseppe M. Peretti, Lawrence J. Bonassar, and Thomas J. Gill. 2009. "Conditions Affecting Cell Seeding onto Three-Dimensional Scaffolds for Cellular-Based Biodegradable Implants." Journal of Biomedical Materials Research Part B: Applied Biomaterials 91B (1): 80–87. https://doi.org/10.1002/JBM.B.31376.

Weinbaum, S., S. C. Cowin, and Yu Zeng. 1994. "A Model for the Excitation of Osteocytes by Mechanical Loading-Induced Bone Fluid Shear Stresses." Journal of Biomechanics 27 (3): 339–60. https://doi.org/10.1016/0021-9290(94)90010-8.

Weissman, Irving L. 2000. "Translating Stem and Progenitor Cell Biology to the Clinic: Barriers and Opportunities." Science 287 (5457): 1442–46. https://doi.org/10.1126/SCIENCE.287.5457.1442.

Westendorf, Jennifer J. 2006. "Transcriptional Co-Repressors of Runx2." Journal of Cellular Biochemistry 98 (1): 54–64. https://doi.org/10.1002/JCB.20805.

Wheeler, D. L., Stokes, K. E., Hoellrich, R. G., Chamberland, D. L., & McLoughlin, S. W. (1998). Effect of bioactive glass particle size on osseous regeneration of cancellous defects. Journal of Biomedical Materials Research: An Official Journal of The Society for Biomaterials, The Japanese Society for Biomaterials, and the Australian Society for Biomaterials, 41(4), 527-533.

Williams, Samuel A., Heather L. Maecker, Dorothy M. French, Jinfeng Liu, Andrew Gregg, Leah B. Silverstein, Tim C. Cao, Richard A.D. Carano, and Vishva M. Dixit. 2011. "USP1 Deubiquitinates ID Proteins to Preserve a Mesenchymal Stem Cell Program in Osteosarcoma." Cell 146 (6): 918–30. https://doi.org/10.1016/J.CELL.2011.07.040.

Wittkowske, Claudia, Gwendolen C. Reilly, Damien Lacroix, and Cecile M. Perrault. 2016. "In Vitro Bone Cell Models: Impact of Fluid Shear Stress on Bone Formation." Frontiers in Bioengineering and Biotechnology 4 (NOV). https://doi.org/10.3389/FBIOE.2016.00087.

Woodward, S. C., P. S. Brewer, F. Moatamed, A. Schindler, and C. G. Pitt. 1985. "The Intracellular Degradation of Poly(ε-Caprolactone)." Journal of Biomedical Materials Research 19 (4): 437–44. https://doi.org/10.1002/JBM.820190408.

Xiao, G., R. Gopalakrishnan, D. Jiang, E. Reith, M. D. Benson, and R. T. Franceschi. 2002. "Bone Morphogenetic Proteins, Extracellular Matrix, and Mitogen-Activated Protein Kinase Signaling Pathways Are Required for Osteoblast-Specific Gene Expression and Differentiation in MC3T3-E1 Cells." Journal

of Bone and Mineral Research : The Official Journal of the American Society for Bone and Mineral Research 17 (1): 101–10. https://doi.org/10.1359/JBMR.2002.17.1.101.

Xiao, Guozhi, Di Jiang, Peedikayil Thomas, M. Douglas Benson, Kunliang Guan, Gerard Karsenty, and Renny T. Franceschi. 2000. "MAPK Pathways Activate and Phosphorylate the Osteoblast-Specific Transcription Factor, Cbfa1 *." Journal of Biological Chemistry 275 (6): 4453–59. https://doi.org/10.1074/JBC.275.6.4453.

Xing, Juan, Yan Li, Manping Lin, Jinfeng Wang, Jinchuan Wu, Yufei Ma, Yuanliang Wang, Li Yang, and Yanfeng Luo. 2014. "Surface Chemistry Modulates Osteoblasts Sensitivity to Low Fluid Shear Stress." Journal of Biomedical Materials Research Part A 102 (11): 4151–60. https://doi.org/10.1002/JBM.A.35087.

Yaghoobi, Maliheh, Sameereh Hashemi-Najafabadi, Masoud Soleimani, and Ebrahim Vasheghani-Farahani. 2019. "Osteogenic Induction of Human Mesenchymal Stem Cells in Multilayered Electrospun Scaffolds at Different Flow Rates and Configurations in a Perfusion Bioreactor." Journal of Bioscience and Bioengineering 128 (4): 495–503. https://doi.org/10.1016/J.JBIOSC.2019.03.015.

Yaghoobi, Maliheh, Sameereh Hashemi-Najafabadi, Masoud Soleimani, Ebrahim Vasheghani-Farahani, and Seyyed Mohammad Mousavi. 2016. "Osteogenic Differentiation and Mineralization on Compact Multilayer NHA-PCL Electrospun Scaffolds in a Perfusion Bioreactor." Iranian Journal of Biotechnology 14 (2): 41. https://doi.org/10.15171/IJB.1382.

Yang, Xiangli, Koichi Matsuda, Peter Bialek, Sylvie Jacquot, Howard C. Masuoka, Thorsten Schinke, Lingzhen Li, et al. 2004. "ATF4 Is a Substrate of RSK2 and an Essential Regulator of Osteoblast Biology: Implication for Coffin-Lowry Syndrome." Cell 117 (3): 387–98. https://doi.org/10.1016/S0092-8674(04)00344-7.

Yao, Qingqing, Yu Liu, Yining Pan, Jacob M. Miszuk, and Hongli Sun. 2020. "One-Pot Porogen Free Method Fabricated Porous Microsphere-Aggregated 3D PCL Scaffolds for Bone Tissue Engineering." Journal of Biomedical Materials Research Part B: Applied Biomaterials 108 (6): 2699–2710. https://doi.org/10.1002/JBM.B.34601.

Yigitbilek, Furkan, Sabena M. Conley, Hui Tang, Ishran M. Saadiq, Kyra L. Jordan, Lilach O. Lerman, and Timucin Taner. 2021. "Comparable in Vitro Function of Human Liver-Derived and Adipose Tissue-Derived Mesenchymal Stromal Cells: Implications for Cell-Based Therapy." Frontiers in Cell and Developmental Biology 9 (March): 697. https://doi.org/10.3389/FCELL.2021.641792/BIBTEX.

Yoshimoto, H., Y. M. Shin, H. Terai, and J. P. Vacanti. 2003. "A Biodegradable Nanofiber Scaffold by Electrospinning and Its Potential for Bone Tissue Engineering." Biomaterials 24 (12): 2077–82. https://doi.org/10.1016/S0142-9612(02)00635-X.

Yusuf, Salim, Eva Lonn, Prem Pais, Jackie Bosch, Patricio López-Jaramillo, Jun Zhu, Denis Xavier, et al. 2016. "Blood-Pressure and Cholesterol Lowering in Persons without Cardiovascular Disease." New England Journal of Medicine 374 (21): 2032–43. https://doi.org/10.1056/NEJMoa1600177.

Zeng, J., Haoqing, H., Schaper, A., Wendorff, J. H., & Greiner, A. (2003). Poly-L-lactide nanofibers by electrospinning–Influence of solution viscosity and electrical conductivity on fiber diameter and fiber morphology. e-Polymers, 3(1).

Zhang, Hailan, Gezhi Hu, Hongyu Wang, Peter Sciavolino, Nancy Iler, Michael M Shen, and Cory Abate-Shen. 1997. “Heterodimerization of Msx and Dlx Homeoproteins Results in Functional Antagonism.” Molecular and Cellular Biology 17 (5): 2920. https://doi.org/10.1128/MCB.17.5.2920.

Zhang, Qingchun, Yun Jiang, Yan Zhang, Zhaoyang Ye, Wensong Tan, and Meidong Lang. 2013. “Effect of Porosity on Long-Term Degradation of Poly (ε-Caprolactone) Scaffolds and Their Cellular Response.” Polymer Degradation and Stability 98 (1): 209–18. https://doi.org/10.1016/J.POLYMDEGRADSTAB.2012.10.008.

Zhang, X., Zeng, D., Li, N., Wen, J., Jiang, X., Liu, C., & Li, Y. (2016). Functionalized mesoporous bioactive glass scaffolds for enhanced bone tissue regeneration. Scientific reports, 6, 19361.

Zhao, Jian, Changfa Xiao, and Naiku Xu. 2013. “Evaluation of Polypropylene and Poly (Butylmethacrylate-Co-Hydroxyethylmethacrylate) Nonwoven Material as Oil Absorbent.” Environmental Science and Pollution Research 20 (6): 4137–45. https://doi.org/10.1007/S11356-012-1397-8/FIGURES/12.

Zhao, Ming, Mei Qiao, Stephen E. Harris, Babatunde O. Oyajobi, Gregory R. Mundy, and Di Chen. 2004. “Smurf1 Inhibits Osteoblast Differentiation and Bone Formation in Vitro and in Vivo.” Journal of Biological Chemistry 279 (13): 12854–59. https://doi.org/10.1074/JBC.M313294200.